Universidade de Aveiro

2022

Holger Mario

Lovon Quispe

Exploração da análise custo-benefício na redução do risco sísmico

Exploring cost-benefit analysis for earthquake risk reduction

Universidade de Aveiro

2022

Holger Mario

Lovon Quispe

Exploração da análise custo-benefício na redução do risco sísmico

Exploring cost-benefit analysis for earthquake risk reduction

Tese apresentada à Universidade de Aveiro para cumprimento dos requisitos necessários à obtenção do grau de doutor em Engenharia Civil, realizada sob a orientação da equipa conformada pelo Professor Doutor Romeu Vicente da Silva, Professor Associado com Agregação do Departamento de Engenharia Civil da Universidade de Aveiro, Professor Doutor Vitor Marta da Silva, Investigador do Departamento de Engenharia Civil da Universidade de Aveiro, e Professor Doutor Tiago Miguel Ferreira, Lecturer do Department of Geography and Environmental Management of the University of the West of England (UWE Bristol).

This work could not be dedicated to someone other than my mother. To whom I owe completely, and who always guided me in my personal and professional growth. I know that, where you are, you will receive this with your characteristic happiness and enthusiasm.

o júri

Presidente

Prof. Maria Adelaide de Pinho Almeida
Professora Catedrática de Universidade de Aveiro

Vogais

Prof. Gabriele Milani
Professor Catedrático do Politecnico Di Milano

Doutora Helen Crowley
Investigadora do Global Earthquake Model

Prof. Serena Cattari
Professora Catedrática da Universidade de Genoa

Prof. Hugo Felipe Pinheiro Rodrigues
Professor Associado da Universidade de Aveiro

Doutor Vitor Emanuel marta da Silva
Investigador da Universidade de Aveiro

Acknowledgements

To achieve the end of this journey would have not been possible without the help of many persons who supported my either academically, or emotionally. This endeavour would not have been possible without all the supervision team. I want to thanks Prof. Vitor Silva, to whom I would like to extend my deepest thanks for the opportunity to develop this work, for his constant support and guidance along this time. Likewise, I am grateful to Prof. Romeu Vicente for his motivation and guidance throughout all the work as well as his welcoming attitude and disposition towards the students. Also, I want to acknowledge to Prof. Tiago Miguel Ferreira for his support and commitment all over this time, his valuable comments and wide collaboration attitude.

I am extremely grateful with my family, who always fulfilled me of motivation and courage towards this life's objective. At this point, I would like to express my deep appreciation for Prof. Nicola Tarque, who guided me from the very beginning of my career as a researcher, for his commitment and motivation. Also, would like to recognize the support of all my friends here in Portugal and in Peru for their motivation and company in this journey. I want to acknowledge the Fundação para a Ciência e Tecnologia (FCT) because of the grant (PD/BD/150406/2019) which permitted me to develop this work.

palavras-chave Risco sísmico, funções de fragilidade, estimativa de fatalidades, custo-benefício, construções de alvenaria.

Resumo

Os edifícios de alvenaria representam mais de 50% do parque habitacional de alvenaria em Portugal de acordo com o recenseamento nacional de 2011. Este tipo de construção revelou ter um fraco desempenho durante os eventos destrutivos ocorridos em Portugal no século passado. Os esforços anteriores para caracterizar a vulnerabilidade sísmica deste tipo de construção concentraram-se principalmente em edifícios individuais. Nesta tese é realizada uma análise custo-benefício para um conjunto de técnicas de reforço compatíveis com edifícios de alvenaria. O Capítulo 1 apresenta, de forma sucinta, os objetivos, motivações, e a estrutura da tese. No Capítulo 2, é apresentada uma revisão da literatura com o objetivo de apresentar aos leitores tópicos relacionados com esta investigação desenvolvida. O Capítulo 3 é dedicado à caracterização geométrica e mecânica de dois tipos de edifícios de alvenaria de pedra mais comuns em Portugal, calcário e granito. É frito um tratamento estatístico a partir do qual são definidas funções de densidade de probabilidade para caracterizar os parâmetros estruturais mais importantes. O Capítulo 4 visa a implementação de modelos numéricos avançados e o desenvolvimento de funções de fragilidade para edifícios de alvenaria. No Capítulo 5 discute-se o estado da prática na avaliação de fatalidades e apresentam-se os resultados da análise estrutural avançada no procedimento de avaliação de fatalidades. No Capítulo 6, são avaliadas com recurso a modelos numéricos um conjunto de técnicas de reforço compatíveis com edifícios de alvenaria em Portugal e são ainda desenvolvidas funções de vulnerabilidade e fragilidade para fatalidades, tendo em conta o impacto dessas técnicas no comportamento sísmico destes edifícios. O Capítulo 7 cobre a implementação das funções de consequência à escala nacional. Finalmente, o Capítulo 8 compila as principais conclusões e apresenta sugestões de futura investigação a desenvolver neste campo.

keywords

Seismic risk, fragility functions, fatality estimation, cost-benefit, masonry buildings.

abstract

Masonry buildings comprise more than 50% of the masonry building stock in Portugal according to the 2011 national census. This construction typology has revealed a poor performance during the destructive events which took place in Portugal in the last century. Past efforts to characterize the seismic vulnerability of this type of construction have focused mostly on individual buildings. In this dissertation, cost-benefit analyses are performed for a set of retrofitting techniques compatible with masonry buildings. Chapter 1 presents the aims, motivations and scope of the research, hence explaining the context of the current research. In Chapter 2, a literature review is presented with the purpose to introduce the reader to topics associated to this research. Important topics are addressed as building stock characterisation, physical damage and fatality assessment, retrofitting and cost-benefit analysis. Chapter 3 is devoted to the geometric and mechanical characterization of the two most common stone masonry building typologies in Portugal, limestone and granite. A statistical treatment is made, and probability density functions are defined for important structural features. Chapter 4 aims at implementing advanced numerical models and developing damage fragility functions for masonry buildings. Chapter 5 discusses the state-of-the-practice in fatality assessment and introduces the outcomes of the advanced structural analysis to propose a new fatality assessment framework. In Chapter 6, retrofitting techniques compatible with masonry buildings in Portugal are modelled and numerically assessed, to develop fragility and fatality vulnerability functions. Chapter 7 comprises the implementation of consequence functions at the national scale. Finally, the main outcomes, principal conclusions and future research is discussed in Chapter 8.

Contents

List of figures

List of tables

Chapter 1

Introduction

This chapter sets the problem in context. The main contribution is targeted at the cost-benefit analysis, however a set of specific objectives aligned with this primary goal of the thesis are identified. This chapter also covers the presentation of the structure of the dissertation.

1.1 Motivation and background

Earthquakes are responsible, on average, for a death toll of 20,000 people per year and constitute approximately 20 % of the annual economic losses due to disasters around the world. In Portugal important seismic events have taken place, such as the ~M6.0 1722 Algarve, ~M8.5 1755 Lisbon, the M6.3 1909 Benavente, M7.8 1969 Algarve and ~M6.0 1722 Azores earthquakes (e.g. Oliveira [1]). These events caused extensive damage in the affected regions, particularly to the masonry building stock (Correia et al. [2]). Masonry buildings have been built to withstand gravity loads but not to sustain horizontal actions, such as seismic loads [3]. The performance of masonry structures to earthquakes has been the target of numerous studies (e.g. Candeias [4], Villar et al. [5], Sumerente et al. [6], Lovon et al. [7], Ferreira et al. [8]), which have identified several reasons for the characteristic high seismic vulnerability. Some of these include the low tensile strength, the massive weight of the structural elements, the poor connection between the vertical and horizontal structural elements, irregularities both in plan and height, the lack of maintenance and the degradation of the masonry units and mortar (i.e. ageing effects). Consequently, the majority of the economic and human losses are associated with this type of construction [9]–[11]. It is thus relevant to further investigate the seismic behaviour of this type of construction and produce information that can be used to assess and mitigate the associated seismic risk.

The latest national housing census [12] states that masonry buildings represent approximately 50% of the building stock in Portugal and comprise 40% of the dwellings. Despite the usefulness of past studies and their valuable contribution to the understanding of earthquake risk in Portugal, several challenges and gaps still remain. Most efforts focused on particular case studies, and thus not all of the masonry building classes have been adequately covered. Moreover, most studies neglected uncertainties related to geometric features and their impact on fragility analyses. However, many studies (e.g. Candeias [4], Ferreira et al. [8], Maio et al.[13]) highlighted the importance of including this source of variability in vulnerability modelling for building archetypes , as the variability of geometric and mechanical properties can affect the associated vulnerability functions significantly. Moreover, different vulnerability derivation methodologies have been used in the past, thus preventing direct comparison of the outcomes due to the associated bias of each method (e.g. Silva et al. [14]). In this study, an innovative procedure was followed for assessing the seismic risk of the most important masonry building classes considering the uncertainty of geometric features.

Ideally, earthquake vulnerability models rely on damage or loss data from past events which allows the development of empirical vulnerability functions by establishing the relation between the probability of damage or loss and a set of hazard intensities (e.g. Rossetto et al. [15]). However, in countries such as Portugal where earthquakes are relatively rare or where a destructive event has not

happened in the last decades, empirical data either do not exist, or might be outdated. In these cases, it is common to rely on analytical approaches (e.g. D'Ayala et al. [16]) for seismic vulnerability assessment. In these methods, numerical models representing one or multiple building classes are created and tested against sets of ground motion records, or a uniform hazard spectrum. The structural response of these models can be used to derive analytical vulnerability functions (e.g. Martins et al. [17], Villar et al. [5]).

Past studies (e.g. D'Ayala et al. [16], Crowley et al. [18]) highlighting the appropriate selection of modelling strategy towards vulnerability assessment, suggest two criteria: a) the target risk metric, b) the complexity of the structural model. Both criteria must be consistent with each other. The target risk metric is the measure of the loss which is trying to be calculated (e.g. annual probability of collapse, annual average non-structural loss, annual average business interruption time). Moreover, the risk metric is associated to an engineering demand parameter (EDP) such as maximum inter-storey drift, maximum inter-storey acceleration, and residual drift. Hence, the model to be selected should be able to predict the EDP, which later will be associated with the risk metric. A more complex model can be capable of predicting more refined EDPs, though it results in higher computational effort. It should be noted that some EDPs can only be predicted by models with a high level of complexity.

Besides the selection of the modelling strategy, the selection of an adequate EDP is of fundamental importance in fragility assessment, as it should be congruent with the damage threshold and with the type of model. Inter storey drift-based damage assessment has been largely used for masonry assessment. However, it assumes uniform damage within each storey, which may not be convenient for some buildings with a particular geometry. The response of structural elements of unreinforced masonry (URM) buildings with flexible diaphragms differs significantly amongst each other, existing panels with in-plane, out-of-plane, or mixed behaviour. A second approach widely used in seismic fragility assessment of masonry buildings is the element-by-element drift-based damage assessment [19]–[21], usually implemented through macro models. The method provides a detailed damage state per element of the structure. Nonetheless, the definition of the structural elements can limit the types of failure mechanisms to be considered. The latter is particularly evident when a failure mechanism involves two structural elements as perpendicular intersections or rigid braces. Thus, this work aims at evaluating two novel EDPs for damage threshold definition. The proposed EDPs allow the treatment of the damage as a continuous parameter in the building.

It should be noticed that most of the studies addressing seismic risk focus mainly on physical structural damage but not on human losses. Based on past earthquakes, it has been demonstrated that the extent of the collapse is associated with the fatality rate inside a building [22]–[25]. It leads to some concerns about the traditional procedures, which consist in assessing fatality risk from physical damage fragility [26], [27], since most extreme physical damage states usually do not disclose the level of destruction of the building. Iida et al. [28] proposed to characterize the extent of the collapse by employing four parameters: internal volume reduction (IVR), plan loss, section loss, and amount of dust. However, current modelling techniques do not allow to quantifying all suggested parameters. Moreover, the relevance of each parameter may vary according to the structural system. Post-earthquake survey data suggests a good correlation between IVR and fatality ratio. This study aims, in part, at implementing an innovative framework for fatality vulnerability assessment in as-built and retrofitted masonry buildings.

Recent developments in the field of numerical modelling make it possible and practical to develop detailed models for a reasonable computational effort. LS-Dyna software [29], [30] has been used to develop cohesive element-based models that can model cracks and collapse explicitly. The models consist of an arrangement of elastic finite-element (FEM) blocks joined by cohesive elements. Similar approaches were proposed in the past but not applied to the vulnerability modelling field [31], [32]. The pursuit of such an approach requires the availability of detailed data regarding the dynamic, geometric, and mechanical properties of each building class.

In general, vulnerability assessment is particularly challenging for building classes due to the need to incorporate the aleatory variability in some of the geometric and mechanical attributes. Some examples of past studies that characterised these properties for a large number of building classes include Bal et al. [33] and Silva et al. [14]. In these studies, technical specifications and drawings of reinforced concrete buildings from Turkey and Portugal were analysed, and statistical models for the most relevant geometric and mechanical properties were derived. Limestone and Granite buildings are the most representative stone masonry buildings in the northern and southern regions of Portugal, respectively. Some aspects of this building typology , such as geospatial distribution [34] and the geometric and mechanical features [35]–[38], have been addressed in previous studies. In this dissertation, technical specifications and drawings from over 200 buildings were analysed to derive statistical models for the most relevant attributes for vulnerability risk assessment, also allowing the identification of the most common building archetypes. This is an important contribution to the current knowledge on vulnerability modelling for masonry building in Portugal by 1) identifying the most common masonry building classes in Portugal obtained from the analysis of the 2011 National Housing Census data [12]; 2) investigating more than two hundred existing masonry buildings to define the most common archetypes, 3) innovatively defining statistical models that include the most relevant geometric attributes, and 4) reviewing the existing literature on mechanical properties for this type of construction.

In the last decades, advances in the definition and assessment of retrofitting techniques are important to reduce fatality and severely injured rates. Nevertheless, this issue still requires study since the progress in the reduction of the global death toll from earthquakes is modest [23], [24]. According to Coburn and Spence [23], it has been demonstrated from past earthquake reports that 75 % of fatalities are caused by the collapse of buildings. However, it should be noticed that other causes of death are attributed to the efficiency of the rescue teams, medical conditions induced by the shock of experiencing an earthquake, accidents curing the disturbance, epidemics among homelessness and triggering of other hazards like fires, tsunamis, landslides, and so on. The reduction of the vulnerability is the main way to reduce seismic risk since other components such as exposure and hazard cannot be reduced, at least not easily. It implies improving the structural behaviour of the building stock in order to reduce damage and human losses. It is mainly achieved by retrofitting techniques, in agreement with the heritage status of most masonry buildings. Recent studies [13], [39] addressed cost-benefit analysis on various retrofitting techniques in order to provide decision tools for risk mitigation. The current dissertation attempts to include the novel physical damage fragility and fatality vulnerability functions herein developed to assess the cost-benefit of retrofitting techniques for masonry buildings in Portugal. Other risk metrics such as life safety and earthquake scenarios will be explored as well.

1.2 Objectives

This research aims ultimately at performing a cost-benefit analysis of retrofitting techniques applicable to unreinforced masonry buildings in Portugal. Other contributions towards the general objective are the use of advanced modelling strategies to explicitly model structural collapse, the introduction of two novel EDPs for physical fragility assessment, the implementation of an analytical framework for fatality vulnerability assessment, the propagation of uncertainties regarding geometric features, and the cost-benefit analysis of retrofitting alternatives. In order to achieve this primary goal, some specific objectives were proposed:

a) Characterizing the geometric and mechanical properties of limestone and granite masonry buildings in Portugal;
b) Fragility modelling of limestone and granite masonry buildings;
c) Vulnerability modelling of limestone and granite masonry buildings;
d) Cost-benefit analysis of seismic retrofitting techniques for URM buildings.

1.3 Outline of the thesis

The content of the thesis has been organized into seven chapters. Chapter 1 is intended to contextualize the reader to the problem this thesis is addressing. The motivation, and the main problem are presented together with its scope and past research. Chapter 2 provides a brief literature review, and basic concepts are explored, such as building stock characterisation, physical fragility assessment, fatality vulnerability assessment, masonry buildings retrofitting, and cost-benefit analysis. Chapter 3 describes the procedure followed towards the characterisation of masonry buildings in Portugal. Important trends regarding the building stock were identified, probability density functions were developed for geometric features, and a review of mechanical properties was performed. Chapter 4 aims to implement cloud analysis together with advanced numerical modelling to develop physical damage fragility functions for limestone and granite masonry buildings. Chapter 5 addresses implementation of a novel fatality vulnerability assessment framework, and performs fatality vulnerability assessment through consequence functions and earthquake scenarios. A comparison is performed with state-of-the-practice approaches. Chapter 6 is devoted to the implementation of retrofitting techniques within the framework for physical damage and fatality assessment. Chapter 7 gathers outcomes from previous chapters and from past studies and employs them to carry out risk and cost-benefit analyses at the national scale. Chapter 8 is devoted to the conclusions and future research arising from the current work.

Chapter 2

Literature review

This chapter aims to provide a background of the state-of-the-art in topics directly related to this research. Section 2.1 focuses on the review of topics related to building stock characterisation, it includes the classification of building portfolios for exposure models, the construction practice of masonry buildings in Portugal, stochastic modelling of geometric features, and identification of mechanical properties. All the aforementioned topics are reviewed from the risk assessment perspective of how a building class should be characterized. Section 2.2 addresses the analytical fragility assessment of masonry buildings. Several studies are available on this topic, and special attention was given to ground shaking intensity measures, damage-to-loss criterion and EDP, and numerical modelling strategies and procedures for developing fragility functions. Section 2.3. was devoted to a review of procedures attempting to assess fatalities due to earthquakes. Finally, section 2.4 is committed to the basis of cost-benefit analysis and the identification of potential retrofitting techniques.

2.1 Building stock characterisation

Building stock characterisation is the first task in seismic risk assessment. Four topics are addressed in this section: exposure models, construction practice over time in Portugal, uncertainty modelling of buildings' features, and mechanical properties.

2.1.1 Exposure models

When assessing the risk of a region with a large number of buildings (often hundreds or thousands), defining the structural system of each building with its individual structural and non-structural characteristics would be impractical [40]. Therefore, the study becomes feasible by grouping the building stock in classes. The grouping process should be made with basis on the overall seismic performance of the building [41], however other features like cost or type of use (e.g., residential, commercial) can be considered. Also, the availability of information and the available resources have an important role when defining the building classes.

Previous studies have addressed the problem of defining building classes for seismic risk assessment, either worldwide [42], [43], at regional [44], [45] or national scales [46], [47]. Building classes are expected to be sufficiently detailed to differentiate significant variances in the vulnerability of each typology according to the local construction techniques, as well as the potential exposed assets. According to FEMA 177 [41], the overall performance of the building is mainly given by the lateral load-resisting system, hence it should be the feature employed for the definition of building classes.

At the national level, Sousa [46] studied the seismic risk in Portugal with special attention to the masonry buildings (see Figure 2.1). In this research, the building stock was largely studied and classified based on the INE 2011 census data [12]. The latter provides measures of building concentration at the municipal level, which are 4037 in Portugal. Along the definition of building classes, a set of factors with influence in the seismic vulnerability were considered such as number of storeys, construction period, and structural system. A total of 20 building classes were defined following the above-mentioned criterion, however a differentiation of buildings constructed with different types of stones was not performed.

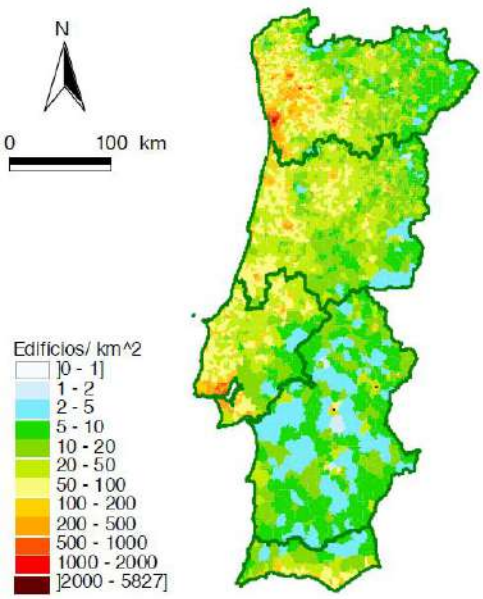

Figure 2.1 Density of masonry residential building stock in mainland Portugal [46]

At the regional level, Crowley et al. [48] developed an exposure model for European seismic risk assessment. This extensive database includes the spatial distribution of the residential, commercial and industrial building count, population, and replacement cost. The database relies on census data per country, and expert's opinion, and the outcomes are publicly available. The study defined building classes using the GEM building taxonomy [42] as shown in Figure 2.2. The main attributes considered in this study are the main construction material, the lateral load resisting system, number of storeys, seismic design code level and lateral force coefficient used in the seismic design. This is the latest study performed at regional level in Europe. However, there have been other attempts of characterizing the European building stock such as Mouroux and Brun [49]. These studies addressed a challenging task, and enormously contributed to the seismic risk research. However, they may not be able to represent local variations of masonry buildings within each country.

Figure 2.2 Example of URM building classified as MUR+STRUB/LWAL/H:1 according to [42]

2.1.2 Construction practice over time in Portugal

The construction practice in Portugal has changed over time either due to the introduction of new materials, or the reassignment of the building's use. It is important to be aware of this process in order to identify changes with important structural consequences. For this purpose, based in the literature review, this work considers four important periods in the development of the construction techniques in Portugal.

a) Unreinforced masonry buildings

Also known as Pre-Pombalino period, it is considered as the first period in the development of construction techniques in Portugal by many authors (e.g. Sousa [46], Costa et al. [47], Appleton [50], Lopes [51], Lamego [52]) . The Lisbon earthquake in 1755 appears to be the factor that bounds this period because of the large destruction it caused in the country. Some authors estimate its magnitude as Mw 9.0. This earthquake produced a subsequent fire and tsunami in the city, and changed, in the long-term, the awareness of the people to natural disasters and the constructive practices of those times. Therefore, almost all buildings constructed before the Lisbon 1755 earthquake belong to this period.

Pre-Pombalino period is also characterized by the use of stone units for the construction of URM buildings. Since stone units are heavy to transport, and because the lack of transportation systems in this period, masonry buildings were constructed with local available materials. Limestone, granite, shale and basalt appear to be the most used in the construction of URM buildings. It is important to realize that these buildings were conceived to deal with gravity loads rather than seismic actions [4], [52], [53]. Nowadays, most of these buildings are considered as vernacular because their characteristics are proper of the country architectonics. Pereira and Romão [34] made a broad survey around the country to define architectural features of vernacular Portuguese buildings, by crossing information provided by the IGP (Geological Institute of Portugal), they defined zones according to the predominant types of materials used in the construction of vernacular masonry buildings in Portugal, as shown in Figure 2.3. Although wood structures appear to be significantly used in this period, nowadays they represent a low proportion of the total buildings stock. Because wooden structures are not included in the scope of this work, the following description will focus on masonry structures.

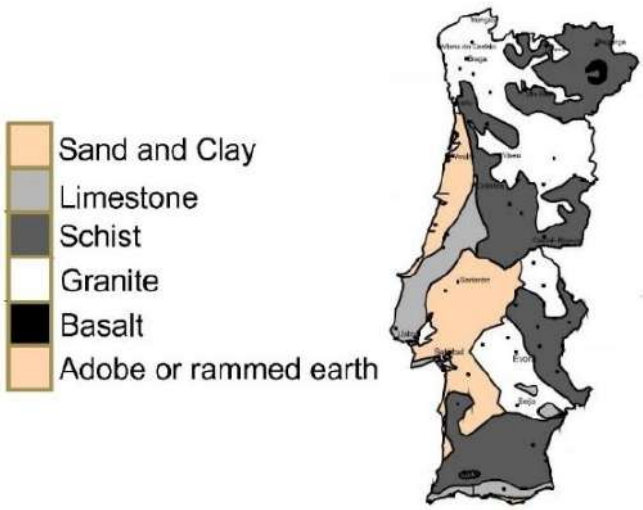

Figure 2.3 Distribution of the materials used in the construction of masonry buildings (adapted from Pereira and Romão [34])

The latest map (Figure 2.3) agree with Pinho [54] and Appleton [55] which suggest that granite and schist were mainly used in the Northern regions and in Beiras. Limestone was mainly employed in Lisbon, West regions, Alentejo and Beira Litoral. Similarly, the construction of buildings of adobe and tapia was practiced in the regions of Aveiro, Ribatejo, Alentejo and Algarve. Finally, basalt is the

most used material in the Azores archipelago [56]. Figure 2.4 shows two examples of granite and limestone pre-Pombalino buildings.

a) b)

Figure 2.4 Examples of unreinforced masonry buildings: a) limestone and b) granite [57]

Previous studies [50], [51], [57] state that there are three types of foundations: direct, semi-direct and indirect. Direct foundations, usually performed in rigid soils, consist in a wider extension of the masonry walls in the earth usually constructed with a poorer quality. Semi-direct foundations comprise a system of masonry arches and piers constructed in order to reach a deeper soil and therefore more rigid. Finally, indirect foundations consist in wood stakes on which the walls rest superficially. The foundations constructed in pre-Pombalino building has not changed significantly in comparison with masonry buildings constructed after this period.

According to LNEC [58], pre-Pombalino walls are constructed either with irregular or carved stones, in most cases joined with lime-sand mortar. Although dry-joined masonry walls can be found, these represent a small portion of the building stock and are frequently associated to monuments. These structures generally present a high walls density and low quantity of openings and are up to three or four floors. In these buildings, it is common to use wood or stone lintels located at the top of the openings to improve the wall-to-wall connexion.

Usually the inter-story system of these buildings is made of timber covering short spans [50] of up to 4 m, even though it is possible to find some masonry vaults mainly used to overcome the durability problem of the wood. Wood beams spaced at 0.20 to 0.40 m usually composes the inter-story system.

The roof is constituted by a wooden framework and its coverage is made up of tiles joint with mortar. In most cases, the wooden structures rely directly on the walls of the structure. However, in some cases the span between the walls can be covered with a masonry vault. This last case is associated to public buildings with higher architectonical value, and a wooden structure is required as well, but it rest on the masonry vault and walls [50].

b) Mixed wood-masonry buildings

Two building types were constructed in this period, locally known as “Pambolino” and “Gaioleiro”. These types of constructions appeared after the 1755 Lisbon earthquake with a specific objective to reconstruct the “Baixa Pombalina” or “Pombalino” downtown. Its name comes from the first minister Sebastião José de Carvalho e Melo, known after as Marquis of Pombal, who ordered the

development of a construction system capable of resisting earthquakes. The aforementioned task that was carried out by the team of Manuel da Maia, included engineers and architects [59].

The system consists in the introduction of a wooden 3D structure as part of the load-resisting system of the building, the wooden structure is used only in the interior walls. Hence, external walls continued being constructed only with stone masonry and mortar. The wooden structure, named Gaiola, comprise a set of rectangular frameworks with Saint Andrew's' crosses, as presented in Figure 2.5a. The next step is filling the gaps of the wooden structure with rubble masonry. Although it is possible to find pre-Pombalino buildings with wooden structures in the internal walls, this practice was not extensive, neither as systematic as in the Pombalino period. The use of wooden structures in the Pombalino period follows a strict symmetry and arrangement (see Figure 2.5b), while the previous construction types were irregular and without any specific configuration. The better junction between the pavements and the internal walls, and the improved resistance to shear forces are some of the main advantages of the wooden structure. The traditional Pombalino building is a 4-story structure used for housing, and in some cases, the ground floor is used for commercial purposes.

With the introduction of the steel and concrete materials for the construction industry in the XIX century, steel beams substituted its wooden counterparts when long spans need to be covered. This replacement was mainly to habilitate the commercial use of ground storeys. Some studies covered the description and analysis of mixed structures [60], [61].

a) b)

Figure 2.5 Example of a) Saint Andrews crosses and b) Pombalino building [62]

In the second half of the XIX century, Portugal entered in a recession period. The economic crisis led to a gradual degradation of the "Pambolino" into the "Gaioleiro" buildings. The latter type of building corresponds to a derogatory way of referring to the "Gaiola" wooden structure because people considered them as a poor-quality building suitable for the birds housing, either because the architectural and structural features. Indeed, a considerable number of Gaioleiro buildings fell down during its construction, and for this reason Appleton [50] consider them as a "Constructive disaster".

The process of degradation was mostly due to the use of a weaker wooden structure, the increment of stories up to 5 or 6 floors, the global reduction of the walls' thickness and its gradual reduction along height. In addition, some architectural characteristics as the lack of illumination and ventilation, long corridors and high concentration of artistic details in the front of the buildings are proper of these buildings.

It should be noticed that this kind of constructions were mainly performed in Lisbon and surrounding districts, but not extensively in the northern regions of the country that were not affected by the 1755 earthquake. In the northern regions, URM buildings continued being employed with some variations as the inclusion of either solid or perforated brick units as material for the construction of masonry walls [4]. There is not a specific date for the end of the mixed wood-masonry buildings, however its construction reduced gradually with the advent of concrete as a construction material in the early XX century.

c) Mixed concrete-masonry buildings

In 1894, the first Portland cement factory started to work in Alcântara valley, Portugal. This success is critical in the evolution of the construction techniques because it disseminates the use of concrete. These types of buildings configure the transition of the old masonry buildings to the modern reinforced concrete structures. Indeed, the introduction of reinforced concrete in structural elements is characterized by occurring progressively during the first half of the XX century.

In the beginning, the use of concrete was restricted to the floors under kitchen and bathrooms with the objective of overcome the durability problem of the wood. Therefore, inter-story systems were hybrid slabs of reinforced concrete and timber. Later, the use of reinforced concrete slabs spread to all the interstory system shaping a "Placa" (Slab in English) which is where its name come from. In 1930, the RGCU (acronym for General Regulation of Urban Construction in Portuguese) forced the use of reinforced concrete beams at each floor level in buildings with more than 2 levels. These beams relied on the exterior walls forming a belt around the slab to avoid out-of-plane mechanisms. The transition of old masonry buildings into "Placa" buildings finished in the 40's with the widely use of solid slabs as the inter-storey system and the replacement of stone units by brick and cement blocks.

Concrete used in this period has low to moderate resistance (C20/25 in the best cases). "Placa" buildings have between 4 and 6 stories. The walls built in this period are made of rubble stone or brick masonry, with the exterior walls' thicknesses measuring approximately between 0.40 to 0.70 m and 0.30 to 0.40 m, respectively, while the interior walls are between 0.15 to 0.25 m. In some cases, the walls' thickness decrease with the height [51]. The partition walls called "Tabique" continued being the same as in the mixed wood-masonry period. The beams constructed around the slabs usually have between 0.20 to 0.40 m according to Appleton [50]. The slabs have roughly of 0.07 and 0.10 m thickness and are simply supported on the masonry walls. Concrete slabs used to be reinforced with one layer with steel bars in tension. Alegre [63] suggested that it is not possible to assure the slabs' continuity between spans, thus the slabs do not work as a continuous floor. Instead, they work as a group of panels delimitated by the walls. In relation to the foundations, direct foundations continued being used, but in this period the first isolated reinforced concrete footings appeared (see [46], [59] for more details). In this period, the first flat roof appeared forming terraces, but wood frames continued being used in most buildings.

Concerning to the architectural features, the "Placa" buildings do not present the same level of artistic details as their previous counterparts. It is characterized by modest facades without ornamental details in the border of the windows nor in the doors.

With the gradual introduction reinforced concrete in structural elements, it did not take long for its use in the vertical elements such as stairs and upper floors. Therefore, some "Placa" buildings with

reinforced concrete columns, in special in the facades, can be found. However, these columns do not show appropriate connection with the horizontal diaphragm. Thus, they are not considered as frame buildings. Further descriptions related to mixed RC-masonry buildings can be found in Correia et al. [61] (see Figure 2.6). "Placa" buildings construction decreased considerably around the 60's, when reinforced concrete frame structures emerged [51].

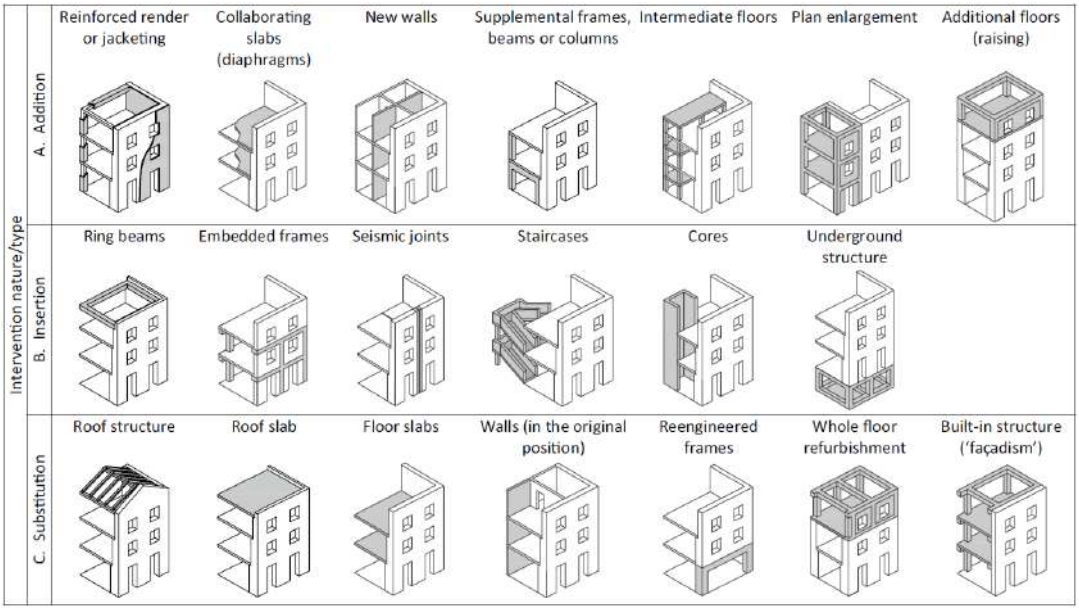

Figure 2.6 Interventions in mixed RC-masonry buildings according to Correia et al. [61]

2.1.3 Uncertainty associated to building-to-building variability

Masonry buildings are known to have a deficient behaviour when affected by seismic events. This behaviour is attributed to some aspects of masonry constructions like its massiveness, the low tensile strength, the poor connexion between elements, lack of maintenance, non-engineered design, and degradation due to weathering. In addition, the vast diversity of masonry assemblies, materials and building configurations leads to a large uncertainty, which has been addressed within the scope of some studies and is explained in this subsection.

One of the main reasons to model the uncertainty regarding geometric features is modelling the building-to-building variability. Silva et al. [64] suggested to interpret building-to-building variability as intra and inter-building variability. Intra-building variability is associated to uncertainties within each specific building like mechanical properties, modelling strategy and analysis method, while inter-building variability is related to differences between single buildings.

Furtado et al. [65] employed 80 architectural drawings to model geometric features of reinforced concrete buildings with infill panels in Portugal. It includes heights, column dimensions and reinforcement details, and slab thickness. Normal and lognormal probability density functions were tested to model the geometric features and chi-square test was used to measure the goodness-of-fit with data. In addition, 1400 infill panels were analysed to identify 13 common arrangements between masonry, windows and doors. Openings sizes were also modelled as random variables. The latter study presents similarities with the research performed by Silva et al. [14] and Bal et al. [33] for RC buildings in Portugal and Turkey, respectively.

Borzi et al. [66] performed a characterisation of masonry buildings made of set of materials like: natural stone, solid and hollow bricks in Italy. Probability density functions were used for sampling buildings and fragility assessment. Data was obtained from the GNDT (National Group for Defence Against Earthquakes, acronym in Italian). Normal, lognormal, and uniform probability density functions were employed to represent the random variables.

Lovon et al. [7] proposed modelling the geometric features of confined masonry buildings in Peru as random variables. Survey data from around 120 drawings was employed to fit geometric features of 1 and 2-storey buildings. Wall density of fully and partially confined walls, wall thickness, height, concrete elements' dimensions, and slab thickness for all storeys were gathered and tested to follow Normal, Lognormal, Gamma and Weibull probability density functions. Goodness-of-fit was measured using Kolmogorov tests. Random variables were employed for fragility assessment considering building-to-building variability within a SDOF simplified modelling framework. A similar work was performed by Sumerente et al. [6] for adobe buildings in the Peruvian Andes.

2.1.4 Definition of mechanical properties

Mechanical properties such as the elasticity modulus, compressive strength and shear strength of masonry walls are fundamental for the seismic vulnerability assessment of this type of constructions. For the sake of order, methods for mechanical properties assessment are organized in this document as non-destructive, in-situ and laboratorial. Focus is given in impactful studies regarding limestone and granite masonry buildings, which are the two most common stones used in Portugal.

Significant differences were found across these studies due to the inherent uncertainty in the material properties of masonry walls. This uncertainty can be attributed to the wide variety of masonry assemblies, founding remarkable differences at unit size distribution, type of mortar, level of tailoring and exposition to the weather (i.e. internal or perimeter wall). Other important source of uncertainty if the type of test, ranging from static, cyclic, or time-history, in-situ, laboratorial, destructive, semi-destructive, non-destructive and others.

In a general perspective it should be said that further experimental research is needed in order to construct a robust database of local URM buildings, but also to store and disseminate this type of data, as performed for other countries (e.g. Augenti et al. [67], Boschi et al. [68], Riahi et al. [69]). This is due to the wide variety of masonry panels and the amplitude of associated mechanical properties taken from different testing techniques.

a) Non-destructive test

Non-destructive test is specially indicated for buildings composing the historical heritage, where engineering interventions are limited. Since these buildings may require maintenance and rehabilitation work, the acquisition of mechanical properties is crucial for its preservation. Cost and handiness are the most important advantages of non-destructive test when acquiring data directly from specific buildings. Precision of non-destructive test has been object of study of many researchers [70]. Focus will be given into two impactful tests nowadays widely used: the sonic test, and operational modal analysis (OMA).

Manning et al. [71] performed direct sonic test in masonry assemblies. This test consists in inducing a pulse into a homogeneous-assumed body, and measuring the velocity of the wave traveling across it. The velocity, and other features of the wave are related to the elasticity modulus of the material and maximum compression resistance of the material. Figure 2.7 illustrates the application of this test. Sonic tests protocols are available in literature like ASTM D2845 [72] and BS 12504-4 [73]. A similar application to sonic tests is GPR, as conducted by Martini et al. [74] for masonry piles in Portugal. This test consists in measuring the wave propagation velocity, attenuation parameters and dielectric constant of the material in order to correlate them with elasticity modulus and strength.

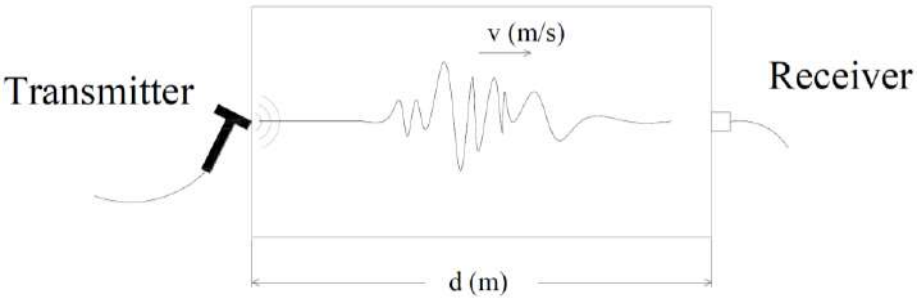

Figure 2.7 Illustration of sonic test [71]

OMA test has been adopted in recent decades as one of the most important non-destructive tests. It consists on measuring vibrations along potential dynamic degrees of freedom of structures, the measure is interpreted in the frequency domain, thus highlighting the natural frequencies of the system due to resonance phenomena. Elasticity modulus can be calibrated to reproduce natural frequencies of masonry structures. It should be noticed that more complex estimations can be performed allowing the identification of modal shapes. Ferreira et al. [75] performed OMA test in masonry buildings in Portugal, and calibrated them with experimental tests as shown in Figure 2.8.

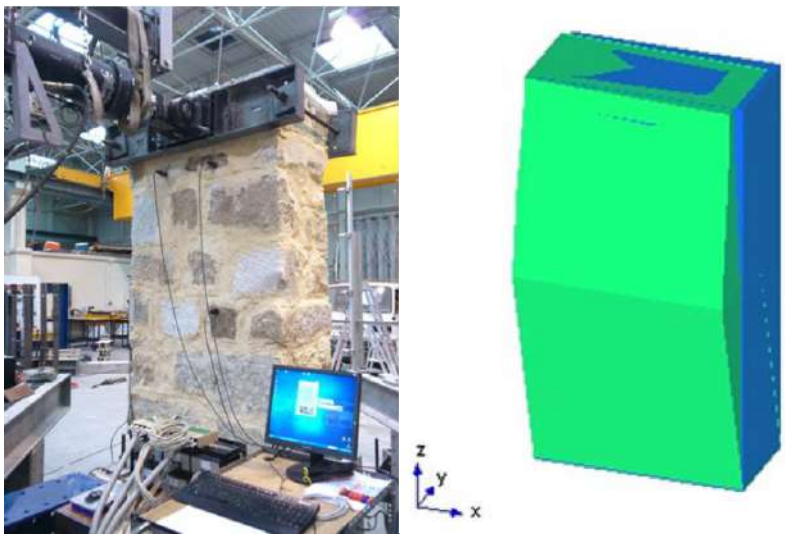

a) b)

Figure 2.8 a) Experimental setup of OMA test on masonry panel, b) out-of-plane modal shape obtained throught OMA test [75]

b) In-situ testing

Obtaining in-situ data from specific buildings is extremely valuable for rehabilitation and retrofitting interventions. This is due to the fact that reproducing a specific type of masonry for laboratory test may lead to biased results since ageing, tailoring level, and mechanical properties in general are not replicated precisely. Thus in-situ tests provide trustable information for specific buildings. Although destructive in-situ tests are available in literature, background will be given in in-situ test with low intrusiveness. Flat-jack test, with different variants, has been largely used for masonry characterisation. In short, the test consists in installing a flat-jack (inflatable device) into a transversal groove inside a wall and apply pressure until the deformation in the wall comes back to its state previous to the perforation. After that, the stress level is measured through pressure gauges connected to the device. Vicente et al. [76] performed flat-jack test in traditional limestone masonry walls in Coimbra, Portugal. Nine tests were performed between exterior and interior walls, stress state, compression strength, and elasticity modulus were calculated per each and compared to laboratory test. One important contribution of this experimental campaign was the employment of single and double flat-jack test for comparison. An important variation of flat-jack test was performed by Simões et al. [59] for old masonry buildings in Lisbon. In brief, it consists in installing additional vertical devices with the objective of producing a plane state stress in the surrounded piece of masonry (see Figure 2.9a), it allows assessing the shear strength which is known to be an important parameter for masonry structures. Flat-jack test protocols are available in literature, such as C1196 – 20 [77] and RILEM TC 177-MDT [78]. It should be noticed, that some non-destructive test can be applied in-situ depending of its handiness. In-situ diagonal compression test has been also performed [79], but is less used that other methods. A scheme of the instrumentation for simple flat jack test is depicted in Figure 2.9b.

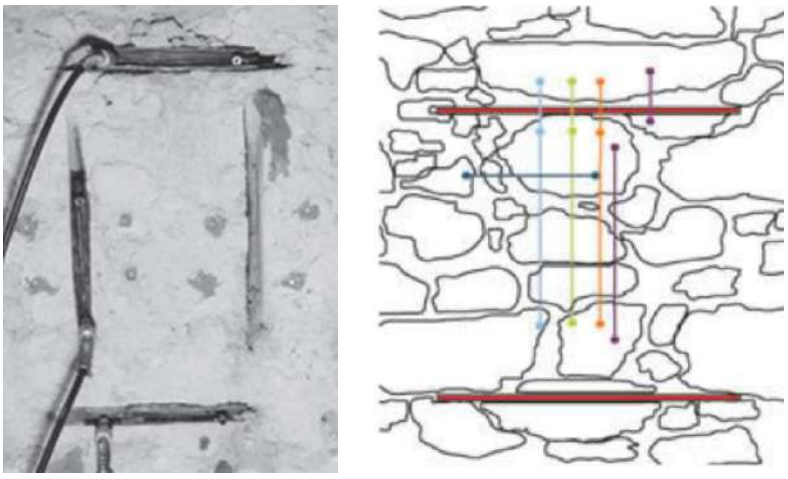

a) b)

Figure 2.9 a) In-situ setup of double direction flat jack test [80], b) schematic intrumentation of simple flat jack test [76]

c) Laboratorial testing

Laboratorial tests allow the investigation of a wide variety of masonry types and loads. It traduces in that it allows the construction of specimens according to our objective research, and test it within the environment we want to reproduce. However, the main limitation of experimental research is the cost that it implies, and the ability to reproduce a specific case of study. Nonetheless, it has been the

main source of data of mechanical properties for structural assessment. Several laboratorial experimental campaigns were conducted in Portugal, herein we selected some innovative and recent research from literature review.

Milosevic et al. [35] tested and modelled limestone masonry panels subjected to diagonal tension. Four specimens, constructed with air lime, and hydraulic mortar were constructed and tested. The main contribution of this study is the assessment of tension and shear strength, since it is well known that these behaviours govern the failure of masonry structures. The analysis of the influence of lime type, and the calibration of fracture mechanical properties using FEM and DEM method was performed as part of this research. An example of specimen subjected to diagonal compression load is shown in Figure 2.10. Protocols for diagonal compression test are available in the literature (e.g. ASTM E519-02 [81])

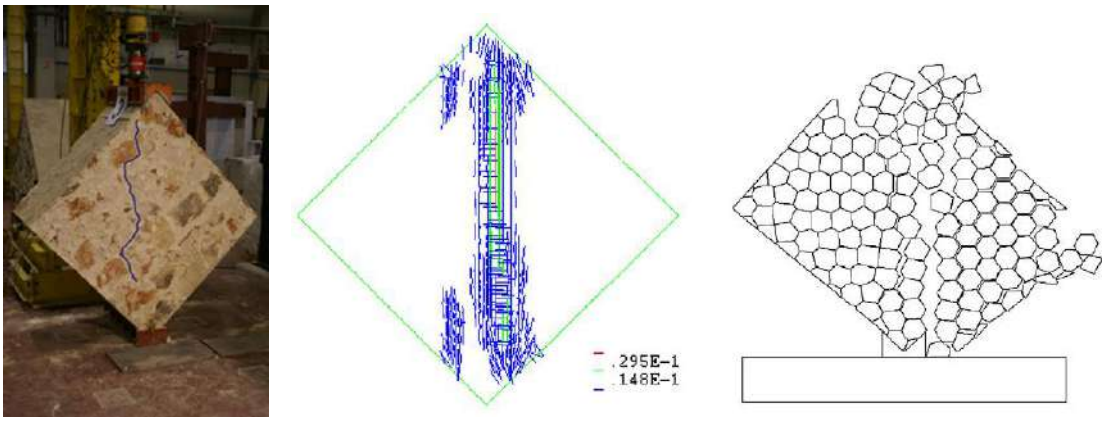

a) b) c)

Figure 2.10 a) Laboratorial setup of diagonal compression test of limestone rubble masonry panel exhibiting crack, b) FEM modelling of diagonal compression test, c) DEM modelling of diagonal compression test [35]

Almeida [82] explored the influence of different levels of tailoring of granite masonry using cyclic compression test in piles, and compression and lateral load in panels. This research defined three levels of tailoring in masonry panels and tested against three levels of load, operational modal analysis was also part of the experimental campaign. Outcomes demonstrates significant variation between mechanical properties (elasticity modulus and compressive strength) according to the regularity of the units and the type of joint (dry or with mortar). The study also provided other parameters like drift capacity, degradation of stiffness, energy dissipation and hysteresis. Retrofitted panels were also tested showing significant increase of mechanical properties. An example of specimen tested to horizontal cyclic load is shown in Figure 2.11. Protocols for compressive testing of masonry prism can be found in [83].

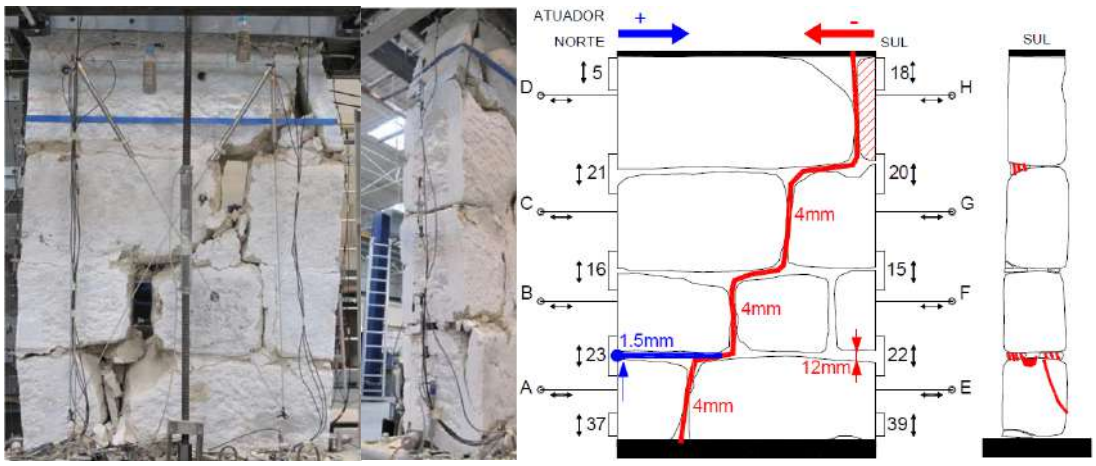

a) b)

Figure 2.11 a) granite masonry panel collapsed after laboratorial test, b) schematic illustration of diagonal crack and instrumentation of granite masonry panel specimen [82]

Vasconcelos [84] conducted an extensive experimental campaign on granite masonry panels. Special attention was paid into the physical and mechanical properties of granites. Compressive and shear behaviour of masonry was explored through non-destructive testing of piles and panels respectively. As an example, Schmidt hammer was used to predict compressive strength, and modulus of elasticity (see Figure 2.12). An important contribution of this work is the correlation of mechanical properties assessed by non-destructive tests and experimental tests, as well as non-destructive indicators and physical properties. Other important aspects of masonry behaviour like energy dissipation and stiffness degradation were also explored.

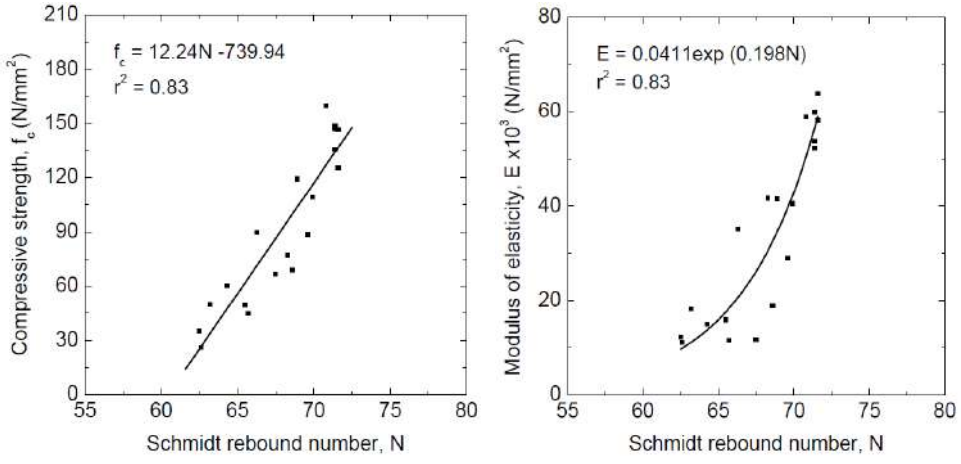

a) b)

Figure 2.12 Correlation between Schmidt rebound number and a) compressive strength, b) modulus of elasticity [84]

The nature of the load (monotonic, cyclic, sinusoidal or time-history) has been demonstrated to have a significant influence in the mechanical characterisation [85]. While the nature of the load becomes more refined, the results tend to belong to a more specific case, thus it may not be possible to generalize the response for other cases. Shaking table test is one of the laboratorial methods with highest reliability, however data from this kind of test is scarce due to limitations on the cost and logistic that it demands. Candeias et al. [38] performed a full-scale granite masonry shaking table test,

conducted at LNEC (National Laboratory of Civil Engineering, in Portuguese). Brick and stone 1-storey masonry buildings were tested until collapse, thus allowing to identify collapse mechanisms.

The vast number of laboratorial tests makes impossible to describe herein all of them, and probably it goes beyond the scope of this text.

2.2 Analytical damage fragility assessment

Fragility functions specifies the probability of a structures suffering certain level of damage as a function of a ground motion intensity measure (IM) [86]. From a statistical viewpoint, fragility functions represent the seismic performance of the overall building class. Ideally, fragility assessment can be obtained from past-events data, however this kind of data is unfrequently gathered after earthquakes. In addition, important events rarely occur in countries with low-to-moderate seismicity, thus fragility assessment based on numerical models provides an effective solution for these cases.

In the fragility assessment procedure there are some aspects and sub procedures that should be defined such as: IM, damage criterion and EDP, numerical modelling and fitting procedure. These will be briefly addressed in this and subsequent sections giving references to key studies. The literature review herein presented will focus on aspects of the analytical fragility assessment, nonetheless there is a large literature available for hybrid or empirical procedures [15].

A fragility estimation requires the definition of an IM and a damage threshold, the former is the domain and represent the level of shaking, while the latter disclosure damage levels through limit values for EDPs. The IM is usually defined by either peak ground acceleration (PGA) or spectral displacement (Sa) at a given period and damping, spectral displacement (Sd) has also been used by some authors [59]. However, with the intention to reduce dispersion, other IMs with higher sufficiency are available, like average Sa [87] and multiple IMs [18] (i.e. a vector of IMs). Some studies devoted to evaluate the efficiency and sufficiency of IMs available in the literature are [88]. EDPs are measures of the structural behaviour obtained from structural analysis. Maximum inter-storey drift, displacement at the top, and maximum base shear are some of the most common EDPs employed for fragility analysis.

2.2.1 Intensity measure

Fragility assessment consists in assigning probabilities of exceedance for each IM, thus IM can be seen as a predictor variable. Analytical fragility assessment procedures use instrumental intensity measures rather than empirical intensity measures (e.g. Mercalli scale). Some aspects desirable of IM definition are: practicality, sufficiency, effectiveness, efficiency and robustness [89].

Practicality refers to the recognition that the IM has some direct correlation to known engineering quantities, and that make sense from an engineering viewpoint. It may be verified through the quantification of the dependence of the structural response with regards to the IM. Sufficiency can be evaluated through statistics analysis of the response for a given set of records. Figure 2.13a and Figure 2.13b show the results obtained by Luco & Cornell [90], who demonstrated the difference between a sufficient IM and an insufficient one. A weak correlation against a strong correlation can be seen in the left and right side respectively. In addition, Figure 2.13c and Figure 2.13d show the analysis of the residuals, no tendency line can be seen in the right side which demonstrate the quality of the predictor, while a clear slope is seen in the left side, less homoscedasticity. Sufficiency also can

be defined on a predictor variable as its capacity do not need of more predictor variables to improve the prediction quality.

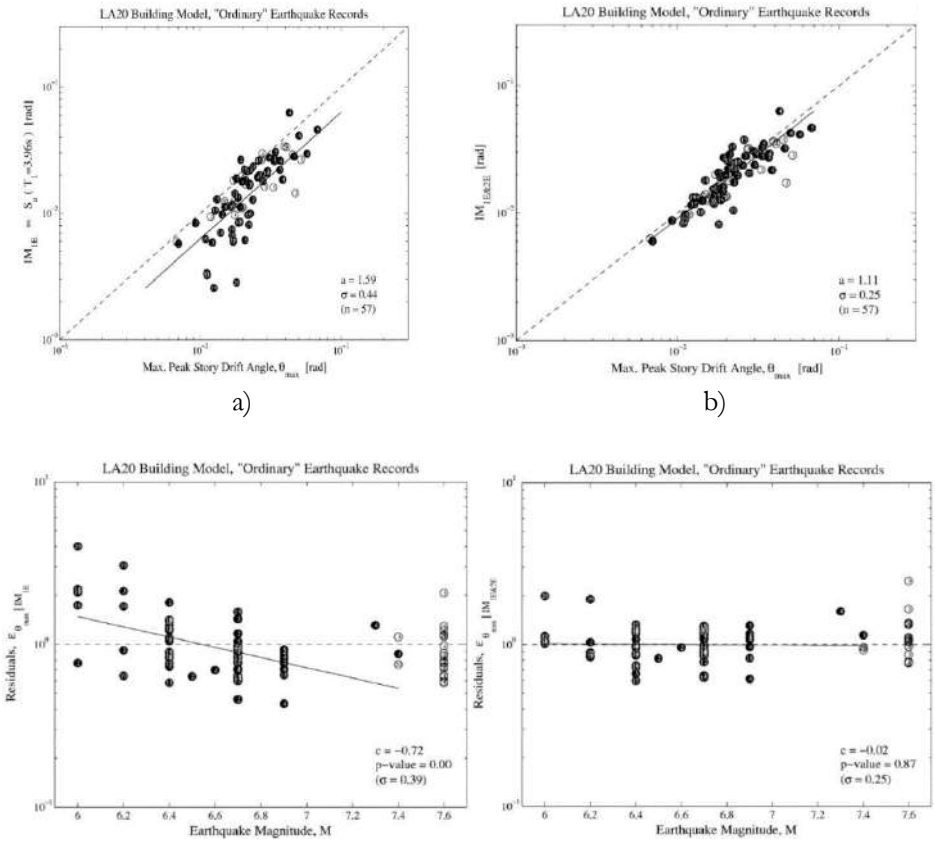

Figure 2.13 a) correlation between IM and EDP exhibiting poor efficiency, b) correlation between IM and EDP exhibiting good efficiency, c) and d) are analysis of residuals for a) and b) examples respectively [89]

The effectiveness of an IM is its ability to assess the mean annual frequency of a given decision variable in a close form [91]. It is different to efficiency, which is a measure of the response precision (i.e. closeness between a set of measures). It can be visualized as the dispersion of the residuals around the model. An efficient IM is supposed to require fewer numerical analyses to achieve a desired level of confidence [90].

Robustness describes the efficiency trends of an IM-EDP pair across different structures [91]. This addresses the issue attempting to identify universally optimum IMs. A good example is the PGA, which perform well for short-period structures, notwithstanding as far as the structure's period increases, the PGA becomes less effective. Conversely, the behaviour of large period structures may show a better correlation with energy-based and long period IMs. For the particular case of period-dependent IMs, the robustness can be evaluated as the gradient of the efficiency across the period, supposed to tend to zero for a highly robust IM (i.e. the period associated to a relative maximum).

Commonly fragility assessment studies use peak ground acceleration (PGA) or spectral displacement (Sa) at a given period and damping (e.g. [6], [7], [14]), peak ground velocity (PGV) and spectral displacement (Sd) has also been used by some authors [59]. However, with the intention to increase

efficiency, other IMs are available, like average Sa [87], Arias intensity [92], and multiple IMs [18] (i.e. a vector of IMs).

2.2.2 Loss, damage criterion and EDP

In most cases, fragility functions aim at assessing physical damage, literature suggests to quantify it either as discrete or continuous damage. Discrete damage approach consists in defining a set of damage states (i.e. levels of deterioration) which usually are sorted gradually. Then, buildings are said to be into a damage state based on a scale, called damage threshold. This criterion assumes that damage degree is uniform within all the building and proposes loss ratios (i.e. ratio between replacement and damaged assets costs) for each damage state. Using the total probability theorem, it is possible to calculated the expected loss ratio as a function of the IM considering the probability of all damage states, this is the vulnerability functions. This approach has been widely used in many studies [5], [7], [33], due to the vast literature available, its handiness and simplicity. Yet, some shortcomings are the impossibility to describe local damage states, and its high dependence on the loss ratios for each damage states. EDPs commonly used within this approach are maximum inter storey drift and displacement at top, they can be defined either as fixed values or as a function of notable points of the pushover curve (i.e. yielding limit, maximum resistance, ultimate strength). This approach is often employed for fragility estimation of building classes. Figure 2.14 shows an example of damage threshold used in [7] to develop fragility functions of confined masonry buildings.

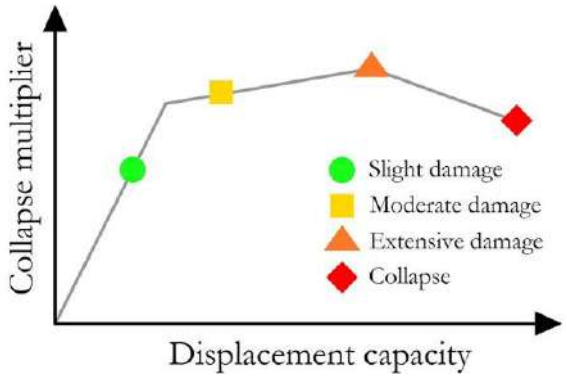

Damage State	Damage Threshold
Slight	$0.7\ \Delta_1$
Moderate	$1.5\ \Delta_1$
Extensive	Δ_2
Collapse	Δ_3

Figure 2.14 Damage threshold depicted in the capacity curve, and damage threshold as function of notable points [7]

Continuous damage approach consists in analysing the damage in each building component, also called component-by-component damage, and calculating the total loss by adding losses of all components. This approach requires fragility functions for each component, and in this case fragility functions for the building are not explicitly calculated, instead vulnerability functions are directly calculated. Common EDPs used in this approach are element drift and maximum inter storey acceleration. The probability of near collapse should be provided in order to define the point in which the buildings losses instability, and loss ratio climbs near to one. This approach is frequently used for single building cases of study. Bias in loss estimation may be lower in this approach, however it requires of a more detailed numerical modelling that predicts EDPs for each component which traduces in a significantly high computational effort. Figure 2.15 shows vulneability functions for building components of for URM developed in [93].

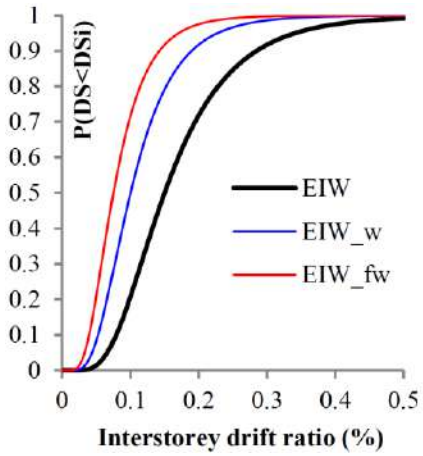

Figure 2.15 Example of component-based vulnerability functions developed in [93]

As previously mentioned the selection of the EDP depends of the approach for loss assessment, nonetheless the efficiency of the EDP for loss prediction is an important factor for its selection. As a clear example of the aforementioned issue is the assessment of non-structural damage. Some past studies suggest to calculate the non-structural damage as a function of the structural damage, using the dame EDP or a percentage of it. However, it is reasonable to think, and has been proved that maximum inter storey acceleration is a better predictor of the non-structural damage. It should be noticed that maximum inter-storey acceleration can only be predicted by non-linear time history analysis, but not by means of non-linear static analysis. Hence, risk modeller should balance the computational and work effort with the need of accuracy in the results. In this sub-section, the relationship between the EDP and the damage quantification, notwithstanding the adopted numerical strategy will depend of the EDP to be predicted. The latter situation is discussed in next sub-section

2.2.3 Numerical modelling strategies for fragility assessment

In the last half century, the community devoted a consistent effort to the computational analysis of masonry structures [94]. Most of the effort was oriented to near-collapse assessment, and current methods for design and analysis of new masonry buildings reached a consistent reliability. However, the numerical analysis of masonry structures is still a challenging task due to its complexity and large uncertainty [94]. Nowadays, a vast number of numerical methods are available in literature and have been implemented in commercial software. Thus, the description of all methods is an unfeasible task, yet some studies devoted effort to the classification of these methods [94], [95]. The herein presented literature review focus in numerical methods which have been applied to fragility and vulnerability assessment.

Fragility assessment requires the analysis of either an archetype structure or a set of buildings, which in both cases will be tested against a set of records. Thus, while searching for the balance between computational effort and accuracy, the level of refinement of the numerical modelling is bounded in its upper limit by the computational effort, and in its lower limit by both the EDP and precision needed. Literature [16], [96] agree in classifying these methods into three types, according to the complexity of the representation: a) multi-degree-of-freedom, b) reduced multi-degree-of-freedom, and c) equivalent single-degree-of-freedom.

a) Multi-degree-of-freedom models

A multi-degree-of-freedom (MDOF) model consist on a detailed three- or two-dimensional [18], [53], [59], [97], [98] model where each structural element is represented individually. Thus, component-by-component loss assessment is possible within this approach. It includes the assessment of damage, loss and downtime within any given framework available in literature [21]. Following this approach, it is possible to make a complete representation of the configuration of the building in plane and height, which permits the analysis of some aspects of earthquake engineering such as torsional effects and analysis of irregularities. Also, within this approach non-structural damage based on inter storey acceleration can be calculated if non-linear time-history is performed.

Simoes [59] performed fragility assessment of URM buildings constructed in the transition between the 19th and 20th centuries in Lisbon. The numerical modelling adopted in the aforementioned study consists in a equivalent column representation, and was performed in the TREMURI [99] software. A set of archetypes were selected, and subjected to non-linear static analysis under uniform and triangular load shapes. One important contribution of this work is the analysis of uncertainties regarding side walls solution, side walls materials, main internal walls materials and partition walls material within a logic tree framework. Additionally, local mechanisms were analysed. Figure 2.16a shows a single element and its degrees of freedom, and Figure 2.16b depicts a representation of a masonry building in TREMURI software.

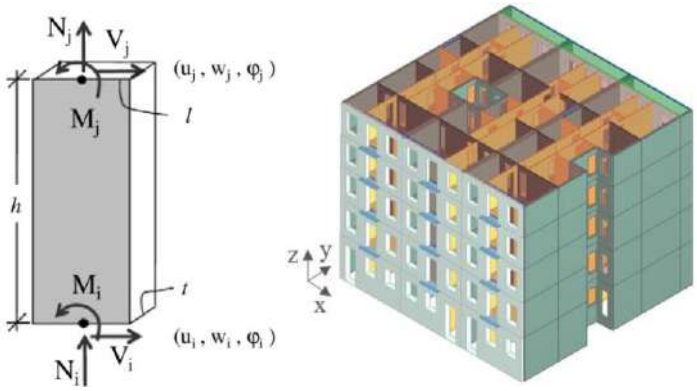

a) b)

Figure 2.16 a) Frame element, and its degrees of freedom, b) masonry building analysed in TREMURI software [59], [99]

Battaglia et al. [100] conducted fragility assessment of masonry aggregates. Uncertainties regarding the number of floors, inter storey height, slab material, and walls materials were analysed by using a logic-tree approach. The numerical strategy consisted in the equivalent column approach implemented in TREMURI software, nonlinear static analysis was performed in both directions and the capacity spectrum method was used to calculate the response of each building against a set of 50 records. Figure 2.17 shows a representation of a masonry aggregate in TREMURI software.

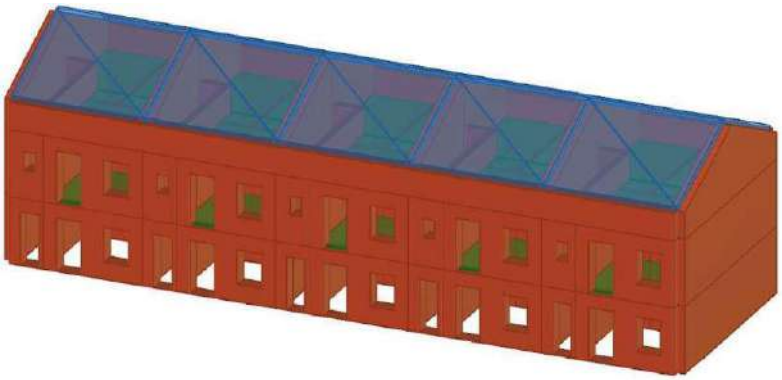

Figure 2.17 Masonry aggregate modelled in TREMURI software [100]

Karbassi & Lestuzzi [101] employed the Applied Element Method for fragility assessment of brick masonry buildings in France. Buildings were tested against 50 records up to the collapse using Extreme Loading for Structures [102] software, Figure 2.18 shows an example of building collapse exhibiting a soft storey mechanism.

Figure 2.18 Masonry building exhibiting soft storey collapse mechanism, modelled in Extreme Loading for Structures [102] software

Other approaches devoted to the collapse modelling of masonry buildings are the erosion and contact surface methods [32], [103]. Erosion technique consist in the deletion of certain elements from the mesh, after a significant number of elements enable the mesh separation collapse is produced. In the other side, contact surface technique consists in joining a set of blocks using cohesive elements, those elements are deleted under a given criteria and blocks are released thus representing the building collapse. Figure 2.19 illustrates examples of the collapse modelling employing the contact surface method. Further research was made for calibration with experimental tests [104].

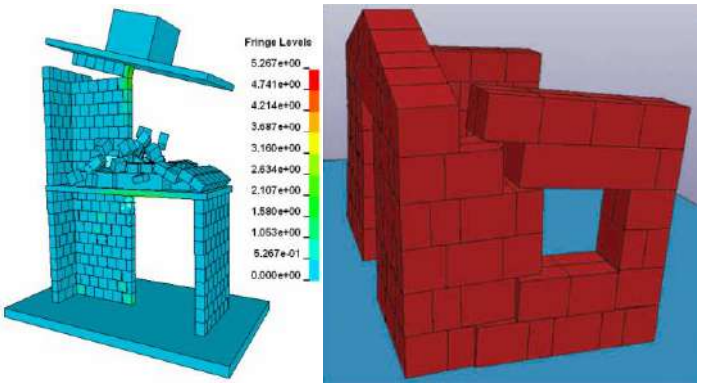

a) b)

Figure 2.19 Brick masonry assembly modelled and calibrated with shaking table test [103], b) stone masonry assembly modelled and calibrated with shaking table test [32]

b) Reduced multi-degree-of-freedom models

Despite the large versatility of MDOF models, they result computationally expensive so they can be reduced to two-dimensional representations. This latter simplification is acceptable for buildings with regular distribution of its structural elements, where the torsional effect does not play an important role in the overall response. In the reduced multi-degree-of-freedom each storey is represented by an equivalent vertical frame that may include translational and rotational degrees of freedom, inter storeys are represented as lumped masses, equivalent hysteretic and damping properties are also assigned. Determining the above-mentioned equivalent properties of the elements is a challenging task that may require high level of expertise by the user. Damage can be assessed at each storey and it is possible to represent the distributed and concentrated failure mechanism. This kind of model is suitable for building typologies in which the torsional effect does not affect significantly its behaviour, and buildings with rigid diaphragms without significant irregularities. It should be noticed that a homogeneous behaviour between elements of the same storey is assumed, and local mechanisms can only be analysed separately

Silva et al. [14] performed reduced MDOF representation of RC buildings in Portugal for fragility assessment. Figure 2.20 illustrates the representation of the numerical modelling performed in OpenSees [105]. The main contribution of this work relies in the comparison between vulnerability assessment methodologies, hence a large set of load shapes and performance assessment methods were evaluated and compared at vulnerability and risk level.

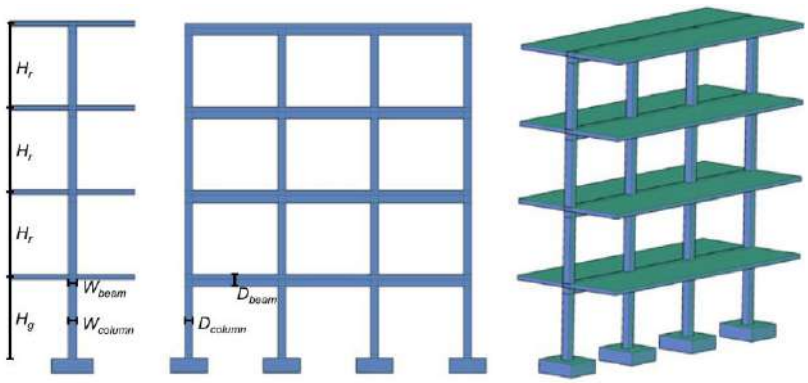

Figure 2.20 Reduced MDOF representation of RC framework employed for fragility analysis [14]

c) Single-degree-of-freedom models

Single-degree-of-freedom (SDOF) models are by far the most used approach for fragility assessment. This is due to the low computational effort they require, and its handiness to calibrate and represent a wide variety of structures. A single-degree-of-freedom model consist on representing the building through an inverted pendulum, hysteretic and damping properties are assigned to the model. This is the simplest way to represent a building behaviour, and allow a large number of analysis, which becomes this model suitable for reliability analysis. The main cons of the single-degree-of-freedom model is the limited information that it can provide from the building. The damage can only be assessed at global building level (i.e. discrete damage), irregularities and torsional effects cannot be considered directly in the analysis.

Borzi et al. [66] proposed to perform simplified pushover analysis into equivalent SDOF systems for stone and brick masonry buildings in Italy. The method consists in calculating a pushover curve by means of the maximum load capacity and the displacement capacity under a set of hypotheses. Soft-storey mechanism is assumed to be prevalent in masonry buildings, and discrete damage threshold is implemented as fixed drift values. Demand is represented by a uniform hazard spectrum and performance is calculated using the capacity spectrum method. Later, Silva et al. [106] updated the methodology to include partially the record-to-record variability, leading less conservative results. Figure 2.21 illustrates the representation of a building as a SDOF employed in the aforementioned study.

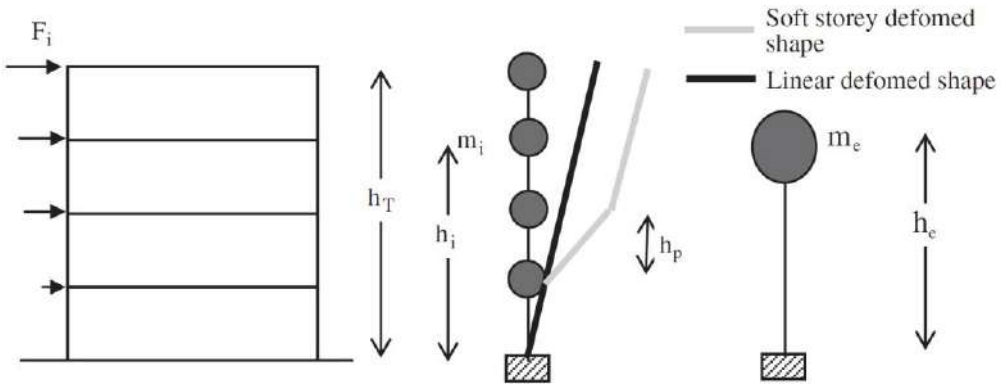

Figure 2.21 Illustration of load shape, soft storey mechanism, and transformation of MDOF into SDOF system in [66]

Lovon et al. [7] used a similar framework applied to confined masonry buildings, this time including the calibration of the displacement capacity with laboratory test of confined masonry panels at full scale and including a damage threshold as a function of the notable points of the capacity curve. Formal and informal buildings were evaluated propagating the uncertainty in geometric and material properties.

Recently, Crowley et al. [18] employed SDOF models including a spring in the base with the purpose to model the soil-structure interaction. An illustration of this model is shown in Figure 2.22 used in the fragility assessment of brick masonry buildings in the Netherlands.

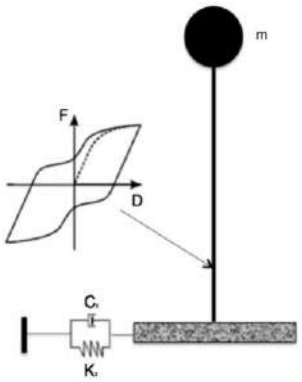

Figure 2.22 SDOF system linked to rheological law for soil-structure analysis [18]

Vast literature has been developed around this approach like: adobe buildings in Peru [97], adobe and brick masonry buildings in Pakistan [107], the building stock in South America [5], and so on. Local mechanisms cannot be evaluated through this approach; however, some studies have addressed this issue attempting to merge both in-plane and out-of-plane collapse mechanisms within a single statistical framework [6].

2.2.4 Procedures for fragility functions development

The development of analytical fragility functions requires the analysis of either an archetype building or a set of buildings subjected to a set of records, after data is fitted to a cumulative density function. Depending upon the procedure in which structural analysis data was obtained, some procedures are further explained. The literature review was made with basis in some studies which addressed this issue [86], [108], [109]. Description about procedures will be given for collapse building, however fragility functions for other damage states can be achieved using the same procedure.

a) Incremental Dynamic Analysis (IDA)

This procedure consists in performing subsequent structural analysis for each record increasing its intensity gradually, the procedure is followed until collapse. Across the procedure, the cumulative probability of collapse given an IM is calculated as the fraction between the number of records that produce collapse at the aforementioned IM. Figure 2.23a illustrates the outcomes of successful structural analysis and Figure 2.23b shows associated the empirical cumulative density functions.

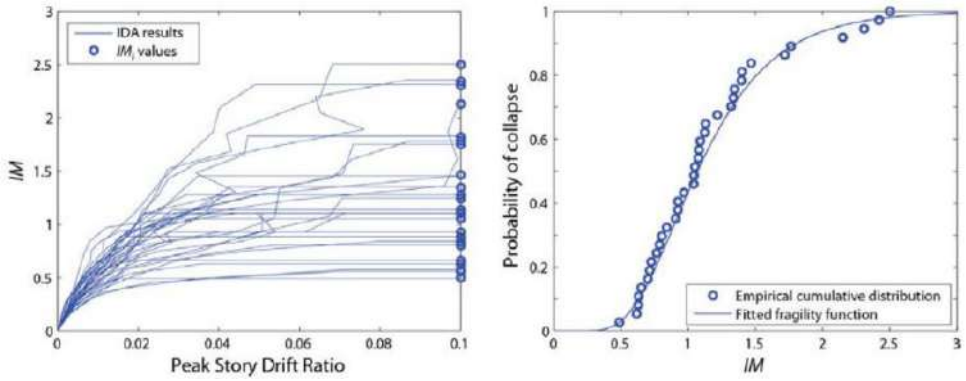

a) b)

Figure 2.23 a) EDP-IM relationships per each record, b) Collapse fragility function obtained through IDA analysis [86]

Frequently, pairs of IM_i and probability of collapse are fitted to a lognormal probability density function through method of moments as shown in Eq. 2.1 and Eq. 2.2:

$$\ln(\theta) = \frac{1}{n}\sum_{i=1}^{n}\ln\left(IM_i\right) \quad \text{Eq. 2.1}$$

$$\beta = \sqrt{\frac{1}{n-1}\sum_{i=1}^{n}\left(\ln\left(\frac{IM_i}{\theta}\right)\right)^2} \quad \text{Eq. 2.2}$$

where θ and β are estimates of the logarithmic mean and standard deviation respectively. Moment methods is traditionally used in IDA since all IM_i at collapse are known. The method was also called as "Method A" by Porter et al. [110], frequently 10 to 20 records are usually enough to provide sufficient accuracy in the estimation of seismic demands when using a relatively efficient IM. Selected IM should meet some requirements, like the possibility to be linearly increased, and not saturating for high values. Further guidelines regarding the selection of IM, records, archetypes, and others can be found in [111]. The main con of IDA method is its high computational cost, and the uncertainty introduced when records are scaled.

b) Truncated Incremental Dynamic Analysis

As discussed by Baker [86] high IM levels are of less interest than low IM levels, thus continue scaling the records after a certain point becomes unnecessary in introduce uncertainty in the fragility assessment. In that cases Truncated IDA can be performed, it consists in defining a maximum IM_{max} as the limit for scaling a given record. Thus, data above this IM is not given, Figure 2.24 illustrates the outcomes of scaling, and cumulative probability of collapse calculated through Truncated IDA.

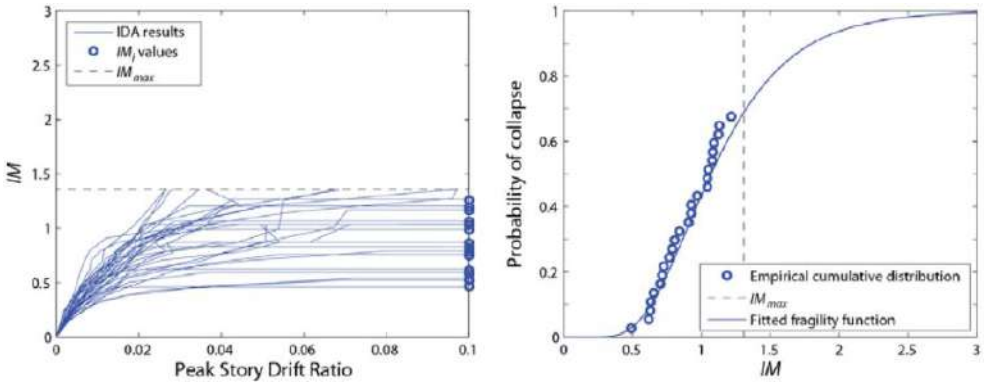

a) b)

Figure 2.24 a) EDP-IM relationships per each record, b) Collapse fragility function obtained through truncated IDA analysis [86]

Since not all IMs are known for each record, the moment of methods cannot be further employed because data is not balanced. Instead, censored maximum likelihood estimation is performed to deal with not observable data, whose likelihood function is shown in Eq. 2.3:

$$Likelihood = \left(\prod_{i=1}^{m} \Phi \left(\frac{\ln\left(IM_i / \theta \right)}{\beta} \right) \right) \left(1 - \Phi \left(\frac{\ln\left(IM_{\max} / \theta \right)}{\beta} \right) \right)^{n-m} \quad \text{Eq. 2.3}$$

where ϕ and Φ are the normal standard probability density function, and cumulative density function respectively, θ and β are the target parameters to be obtained by means of optimizing the Likelihood functions, n is the total number of records, and m is the number of records which leads to collapse. It should be noticed that the likelihood function herein presented is applicable when representing fragility function as a lognormal cumulative function, and can be adapted for alternative probability density functions accordingly.

c) Multiple Stripes Analysis (MSA)

This procedure consists in performing the structural analysis for a set of discrete IM levels rather than increasing the IM up to collapse. [112] suggest to employ a different set of records for each IM of interest. Thus, the modeller may not observe a strict increase of the collapse probability across IMs, but the true probability of collapse is supposed to increase as IM increase. Figure 2.25 illustrates the outcomes of structural analysis and fitting procedure.

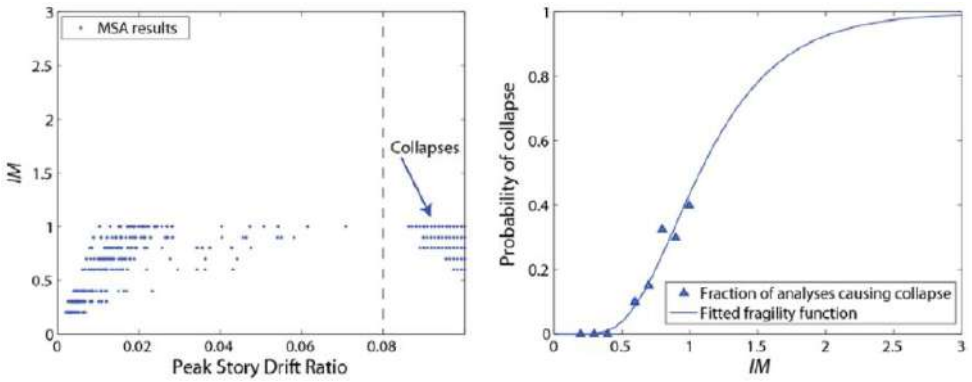

a) b)

Figure 2.25 a) EDP-IM relationships per each record, b) Collapse fragility function obtained through MSA analysis [86]

For a given IM of interest, the number of collapses is assumed to follow a Binomial distribution, hence the probability of having z collapses for n records are given by Eq. 2.4:

$$P(z \text{ collapses in n records}) = \binom{n}{z} p^z (1-p)^{n-z} \quad \text{Eq. 2.4}$$

where p is the probability of a ground motion leading the structure to collapse. The latter can be replaced by a lognormal cumulative density function into a likelihood estimation framework, as is shown in Eq. 2.5:

$$Likelihood = \prod_{j=1}^{m} \binom{n_j}{z_j} \Phi\left(\frac{\ln\left(x_j/\theta\right)}{\beta}\right) \left(1-\Phi\left(\frac{\ln\left(x_j/\theta\right)}{\beta}\right)\right)^{n_j - z_j} \quad \text{Eq. 2.5}$$

the parameters β and θ are obtained by optimizing the Likelihood function. It should be noticed that the formulation does not require multiple observations for a given IM, thus being useful when using unscaled records. In addition, it is recommended to use the records only once, since it is assumed the independence in the likelihood at each intensity.

d) Cloud Analysis

Cloud Analysis is probably the fragility assessment method with higher effectiveness. This is due to its handiness be included in the risk assessment in a closed form. The procedure has its background in a generalized bi-dimensional linear regression between IM and EDP performed in the logarithmic space. The method has been largely explained and tested in [108], where a closed form is proposed. Frequently, the parameters of the linear regression are estimated either through least squares or maximum likelihood regression assuming normal disturbance around the mean as shown in Eq. 2.6:

$$y = a + b \cdot x + \varepsilon \quad \text{Eq. 2.6}$$

where x and y are the logs of IM and EDP respectively, p_1 and p_2 are the parameters of the linear regression, and ϵ is the disturbance, assumed to follow a normal distribution with mean equal to zero, and constant standard deviation (homoscedasticity).

Incremental Dynamic Analysis and Multiple-stipe Analysis are procedures widely used in literature, however in some cases they require a large computational effort the fact of performing subsequent analysis with scaled records. Cloud analysis has been progressively employed in recent structural fragility studies due to the low computational effort it requires, and its capability to model broad types of uncertainties such as record-to-record, mechanical material properties and component capacity [108], [113], [114].

Eq. 2.6 can be reshaped in terms of IM and EDP, as is shown in Eq. 2.7 and Eq. 2.8:

$$E\left[\log\left(EDP\right)\middle|IM\right] = a + b \cdot \log\left(IM\right) \quad \text{Eq. 2.7}$$

$$\sigma = \sqrt{\frac{\sum_{i=1}^{n}\left(\log\left(EDP_i\right) - E\left[\log\left(EDP\right)\middle|IM\right]\right)^2}{n-2}} \quad \text{Eq. 2.8}$$

Where $\mathrm{E}[\log(EDP|IM)]$ stands for the expected logarithm of EDP given an IM, a and b are the regression parameters, σ is the logarithmic standard deviation for the expected EDP given the IM, EDP_i corresponds to the i-EDP value obtained from the non-linear analysis. After the linear generalized model was calculated, fragility functions can be assessed by following the procedure depicted in Figure 2.26.

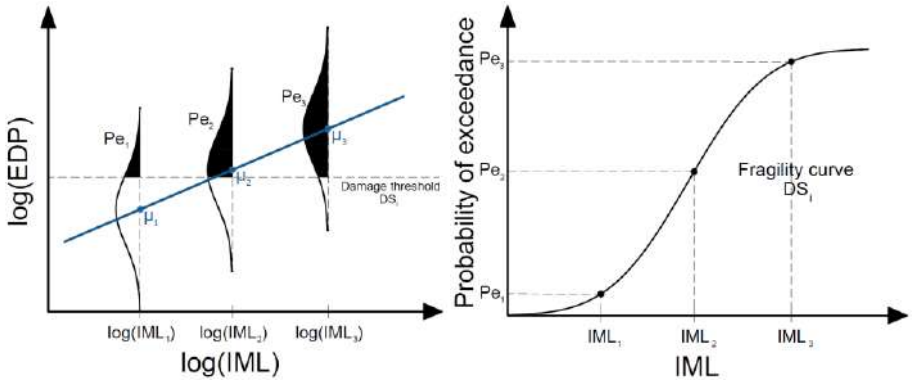

Figure 2.26 Probability of exceedance in a) linear best fit, b) fragility function (Adapted from [115])

Figure 2.26a shows the best fit in the log space represented by the blue line. Three IMLs are shown with its corresponding expected values μ, assumed to be the mean of the normal functions around them with a constant standard deviation. Probabilities of exceedance Pe are calculated as the shaded area above the damage threshold for each IMLs, after that these probabilities are plotted with its corresponding IMLs as shown in Figure 2.26b. Hence, the fragility function is given by Eq. 2.9:

$$P\left[EDP \geq ds_i \middle| IM\right] = 1 - \Phi\left(\frac{\log\left(EDP_{dsi} - E\left[\log\left(EDP \middle| IM\right)\right]\right)}{\sigma}\right) \qquad \text{Eq. 2.9}$$

Where EDP_{ds_i} is the EDP damage threshold, and σ represent the total variability. The aforementioned uncertainty can be easily updated to include any class of uncertainty, for example [115] propose to calculate the total variability as a combination of building-to-building and record to record variability, as shown in Eq. 2.10:

$$\sigma_{total} = \sqrt{\sigma_{btb}^2 + \sigma_{rtr}^2} \qquad \text{Eq. 2.10}$$

e) Other approaches

Previously showed approaches are the most formalized, and for which the largest guidelines can be find in literature. However, there are several studies successfully applied to the field of fragility assessment, which will be briefly addressed herein.

[14] propose to employ least squares regression to fit empirical cumulative probabilities to cumulative lognormal functions. Several studies were carried out following this procedure [6], [7], [14], [33], leading to good results. The procedure has been progressively improved, and [106] proposed a procedure that is capable consider the building-to-building variability. Martins & Silva [116] employed this approach to model the building-to-building and record-to-record variability.

Multi-dimensional generalized linear models are also available in literature [18] for fragility assessment. This procedure may improve the prediction of EDP by using an IM vector. Similar work has been conducted using generalized additive models.

Gaussian kernel-smoothing is a non-parametric regression method that is especially useful to model erratic behaviour od dependent variables, there are some attempts [109] that carried out fragility assessment using this approach. However, bias in the extremes of the fragility function is a common issue of this method. In recent years, Machine Learning approaches have also take place in the fragility modelling field, further information can be found in [117].

2.3 Fatality vulnerability assessment

Human casualty estimation is one of the most challenging tasks of the risk assessment. Those have demonstrated to be governed by a large uncertainty from event to event. Some of the main sources of casualties are the building collapse, machinery accidents, heart attacks and subsequent hazards derived from the main shock such as landslides, mudflows, and fires. Figure 2.27 roughly depicts the sources of human casualties in seismic events, data was gathered by Coburn & Spence [23]. As is depicted in Figure 2.27 most of deaths are produced by collapse of masonry buildings (around 75 %).

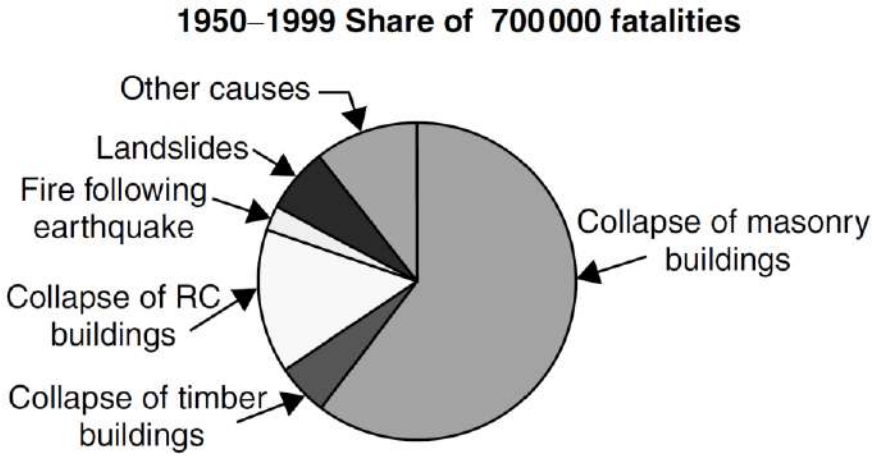

Figure 2.27 Distribution of deaths in earthquakes between 1950-1999 according to its cause [23]

Traditional approaches for human casualty estimation consist in assigning lethality ratios to each building class in order to normalize the fatality rates to each building class' performance, similar to physical damage assessment. Coburn & Spence [23] found that lethality ratio also depends on the collapse mechanism, occupancy levels, ground motion peculiarities, occupant behaviour and recue effectiveness. In recent decades, physical damage-based fatality assessment procedures were implemented, such as described in [26], [27], the latter are based in the assumption of strong correlation between building damage and the number of casualties. Nonetheless, field data-based studies [22] suggest that casualties may vary significantly in buildings which suffered extreme damage depending of the level of collapse [118]. To overcome this issue, some studies [119] have explored the correlation between different EDPs and number-severity of casualties in post-earthquake data. Further description of methods addressing fatality assessment will be reviewed in next subsections, the review focus in consequence functions developed thus other important topics like occupancy and dynamic population are not addressed.

2.3.1 Empirical fatality vulnerability assessment

Procedures based in post-earthquake field data are herein addressed. This kind of data are scarce, since governments efforts focus in rescue, and care for affected people instead of post-earthquake

data gathering. Empirical assessment procedures were proposed either using earthquake magnitude of seismic intensity.

Samardjieva & Badal [120] employed worldwide data during the 20th century until 1999 to perform regression to predict human losses starting from earthquake magnitude and population density. As is shown in Eq. 2.11:

$$\log(N_k)(D) = a(D) + b(D)M \qquad \text{Eq. 2.11}$$

where N_k is the number of victims, D is the population density, M is the earthquake magnitude (in moment magnitude), a and b are the regression parameters. Figure 2.28 shows the data and regression equations developed in the aforementioned work, together with regression and correlation coefficients.

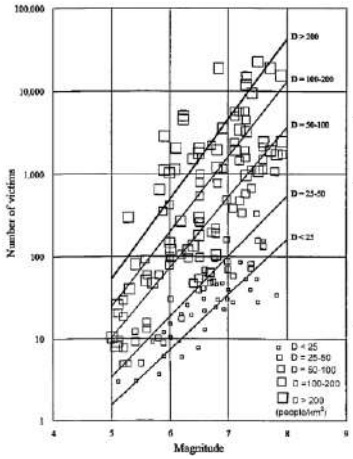

a)

Population Density (people/km²)	1900–1950				1951–1999			
	a	*b*	*r*	*σ*	*a*	*b*	*r*	*σ*
$D < 25$	−3.41	0.66	0.88	0.341	−3.11	0.67	0.84	0.343
$D = 25–50$	−3.00	0.71	0.90	0.295	−3.32	0.75	0.85	0.342
$D = 50–100$	−2.60	0.75	0.92	0.295	−3.13	0.84	0.82	0.345
$D = 100–200$	−2.17	0.77	0.92	0.292	−3.22	0.92	0.70	0.397
$D > 200$	−2.09	0.86	0.83	0.344	−3.15	0.97	0.75	0.348

b)

Figure 2.28 a) correlations between number of victims and magnitude, b) parameters for Eq. 2.11 according to population density [120]

Earthquake scenarios were also developed in the above-mentioned approach in Spain and Japan at regional level. Some of the cons of this approach are the large uncertainty, incompatibility with instrumental IMs, impossibility for specific building assessment, and so on. In addition, the method does not disclosure outcomes for different building classes, nor regions with different seismicity. Also, the evolution of the exposure cannot be explicitly taking into account, whereas data is reported after significant span of time for which exposure is different.

Jaiswal et al. [121], within the USGS Prompt Assessment of Global Earthquakes for Response (PAGER) research program, propose empirical fatality vulnerability functions for each country with basis on observations of a large data set. The USGS ShakeMap is used for automatic generation of Mercalli macro-seismic intensity (MMI) scale. Fatality vulnerability functions are fitted to the form shown in Eq. 2.12:

$$\nu(S) = \Phi\left[\frac{1}{\beta}\log\left(\frac{S}{\theta}\right)\right] \qquad \text{Eq. 2.12}$$

where Φ is the standard lognormal cumulative density function, S is the Mercalli macro-seismic intensity (MMI), θ is the logarithmic mean, and β is the logarithmic standard deviation. The uncertainty associated to the fatality ratio is assumed to follow a beta distribution. Despite the significant contribution of this study, some issues remain such as the disclosure between building classes, the analysis of the effect of recue quality, and the analysis of specific building cases.

2.3.2 Physical damage-based fatality vulnerability assessment

Some studies propose to assess fatalities with basis on the structural seismic performance of the buildings [26], [27], represented by the physical damage. In general, the procedures consist in performing a convolution between physical damage fragility functions and loss ratios corresponding to each damage state. Hence, the outcomes are highly dependent of these parameters and some studies devoted effort to establish fatality ratios for specific countries or building stocks.

HAZUS [27] provides a wide framework for many kinds of losses, fatality assessment is not an exception. Figure 2.29 shows the logic tree approach proposed in the above-mentioned study, it consist in four fatality ratios for each damage state. Additionally, the probability of collapse given that a building achieves damage state four should be computed, and a specific fatality ratio is assigned for this context, finally, the probability of being killed is calculated as shown in Eq. 2.13. HAZUS [27] provides all parameters used in this approach, however the main con of the aforementioned procedure is the limited applicability of such parameters inside the United States, and similar building stocks. However, this approach has been widely used in many studies such as [13], [122]. Despite the great contribution that HAZUS is for the earthquake fatality assessment, it should be noticed that rates provided by HAZUS were calibrated with basis in frequent earthquakes, hence underestimating human losses for high magnitude events.

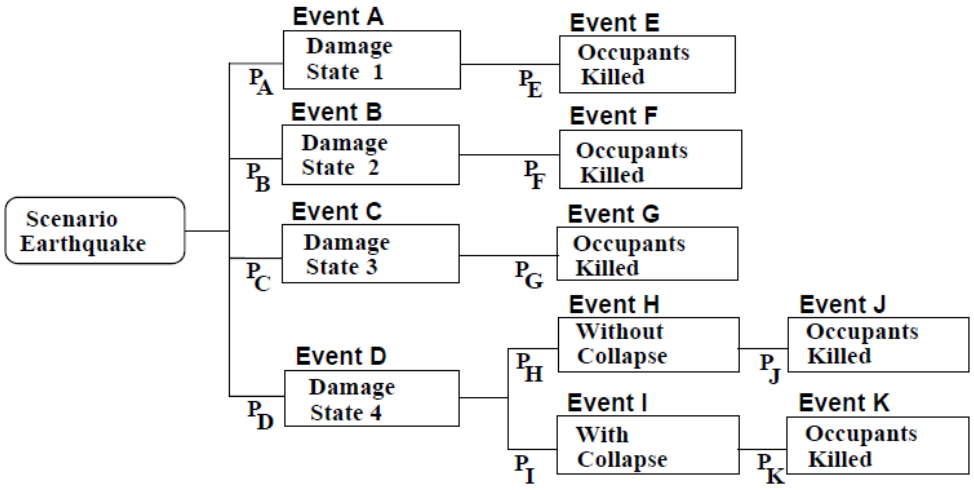

Figure 2.29 Logic three proposed in [27] for fatalities assessment

$$P_{killed} = P_{killed|collapse} + P_{killed|no-collapse} \qquad \text{Eq. 2.13}$$

Spence [26] studied post-earthquake field data in Europe, established an injury classification and developed fatality ratios either for fatalities and injuries levels. The factors indicate the probability of being killed given that the building achieves damage state 4. Table 2-1 shows the injury distributions for specific building types. This study was carried at regional level for Europe, this is not sensible to

local variations of building classes. Some contributions of the study are the development of earthquake scenarios for three cities in Europe, and a framework for the treatment of uncertainties.

Table 2-1 Casualty factors for masonry buildings in Europe, adapted from Spence [26]

Number of storeys	Damage State D5					
	IU	I1	I2	I3	I4	I5
1	23.6	50.0	12.0	8.0	0.4	6.0
1-3	16.5	50.0	15.0	10.0	0.5	8.0
≥4	9.4	50.0	18.0	12.0	0.6	10.0

2.3.3 Extend of collapse-based fatality vulnerability assessment

Despite the handiness of all physical damage-based fatality assessment procedures, the correlation between damage and fatalities is still questionable for some building classes. Thus, some studies attempted to find predictors with higher efficiency, which traduces into new predictors EDPs. Most of the new EDPs are focused in the quantification of the extend of collapse, depicted in Figure 2.30. Coburn & Spence [23], emphasises the variation of the collapse extend in buildings that were classified as having the same damage extend. This variation may imply a different fatality ratio, which cannot be perceived in traditional physical damage states.

a) b) c)

Figure 2.30 Illustration of building with extreme damage level, exposing different level of collapse a) 10, b) 50, and c) 100 % [123]

Iida et al. [28] proposed to employ a vector of predictors for fatality assessment. The four variables employed are the plan loss, the section loss, the volume loss and the amount of dust. All of them characterize the extend of the collapse, the mentioned approach is performed with basis on post-earthquake survey data of timber buildings during the Noto Hanto and Niigataken earthquakes, which took place in Japan in 2007. Figure 2.31 shows the predictors parameters defined by Iida et al. [28] together with possible types of injuries. The multivariate prediction of fatalities, as well as the identification of potential injuries types are the most important contributions of this work.

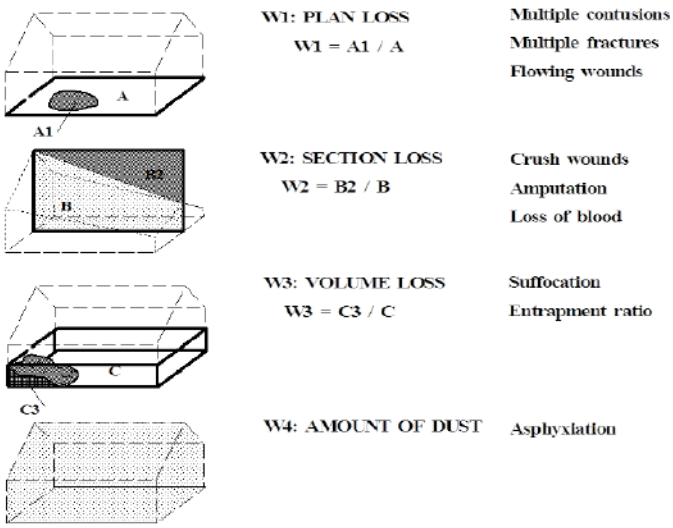

Figure 2.31 EDPs fatality predictors proposed by Iida et al. [28]

Abeling & Ingham [118] performed fatality assessment based in volume loss for masonry buildings in New Zealand after Mw 7.1 Darfield and Mw 6.2 Christchurch earthquakes. This predictor parameter was previously employed by Okada [123], for fatality prediction of fatalities of masonry buildings in Japan. Data of around 600 buildings was gathered, and a correlation between volume loss and fatality ratio was proposed as is shown in Figure 2.32. Volume loss damage states were proposed for different levels of collapse, and they were assigned fatality ratios. The study also provides earthquake scenarios for brick masonry buildings in New Zealand. The volume loss to fatality ratio relationship is maybe the most important contribution of this study, which has been implemented in further studies for fatality loss assessment.

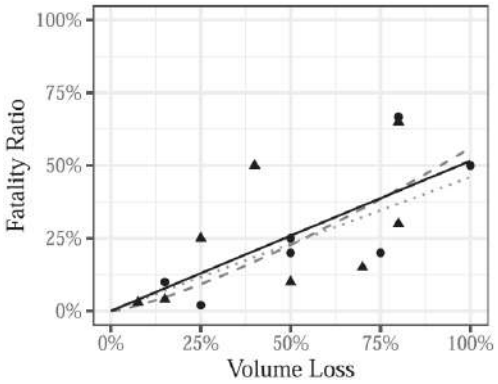

Figure 2.32 Volume loss – fatality ratio relationship proposed in [118]

Crowley et al. [18] applied advanced numerical modelling based implemented in Ls-Dyna software [30] to assess the level of collapse of masonry buildings in Netherlands. The EDP herein employed for fatality prediction is the ratio between the are covered by debris and the area of the building. This approach was complemented with Coburn and Spence [23] fatality assessment parameters addressing type of material and effectiveness of rescue activities. The numerical approach herein implemented consist in the deletion of elements when they achieve some given criteria, an example of collapse mechanism is shown in Figure 2.33. The personnel fatality vulnerability is calculated as shown in Eq. 2.14

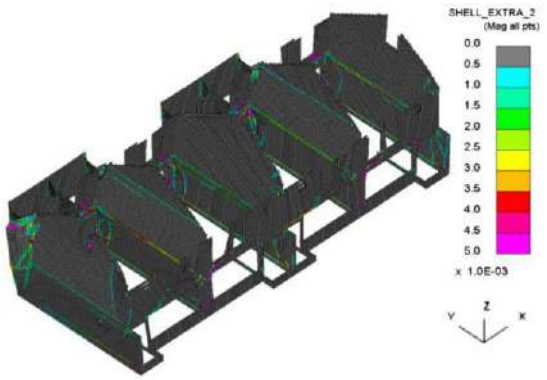

Figure 2.33 URM collapse mechanism calculated in [18]

$$P_{d\_inside|collapse} = \frac{A_{debris}}{A_{floor}}\left[M4 + M5(1 - M4)\right] \qquad \text{Eq. 2.14}$$

Where $P_{d\_inside|collapse}$ is the probability of a random person dying inside a building giving that the building collapse, A_{debris} is the area that the debris cover, A_{floor} is the area of the floor, $M4$ is the probability of dying immediately given that a person is trapped, $M5$ is the probability of surviving trapped occupant to die subsequently to the rescue.

2.4 Retrofitting techniques for masonry buildings

Several retrofitting techniques have been proposed for URM buildings exposing different levels of intrusiveness and cost. This fact, added to the wide variety of masonry buildings results in an enormous amount of retrofitting alternatives. Interventions involving low intrusiveness are well valuated in the field of retrofitting URM buildings, since they are part of the architectural heritage of the built environment. Authenticity of the building components, and reversibility of the intervention are also considered as important criteria when dealing with architectural heritage. A brief review of the studies devoted to retrofitting of masonry buildings with application in Portugal will be herein performed.

Ferreira et al. [39] proposed a set of three retrofitting strategies, sorted by their intrusiveness and cost for the historical centre of Horta city, the author evaluated the effectiveness of the retrofitting strategies employing the vulnerability index method. The cost associated to the retrofitting strategy from 1 to 3 are 35, 100 and 250 €/m2 respectively, and ranges from lowest to highest intrusiveness. The strategies are composed by a set of 6 structural solutions, Figure 2.34 shows the measures per each retrofitting strategy and Figure 2.35 illustrates the retrofitting solutions.

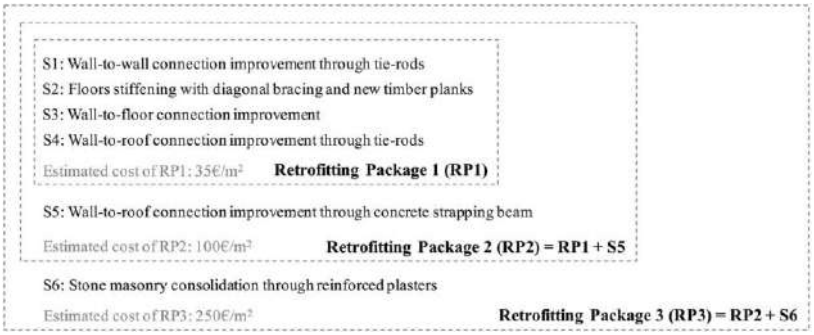

Figure 2.34 Retrofitting packages sorted by level of intrusiveness and cost, proposed in [39]

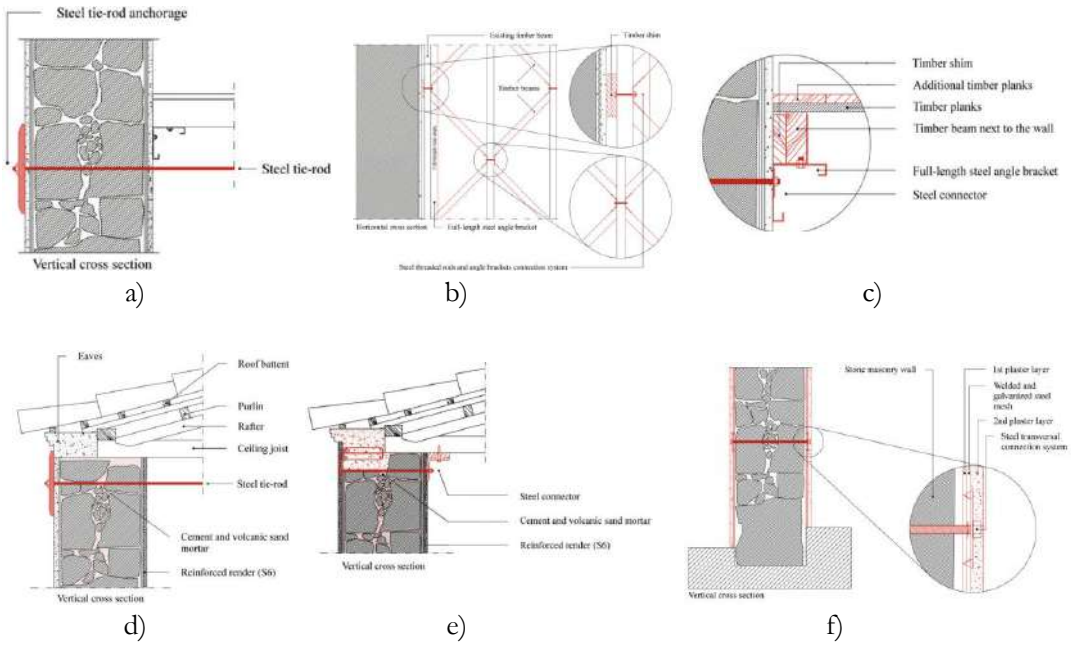

Figure 2.35 Retrofitting solutions proposed in [39]. S1-S6 from Fig. 32 corresponds to a) to f) respectively

Bento [124] proposed retrofitting strategies for mixed RC-URM buildings in Lisbon. In its works, the author summarized the retrofitting approach in 5 steps: securing all unconstrained parts from falling, strengthen specific structural elements, improving wall-to-wall and wall-to-diaphragm connections, increasing the in-plane stiffness and strength of floors and diaphragms, adding new structural elements (if necessary). Relevant important measures discussed by the author are the strengthen of masonry walls through grout injection, and cement coating reinforced either with still or polymers as shown in Figure 2.36. The author also suggests the use of tie-rods to improve the wall-to-wall and wall-to-diaphragm connection as previously explained. In addition, the author also highlights the retrofitting of timber slab by the addition of steel strips at its top and/or bottom, which have been proved in laboratory tests by Piazza et al. [125] as shown in Figure 2.37.

Figure 2.36 Application of retrofitting solutions a) mortar injection, b) steel mesh coating, c) polymer mesh coating [124]

a) b)

Figure 2.37 Seismic retrofitting of timber slab a) steel strips at top, b) steel strips at bottom [124]

Coías [126] performed a wide revision of low intrusive techniques for structural rehabilitation of old buildings (URM and timber) in the framework of the RECOPAC project. The author divides the structural solutions into two groups: the strengthen of masonry components, and the improvement of the global behaviour. The first group includes fifth options: the use of tie-rods as confinement of walls, the coating of masonry elements, reconstitution of masonry elements through rearrangement of masonry units and reparation of local damage, the reconstitution of masonry sections using other materials, and the insertion of new structural elements. Figure 2.38 illustrates the use of structural solutions in group 1.

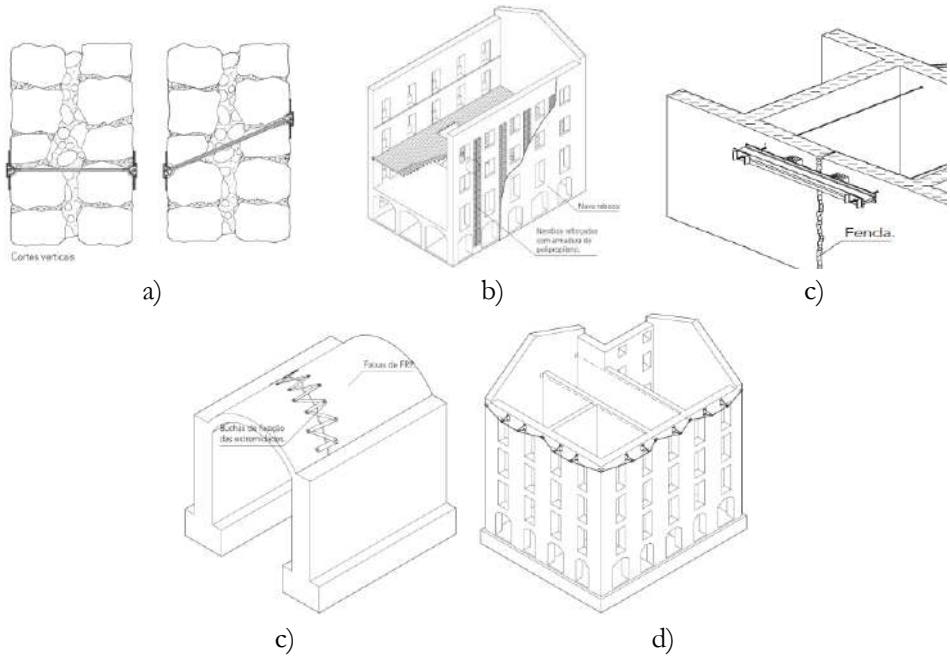

a) b) c)

c) d)

Figure 2.38 Group 1 of structural solutions proposed in [126], a) the use of tie-rods as confinement of walls, b) the coating of masonry elements, c) reconstitution of masonry elements through rearrangement of masonry units and reparation of local damage, d) the reconstitution of masonry sections using other materials, and e) the insertion of new structural elements.

A deeper review of the retrofitting approaches shown in Figure 2.38 and Figure 2.39, as well as similar implementations, can be found in [126]. The latter study also addresses the foundations retrofitting in masonry buildings, which is an important issue of the seismic performance specially when buildings are located in soft soil.

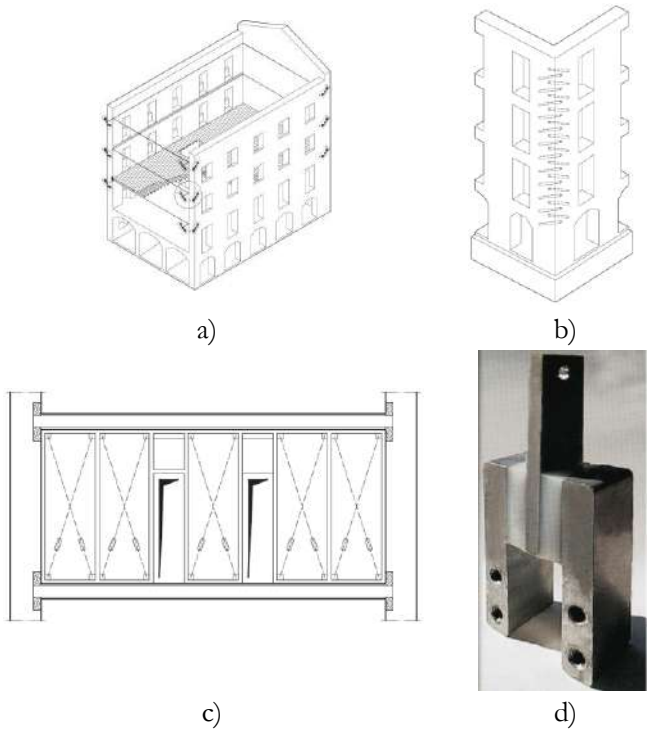

a) b) c) d)

Figure 2.39 Group 2 of structural solutions proposed in [126] a) the installation of bracing elements, b) the installation of elements to improve the connection between structural elements, and c) installation of seismic damping devices, d) seismic damping device

Post-tensioning URM buildings is also an effective retrofitting technique for aseismic actions [127]–[130]. In the beginning the used of horizontal metal ties was used to eliminate the horizontal thrust of arches, vaults, and roofs, vertical tie-bars were introduced for seismic retrofitting later. Either horizontal or vertical bards are suitable to provide a better wall-to-wall and wall-to-floor connection, therefore ensuring a box-type behaviour. Depending of the aesthetical features to preserve, bars should be installed inside rather than outside the building, thus also providing protection to corrosion. Vertical bars installation allows the enhancement of the in-plane behaviour of masonry walls, while horizontal bars reduce the risk of out-of-plane failure mechanisms. Schemes of steel confinement devices installed outside a stone masonry building are shown in Figure 2.40.

a) b)

Figure 2.40 Installation of a) external tendons, and b) stainless steel cables, for seismic retrofitting [130]

2.5 Cost-benefit analysis

Cost-benefit assessment is a socioeconomic analysis used to evaluate the effectiveness of a set of decisions, herein consisting in different retrofitting strategies. The cost to benefit ratio is calculated for each retrofitting strategy and is used as a decision tool. Revenues comes from the reduction of material and human losses due to the less vulnerability, while the cost is associated to the resources employed in the intervention of the building. Assigning economic value for human losses is a highly polemical approach, but is necessary since otherwise losses may be underestimated, thus retrofitting strategies result less attractive. The importance of exploring cost-benefit of retrofitting alternatives relies in the fact that some strategies do not warrant the investment performed, but also for the optimization of resources.

The economic value assigned to human life has been proposed to calculated of many ways such as the amount society is willing to pay in order to save a life, the remaining lifespan, the future earning potential, the investment performed by the state in the person, the compensation the state is willing to pay for fatalities caused by natural disasters, and others.

The prediction of human losses due to seismic events has mainly focused in casualties, but not injuries, thus underestimating the costs associated to human losses. The study of costs associated to the recovery of injured persons such as hospitalization, therapy, among others are part of the current research. Coburn & Spence [23], as well as Coburn et al. [22] performed research attempting to assess the number of injured people for a seismic scenario. Eq. 2.15 proposed in [23] allows a rough estimation of injuries due to seismic events.

$$L = M1 \cdot M2 \cdot M3 \cdot \left[M4 + M5 \cdot (1 - M4) \right] \qquad \text{Eq. 2.15}$$

Where $M1$ is the population per building, $M2$ is the occupancy at time of earthquake, $M3$ is the percentage of trapped occupants, $M4$ is the injury distribution at collapse, and $M5$ is the mortality post-collapse. Figure 2.41 illustrates the assessment of the factors above explained.

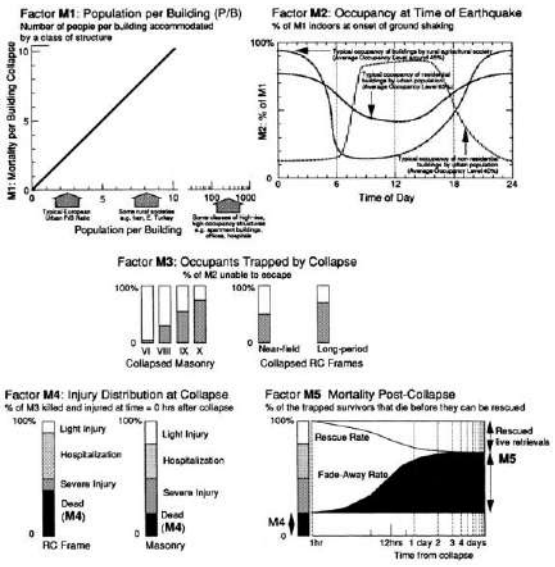

Figure 2.41 Factors M1 to M5 used in the estimation of human injuries and casualties proposed by Coburn & Spence [23]

The benefit of retrofitting interventions is given at a random time in the future, when an earthquake occurs, thus being associated to a large uncertainty. The latter can be modelled and quantified through the probabilistic seismic hazard, and building vulnerability. Liel & Deierlein [131] propose to discount future retrofitting revenues to the present by applying a constant interest and accounting for inflation phenomenon. A similar approach, taken on the interest rate instead of the present value can be done with the purpose to calculate a rate of return, useful for comparison with other investment projects.

Cost benefit analysis was traditionally performed at fixed values of investment and revenues, however [131] propose to implement the cost-benefit approach into a performance-based framework. The first step consists in the assessment of the average annual loss, performed according to Eq. 2.16.

$$EAL = \int_{IM=0}^{\infty} E\left[L\middle|im\right]\left|d\lambda_{IM}\right| \qquad \text{Eq. 2.16}$$

Where EAL is the expected average annual loss, $E[L|im]$ is the expected loss given the im intensity measure usually represented by a consequence function, λ_{IM} is the derivative of the ground-motion hazard curve which describe the likelihood of ground motions occurring that exceed a particular intensity at the building site. The same equation can be employed for human and economic losses by replacing the corresponding consequence function, leading to Eq. 2.17:

$$E\left[B\right] = E\left[B_F\right] + E\left[B_I\right] + E\left[B_L\right] \qquad \text{Eq. 2.17}$$

Where $E[B]$ is the expected benefit due to lives saved $E[B_F]$, costs saved due to reduction of injuries $E[B_I]$, and benefit associated to the reduction of damage due to retrofitting action $E[B_L]$.

The next step consists in the estimation of the expected benefit; it is the reduction of the probabilistic loss with its corresponding annual discounting. All Eq. 2.18 illustrates the latter step:

$$E\left[B_F\right] = \left(EAF_0 - EAF_R\right)\sum_{t=1}^{T}\left(1+r\right)^{-t}$$

$$E\left[B_I\right] = \left(EAI_0 - EAI_R\right)\sum_{t=1}^{T}\left(1+r\right)^{-t} \qquad \text{Eq. 2.18}$$

$$E\left[B_L\right] = \left(EAL_0 - EAL_R\right)\sum_{t=1}^{T}\left(1+r\right)^{-t}$$

Where $E[B]$ is the expected benefit, EAF_0 and EAF_R are the expected average annual loss associated to fatalities before and after the intervention respectively, EAI_0 and EAI_R are the expected average annual loss associated to injuries before and after the intervention respectively, EAL_0 and EAL_R are the expected average annual loss associated to physical damage before and after the intervention respectively, T is the period of evaluation, usually associated to its durability, r is the devaluation rate, commonly assumed as the inflation of the currency.

Arya [132] studied retrofitting experiences applied on unreinforced masonry buildings. This study found that retrofitting of an existing building may cost around 2 to 3 times the cost of constructing the building with seismic provisions from the beginning, while this ratio goes up to 4 to 8 time for repairing a damaged building. Ferreira et al. [39] proposed cost of retrofitting for three levels of interventions based in the revision of retrofitting structural designs developed during the rehabilitation process of the Faial island, Portugal in 1998. The proposed costs are 35, 100 and 250 €/m² for retrofitting packages RP1 to RP3 sorted according to its intrusiveness as described in Figure 2.34.

Diz et al. [133] proposed retrofitting intervention costs with basis on information gathered from 40 execution projects. The projects were randomly selected from a database of 3700 retrofitting designs made after the Azores earthquake in 1998. Retrofitting cost for reinforced plasters and strengthening of connections, are proposed to be in average 128 and 23 €/m² respectively. Retrofitting of foundation beams is assumed to cost 775 € per linear meter of wall.

The last step in the cost-benefit analysis is the assessment of the ratio between cost of the intervention and benefit is calculated. Ferreira et al. [39] analysed the impact of retrofitting strategies at large scale. Savings were estimated at different levels of seismic intensities for a set of 3 retrofitting packages with different level of investments and intrusiveness. Maio et al. [13] performed cost-benefit analysis for retrofitting strategies proposed in Ferreira et al. [39] for masonry buildings in Portugal. Figure 2.42 shows the outcomes of different retrofitting strategies from 1 to 3 sorted by its level of intrusion and investment from lower to higher. Three building archetypes were evaluated (e.g. A, B, C and D). Retrofitting strategies appear to show promising values with ratio values above 3.

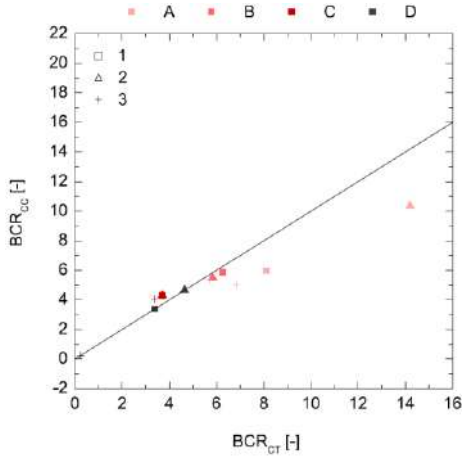

Figure 2.42 Benefit-cost ratios form URM buildings calculated in [13]

Segovia-Verjel et al. [134] performed cost benefit analysis on URM schools in Spain normalizing the costs between a set of retrofitting techniques to the lowest intervention. Three techniques were analysed consisting of encirclement L-profile (EL), steel grid (SG) and carbon fibber reinforced polymers (CFRP), ratios between normalized costs and cost-benefit ratios are shown in Figure 2.43.

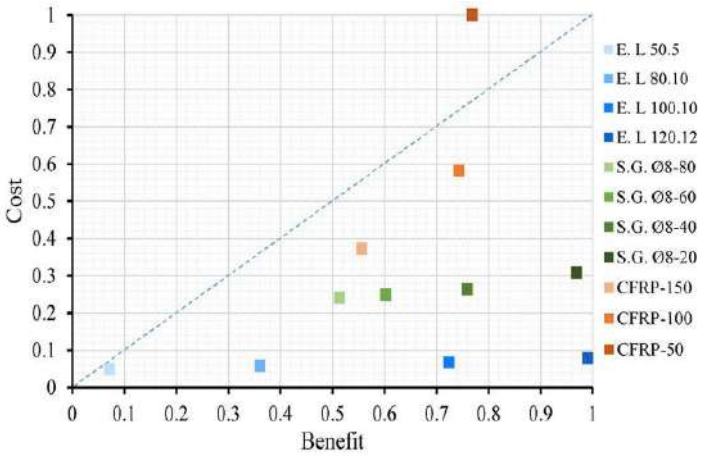

Figure 2.43 Benefit-cost ratios form URM buildings calculated in [134]

Cost-benefit approach has also been implemented for old RC buildings in the United States in [131]. Buildings with different heights were evaluated together with different retrofitting strategies. Cost-benefit ratios were calculated for different costs per life saved and inflation rates, outcomes are shown in Figure 2.44a and Figure 2.44b respectively.

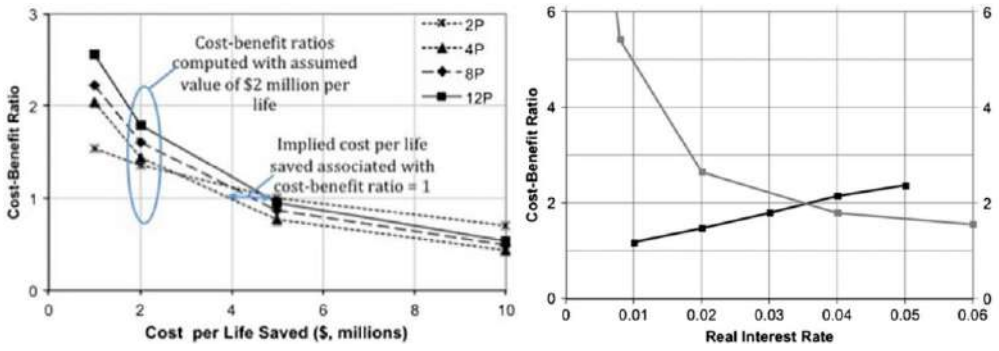

a) b)

Figure 2.44 Effect of a) cost per life saved, and b) real interest rate, in cost-benefit ratio [131]

2.6 Final remarks

In this chapter, an extensive but necessary literature review was performed in order to identify past studies related to our research topic. The vast literature available in internet forces the author to select representative studies following two criteria: the most recent state-of-the-art literature, and the applicability to the region of interest.

Regarding building characterisation, the review included approaches for the classification of buildings within context of the seismic risk evaluation. Also, a detailed review was performed about the evolution of the constructive practice of masonry in Portugal. Some effort was made on the definition of mechanical properties of masonry buildings, the types of testing procedures and past studies addressing masonry building in Portugal. It was identified a significant number of studies attempting to determine the mechanical properties of masonry buildings in Portugal by means of destructive, semi-destructive and non-destructive tests

The analytical damage fragility assessment is an arising field, where significant research is going on currently. Some important topics were addressed as the efficiency and sufficiency, the loss-damage-

EDP definition and the fragility deriving procedure. Several modelling strategies were addressed, and classified by its complexity and prediction capabilities.

Fatality vulnerability assessment is a key topic, which this work aims at strongly contribute. As stated by Spence [23], despite the large research performed towards the physical damage calculation, the human losses assessment is still a gap in the seismic risk field. The literature review on this topic includes empirical procedures, physical damage-based procedures, and extent of collapse-based approaches. The current work aims at implementing a framework based in advanced numerical modelling for fatality vulnerability prediction, the literature in this topic is still scarce, but most important contributions were considered in this chapter.

Cost-benefit analysis is a widely used tool for decision-making. Past studies implemented cost-benefit analysis for the feasibility analysis of retrofitting solutions. It was found that the methodology was successfully implemented for RC and masonry buildings worldwide, and also in Portugal. At this point, some past studies focused only in the economic loss, but not in the human losses. Also, most of the studies consider only the direct losses, but not second-order (i.e. indirect) losses.

Chapter 3

Characterisation of masonry buildings in Portugal

This chapter offers a brief description of the Portuguese masonry building stock and associated construction practices. Field data was analysed, and after a statistical treatment, some probability density functions were proposed for important structural features. A set of archetypes are identified according to the opening's ratio, and finally, a review of mechanical properties for limestone and granite masonry buildings in Portugal. Outcomes of this chapter were published in a journal article doi: 10.1016/j.engstruct.2021.111857

Lovon H., Silva V., Vicente R., Ferreira T.M., Costa A. (2021). Characterisation of the masonry building stock in Portugal for earthquake risk assessment. *Engineering Structures*, (233), 111857.

3.1 The Portuguese masonry building stock

The National Institute of Statistics (INE) of Portugal performs a decennial census across the country [12], which collects a wide spectrum of information regarding the residential building stock. The latest housing census survey was performed in 2011, and it provides information at the subsection level, which is the minimum area covered during the field survey. According to the census data, the proportion of masonry buildings, reinforced concrete, and other materials are 51.5%, 47.7%, and 0.8%, respectively, corresponding to a total of 3,353,610 buildings. The types of stone used in the construction of masonry buildings depend mainly on the available local materials. Limestone and granite are the most common types of stone used in masonry buildings in Portugal [34]. Figure 3.1 illustrates examples of typical limestone and granite masonry buildings located in urban areas in Portugal.

a) b) c) d)

Figure 3.1. Example of a), b) Limestone c), d) granite masonry buildings

Pereira & Romão [34] defined zones according to the predominant type of materials used in the construction of vernacular masonry buildings in Portugal. The resulting map identifying the most likely type of masonry was obtained by crossing information provided by the Geological Institute of Portugal and a broad survey carried out by the National Association of Architects. In this study, the map developed by Pereira and Romão [34] and the data from the national housing survey were

combined to estimate the fraction of each masonry building class in Portugal (see Table 3-1). A density map was created to analyse the distribution of unreinforced masonry buildings in Portugal using a Quartic Kernel density interpolation (with a pixel size of 0.1 km with a search ratio of 1 km), as presented in Figure 0.2. This map presents masonry buildings with a flexible (timber) and rigid (reinforced concrete, RC) floors separately, as this is one of the attributes captured by the national housing census. There is a notorious concentration of masonry buildings in the west of the country, where the population density is higher.

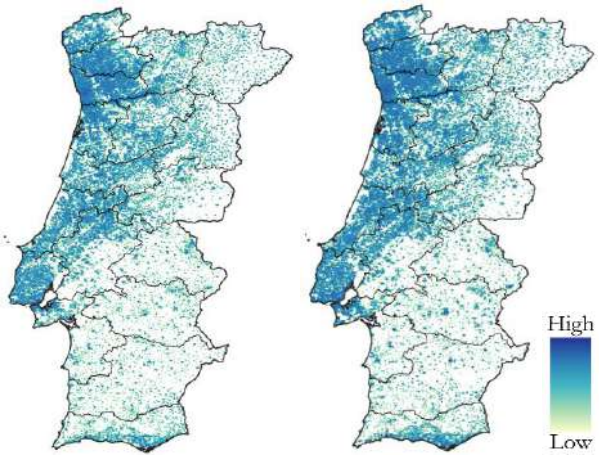

Figure 3.2 Density map of URM buildings a) without RC slab, and b) with RC slab

According to the decennial census [12] performed by the National Institute of Statistics (INE) of Portugal, the masonry building stock constitute around 3.3 million buildings, and approximately 4 million people live in these buildings. Figure 3.3 shows the buildings date of construction together with the number of storeys of masonry buildings in Portugal.

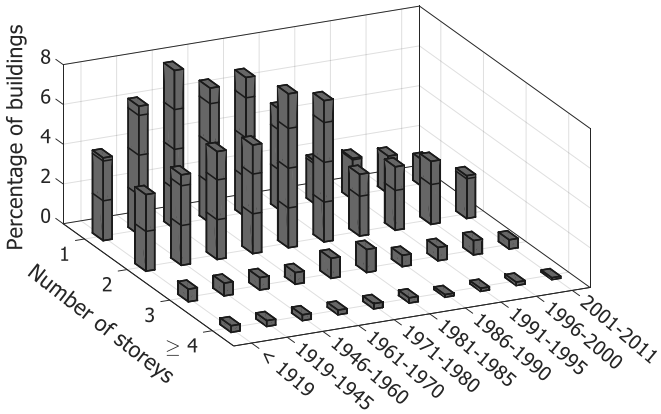

Figure 3.3 Distribution of masonry buildings per construction period and a) number of storeys

The census reveals that approximately 40 % percent of the population lives in masonry buildings. Census data of occupancy and structural system at municipal level has been crossed with the objective to assess the percentage of people and building stock exposed to a certain level of seismic hazard (see Figure 3.4).

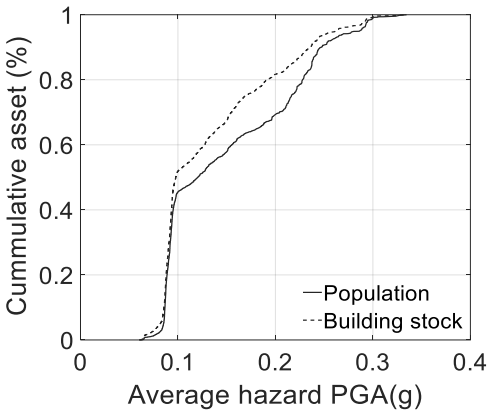

Figure 3.4 Cumulative percentage of assets exposed to an average seismic hazard in PGA (g)

Limestone and granite masonry buildings were constructed before and during the beginning of the XX century. By half of this century, the transition to the modern reinforced concrete buildings occurred. In this transition period, a concrete slab was gradually incorporated as part of the construction practice, first at the level of the ground floor where kitchens and bathrooms were often located, and finally as the entire inter-storey system. In the southern regions of Portugal, particularly in Lisbon, the construction of URM buildings was interrupted after the 1755 M8.5 Lisbon earthquake. After this event, the mixed wood-masonry buildings (locally known as Pombalino, and later the Gaioleiro – Simões [62]) replaced the URM construction temporarily, up to the beginning of the last century when the transition to modern reinforced concrete buildings started.

According to Appleton [50], there are three main types of foundations in limestone and granite masonry buildings: direct, semi-direct, and indirect. Direct foundations, usually performed in rigid soils, consist of a wider extension of the masonry walls in the earth usually constructed with poorer quality. Semi-direct foundations comprise a system of masonry arches and piers constructed in order to reach deeper soil and, therefore, more rigid. Finally, indirect foundations consist of wood stakes on which the walls rest superficially. In most cases, the type of stone used for the walls is also used for the foundations. Less frequently, isolated reinforced concrete footings were also used in masonry buildings constructed in the transition to the modern reinforced concrete buildings (e.g. Sousa [46], Lamego [52]).

The limestone and granite masonry walls are constructed either with irregular or tailored stones and in most cases with lime-sand mortar irregular bed joints. Although dry-joined masonry walls can also be found, these represent a small portion of the building stock and are frequently associated with monuments [135]. In general, masonry buildings present a high wall to floor area ratio and a low quantity of openings. These features are demonstrated to have a meaningful influence on the stiffness, fundamental period, load capacity, and energy dissipation of the masonry buildings. The importance of these parameters has been addressed in several past vulnerability studies, e.g. [14], [16], [58].

Regardless of the type of masonry, the openings are usually topped by timber or stone lintels. For the case of masonry buildings with flexible floors, the inter-storey system consists of timber beams usually spaced between 0.20 to 0.40 meters. In some cases, the use of vaults is reported in buildings with the higher architectural value. The inter-storey system in buildings with rigid floors consists of a simply supported concrete slab with a thickness of around 0.10 meters, usually reinforced with

solely one layer of longitudinal steel reinforcement in tension. According to Alegre et al. [63], it is not possible to ensure the continuity of the slabs between spans, and thus these elements do not work as a continuous floor system. Hence, the walls and slabs are not coupled at the intersection (between spans), resulting in a higher moment at mid slab spans for gravity loads, and higher displacement and flexural moment demand on walls for lateral loads. The majority of the roofs present a slope according to the weather conditions of the region. A timber framework constitutes the roof system and has a ceramic tile finishing jointed with mortar. The timber trusses rely directly on the walls, but in some cases, the span between the walls can be covered with a masonry vault. This latter case is associated with public buildings with higher architectonical value [51].

3.2 Characterisation of the geometric properties

The characterisation of the geometric properties of the masonry building stock was performed following three main steps: 1) identification of the macro building classes in accordance to the latest national housing census, 2) collection of data from drawings and technical specifications regarding the geometric properties of existing masonry buildings, and 3) definition of statistical models for each geometric parameter. As further described in this section, the revision of the detailed drawings (and existing literature) also allowed defining the most common archetypes for this type of construction.

3.2.1 Identification of the macro masonry building classes

When assessing seismic risk for a region with a large number of buildings, it is impractical to define the structural system of each building according to its individual structural and non-structural characteristics (Meslem and Lang [40]). The assessment becomes feasible by grouping the building stock according to a number of building classes. The grouping process is performed based on the overall performance of the buildings to seismic actions and the availability of the information for the building inventory (Yepes et al. [136]). Previous studies have addressed the challenge of defining a building taxonomy for seismic risk assessment at different scales: national (Silva et al. [14], Campos et al. [47]), regional (Crowley et al. [48]) or global (Brzev et al. [42], Jaiswal and Wald [137]) scales. A building taxonomy is expected to have sufficient detail to capture the particularities of each building class according to the local construction techniques. Yepes et al. [136] suggested defining the building classes according to characteristics that influence the seismic performance, such as the main material of construction, lateral load-resisting system and the number of storeys. Table 3-1 lists the macro masonry buildings classes defined in the present study, along with the respective percentage in the entire residential building stock. The building classes defined herein are intended to take advantage of the data from the 2011 Census, and therefore the definition of the building classes considered the quality and level of detail of the national census data. As further described in this section, the revision of the detailed drawings (and existing literature) also allowed defining the most common archetypes for this type of construction.

Table 3-1 Macro masonry building classes for masonry buildings in Portugal.

N°	Attributes		Number of storeys	Label	Percentage (%)
	Lateral load-resisting system	Type of Diaphragm			
1	Unreinforced masonry with limestone walls	Flexible	1 to 6	URML_F	4.8
2		Rigid	1 to 6	URML_R	12.3
3	Unreinforced masonry with granite walls	Flexible	1 to 6	URMG_F	7.1
4		Rigid	1 to 6	URMG_R	19.7
5	Mixed wood-masonry walls	Flexible	3 to 6	MWMP_F	N/A
6	Others (e.g. adobe, schist, rubble stone or rammed earth)	Indistinct	Indistinct	M_O	7.6

3.2.2 Definition of the geometric properties

The evaluation of the geometric properties of the limestone and granite buildings in Portugal was performed through the analysis of drawings and technical specifications from existing masonry buildings. From the initial set of over 200 building drawings, 100 cases were selected for the limestone buildings, while 85 were used for the granite buildings. Several buildings were excluded from these analyses due to the lack of detail in the drawings, unusual geometry due to the use of the building (e.g. public services), or inclusion of other types of materials (e.g. concrete walls). For the data processing, the X-direction was considered along the façade, while the Y-direction was assumed to be perpendicular. Both structural and non-structural walls were analysed, in order to allow future studies regarding the assessment of loss of functionality or estimation of the amount of debris. The analysis of these databases allowed the collection of metrics such as the size of the buildings in the two directions, heights, the thickness of the walls, and percentages of openings in the façades.

The collection of a sufficient number of building drawings per building class (see Table 3-1) may lead to an unpractical number of samples. To overcome this issue, data from different building classes were grouped under the assumption that no statistical differences are expected between them. This hypothesis was verified using ANOVA (Analysis of Variances) tests [138], which allows testing whether samples from different classes can be assumed to belong to the same group. This statistical test assumes that the distribution of the residuals follows a normal (gaussian) distribution, so when assuming other statistical distributions (e.g. lognormal), the data was adjusted accordingly. Notwithstanding, it was decided to keep the statistical analysis between the limestone and granite buildings separated, as one of the primary purposes of this study is to provide basic information for the derivation of analytical vulnerability functions for each construction type. The dispersion of the geometric variables was depicted using boxplots, outliers are represented by asterisks. For the definition of the statistical models for each geometric variable, normal, lognormal, Weibull, and Gamma distributions were considered. The best probability density functions for each variable were chosen using the chi-square goodness-of-fit test. A similar procedure was followed by Silva et al. [14] and Bal et al. [33] for reinforced concrete buildings in Turkey and Portugal, respectively.

For the sake of simplicity and to avoid categories with a small number of samples, all buildings were grouped into 4 categories with respect to the number of storeys. Henceforth, these groups will be designated as building categories, as illustrated in Figure 3.5.

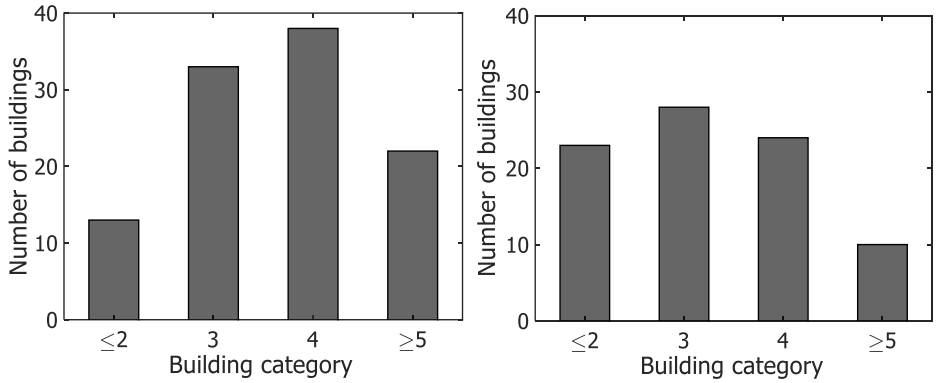

Figure 3.5 Distribution of buildings according to the height category for a) limestone buildings, b) granite buildings.

a) Ground floor height

The inter-storey height of the ground floor is often different from the height of the upper storeys (e.g. Silva et al. [14], Bal et al. [33], Sumerente et al. [6]). For this reason, this variable is analysed in this section, while the height of the upper flows is covered in the following section. Figure 3.6 presents the dispersion of the ground floor height for limestone and granite buildings, while Figure 3.7 depicts the histogram, fitted distribution, and the goodness-of-fit results.

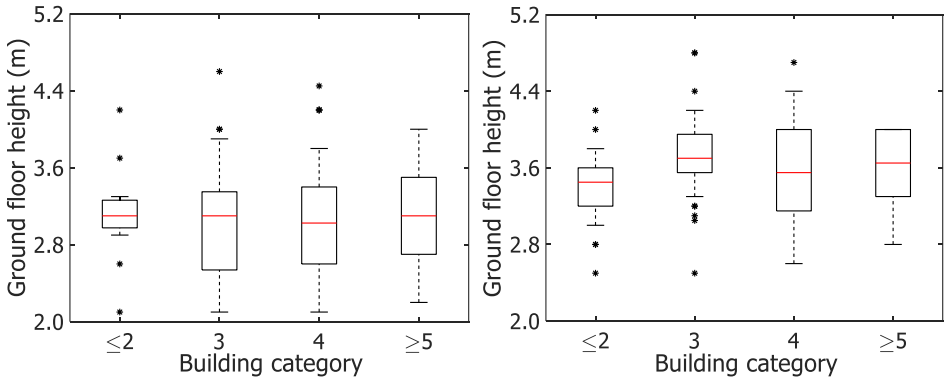

Figure 3.6 Dispersion of ground floor height for all building categories of a) limestone, and b) granite masonry buildings

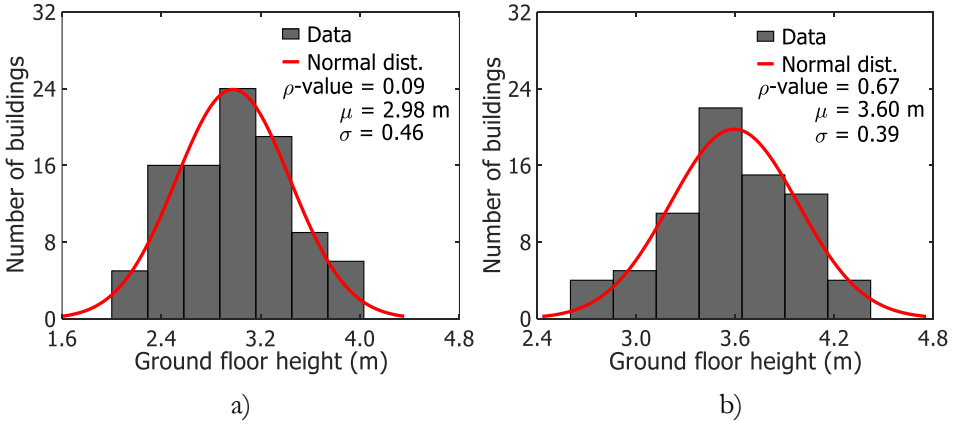

Figure 3.7 Histogram, fitted distribution, and goodness-of-fit results for the ground floor height for a) limestone b) granite masonry buildings

A significant difference between the ground floor height of limestone and granite buildings was observed. On average, granite buildings are 20% higher than limestone buildings. This difference is most likely due to the different architectonic and construction practices typical of the regions where these buildings are located. As previously mentioned, granite buildings are more common in the north of the country, while limestone masonry buildings can be found mostly in the centre and south of Portugal. Nonetheless, the standard deviation of the ground floor height is similar for both cases.

b) Upper storeys height

For the analysis of the upper storeys' height, each inter-storey height of the upper floors was considered as one data point. Some buildings present attics on the uppermost floor, which were not included in this study. One-storey buildings were also not considered for the analysis of this variable and were included in the previously described variable instead. Figure 3.8 shows the dispersion of the regular storey height for limestone and granite buildings, while Figure 3.9 presents the histogram, fitted distribution, and the goodness-of-fit results.

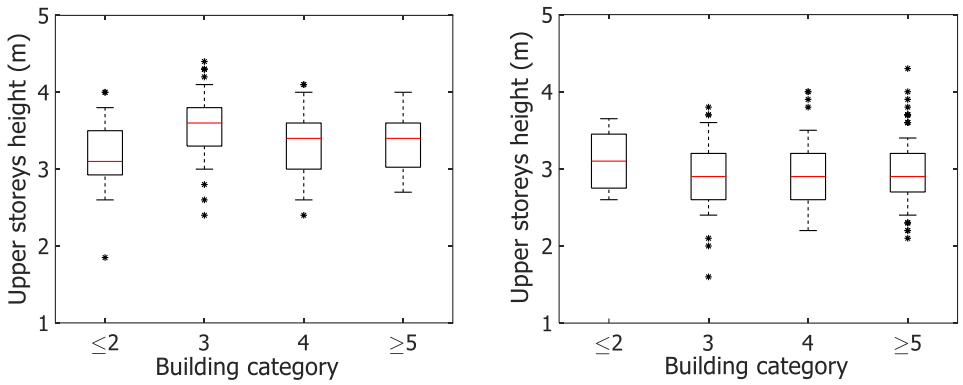

Figure 3.8 Dispersion of the upper storeys height for a) limestone, and b) granite masonry buildings

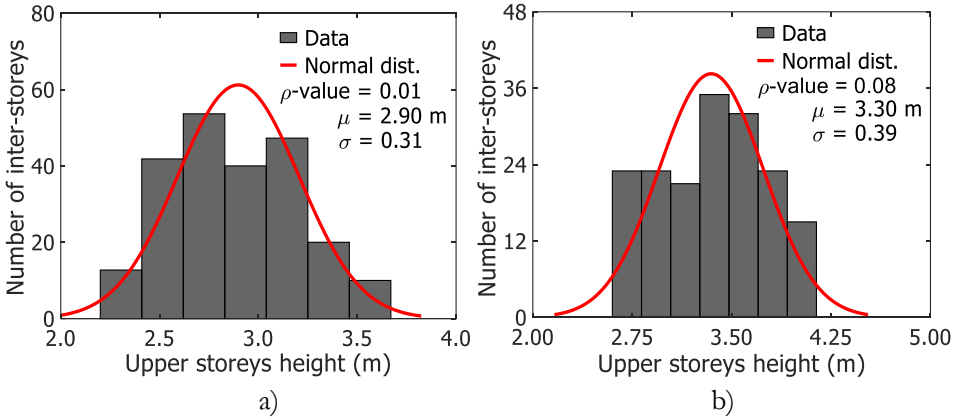

Figure 3.9 Histogram, fitted distribution, and goodness-of-fit results for the upper storeys height for a) limestone b) granite masonry buildings

c) Length of the building in the X and Y directions

The overall dimensions of the buildings (length in both directions) play an important role in the estimation of debris, as the volume of the building depends directly on this parameter. Moreover, discrepancies between the length in the X and Y directions also allow evaluating horizontal

irregularities. The ratio of the length in the two directions may have an important influence when one direction is four times larger than the other (e.g. Tomaževič [85]), and it can influence the seismic performance of the structure (e.g. Candeias [4], Borzi et al. [66]). A two-way ANOVA analysis was performed in order to identify possible correlations between the lengths in the X and Y directions (i.e., whether a large length in one direction means that there is a high likelihood of also having a large length in the other direction). The results indicated no significant correlation, and, consequently, these variables were modelled separately. The relationship between the lengths of the buildings in each direction is presented in Figure 56 for both types of masonry buildings. Figure 3.10, Figure 3.11 and Figure 3.12 present the histogram, fitted distribution and the goodness-of-fit results for the limestone and granite buildings in the X and Y directions, respectively.

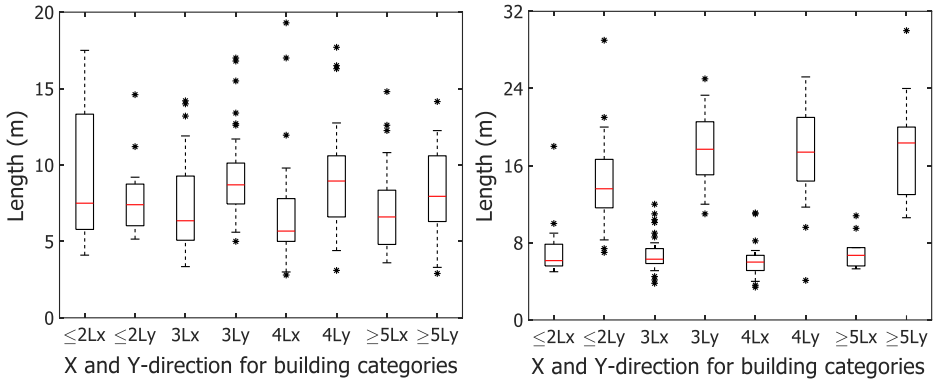

Figure 3.10 Dispersion of the lengths in X and Y direction for all building categories of a) limestone, and b) granite masonry buildings

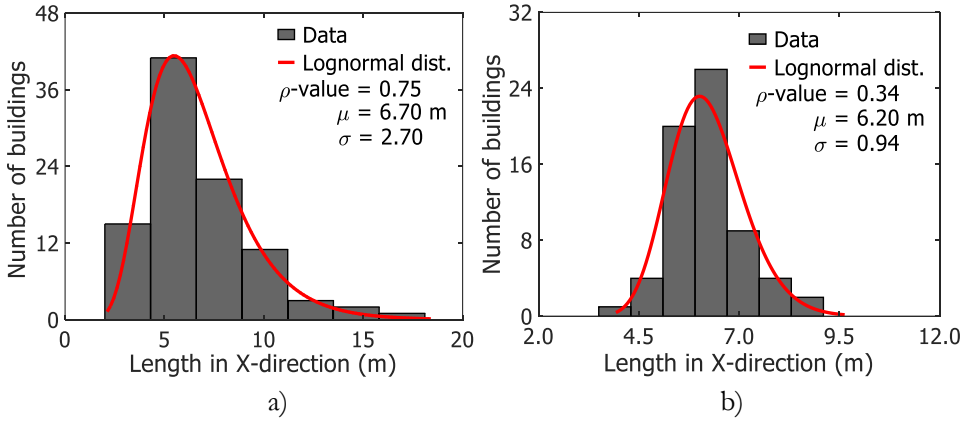

Figure 3.11 Histogram, fitted distribution and goodness-of-fit results for the length in the X-direction a) limestone b) granite masonry buildings

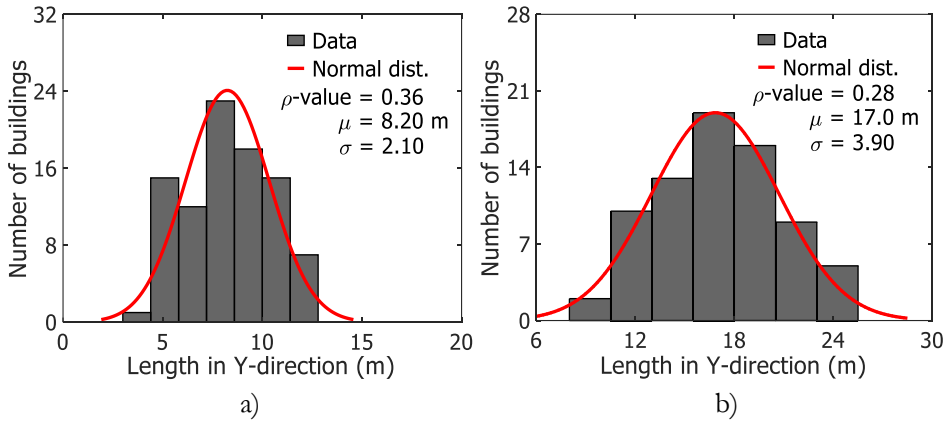

Figure 3.12 Histogram, fitted distribution and goodness-of-fit results for the length in the Y-direction a) limestone b) granite masonry buildings

d) Thickness of the walls

The thickness of the walls is directly related to their in-plane stiffness, which, in turn, plays an important role on the capacity of the building to dissipate energy during a seismic event (e.g. Candeias [4], Borzi et al. [66], Lovon et al. [7]), the reason why this parameter is also analysed herein. Figure 3.13 presents the dispersion of the thickness of the walls per height category, for limestone and granite buildings. It is relevant to note that for the vast majority of the buildings analysed in this study, the thickness of the upper storey walls decreases. Such a trend is somewhat expected as lower storeys require thicker walls to support the weight of the upper storeys. In this section, a statistical model for the mean thickness of the walls is presented, and then additional information is provided regarding the expected reduction in this variable within each building typology.

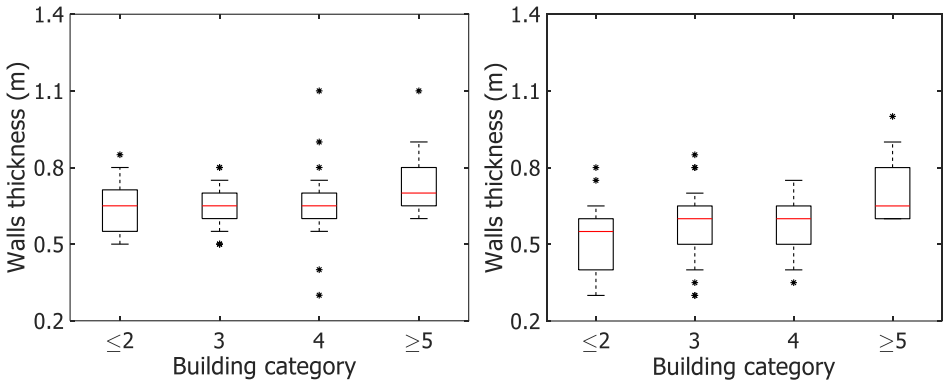

Figure 3.13 Dispersion of wall thickness at the ground floor for a) limestone, b) granite buildings

The influence of the number of storeys in the mean thickness of the walls was tested using the ANOVA analysis. The results suggest that there are no statistical discrepancies when grouping all building into two subcategories: buildings with 3 or fewer storeys (≤3) and buildings with more than 3 storeys (>3). Following this categorisation, a statistical model was fitted for each subcategory (see Figure 3.14 and Figure 3.15).

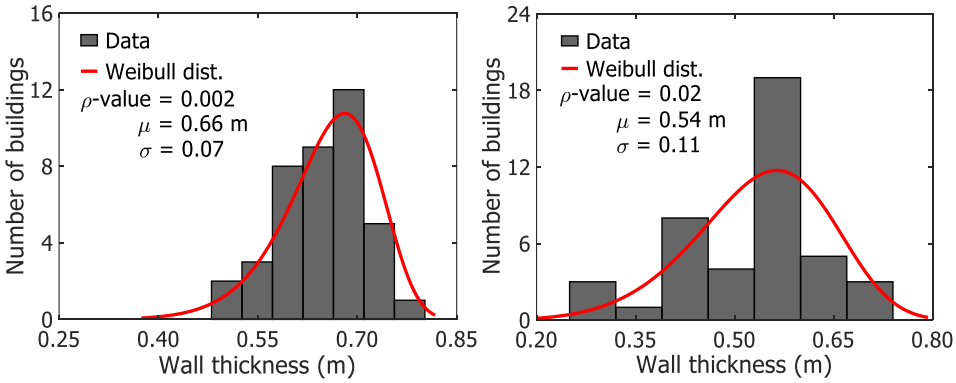

a) b)

Figure 3.14 Histogram, fitted distribution and goodness-of-fit results for the thickness of the walls for a) limestone and b) granite masonry buildings with a number of storeys equal or lower than 3

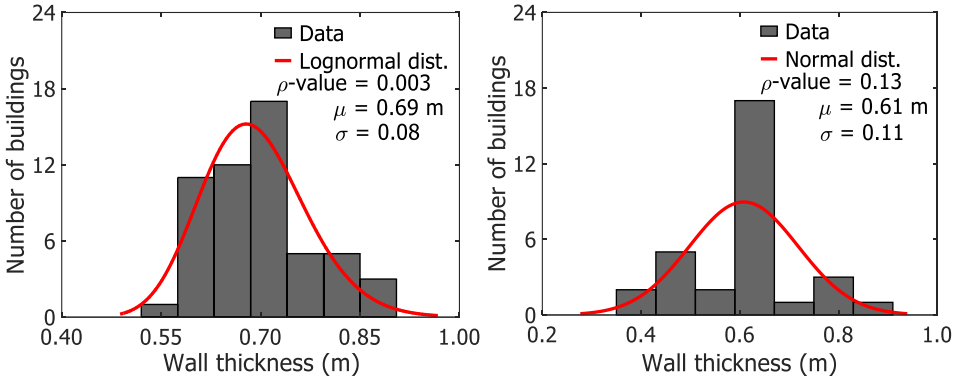

a) b)

Figure 3.15 Histogram, fitted distribution and goodness-of-fit results for the thickness of the walls for a) limestone and b) granite masonry buildings with more than 3 storeys

As previously mentioned, the thickness of the wall tends to be larger at lower storeys, and it decreases inversely proportional to the height of the building. In fact, only 10.9 % and 40.2 % of the limestone and granite buildings did not present any reduction, respectively. This tendency in wall thickness reduction can be observed in Figure 3.16, where the mean thickness per each storey is presented according to the building height categories.

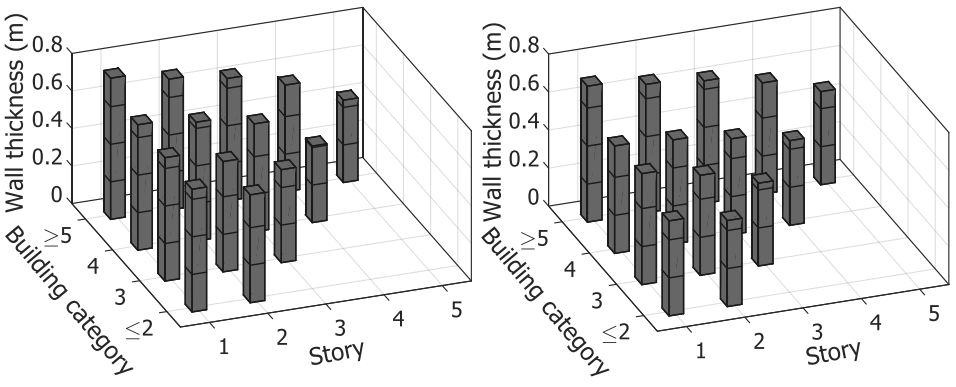

a) b)

Figure 3.16 Wall thickness of each storey per buildings height category for a) limestone, and b) granite buildings

For mathematical convenience, the wall thickness reduction was evaluated instead of the width itself. This reduction is represented by the ratio between the wall thickness at the storey under analysis and wall thickness of the storey below. The ANOVA analysis did not indicate any statistical evidence that the mean wall thickness reduction is influenced by the building height category, as presented in Figure 3.17. The statistical model fitted for this variable is presented in Figure 3.18.

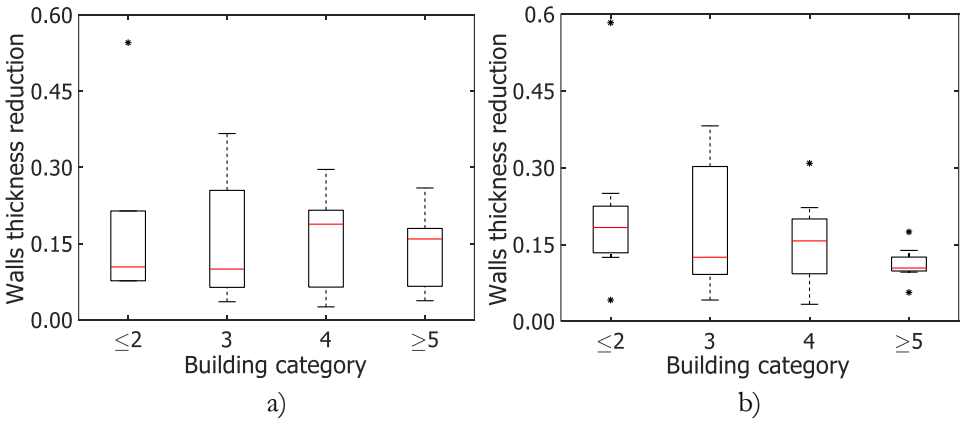

Figure 3.17 Dispersion of the mean wall thickness reduction for the building height categories for a) limestone and b) granite masonry buildings

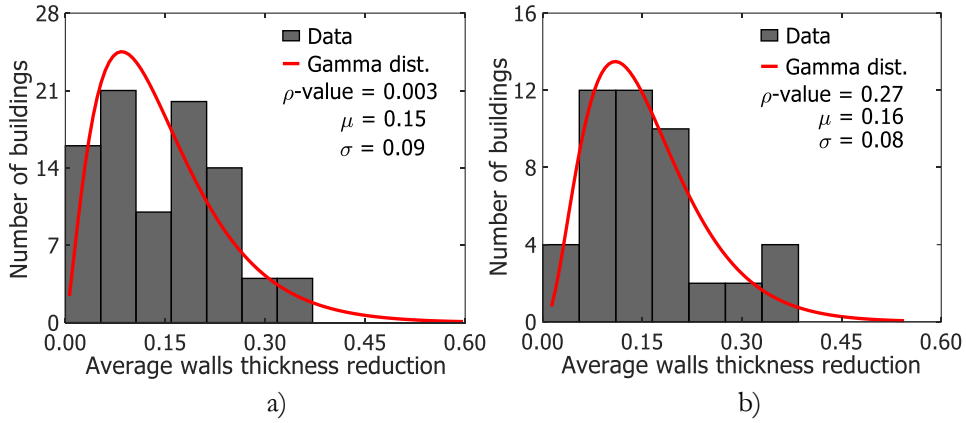

Figure 3.18 Histogram, fitted distribution and goodness-of-fit results for the mean wall thickness reduction for a) limestone and b) granite masonry buildings

e) Percentage of openings in the façade

The percentage of openings in the façade plays an essential role in the seismic performance of the building since the location and the size of the openings define the configuration and dimension of the structural elements of the walls, i.e. piers and spandrels. The percentage of wall openings, associated to their location in the façade, can also trigger specific collapse mechanism resulting from the in-plane weakening of the wall, a phenomenon well-discussed by Mendes et al. [139]. No significant differences were observed between the percentage of openings across the different building height categories, but important discrepancies were observed between the percentages of openings for the ground floor storey and upper floor storeys. The dispersion of this variable is presented separately in Figure 0.19 and Figure 0.20 for the limestone and granite masonry buildings, respectively.

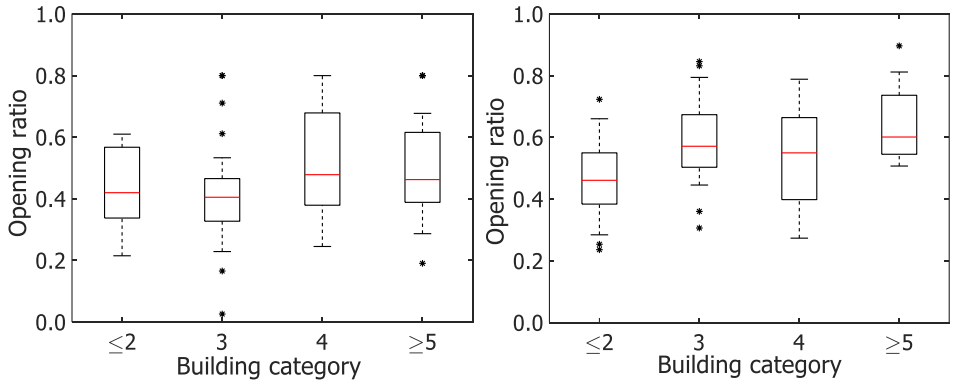

Figure 3.19 Dispersion in the percentage of openings for the a) façade of the ground storey b) façade of the upper storeys for limestone buildings

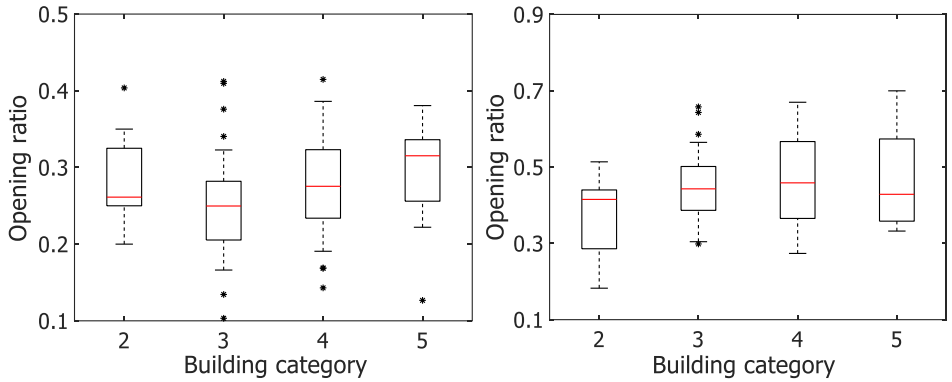

Figure 3.20 Dispersion in the percentage of openings for the a) façade of the ground storey b) façade of the upper storeys for granite buildings

The statistical models for this variable were also performed considering the ground floor and upper floor storeys separately, as shown in Figure 3.21 and Figure 3.22 for the limestone and granite buildings, respectively.

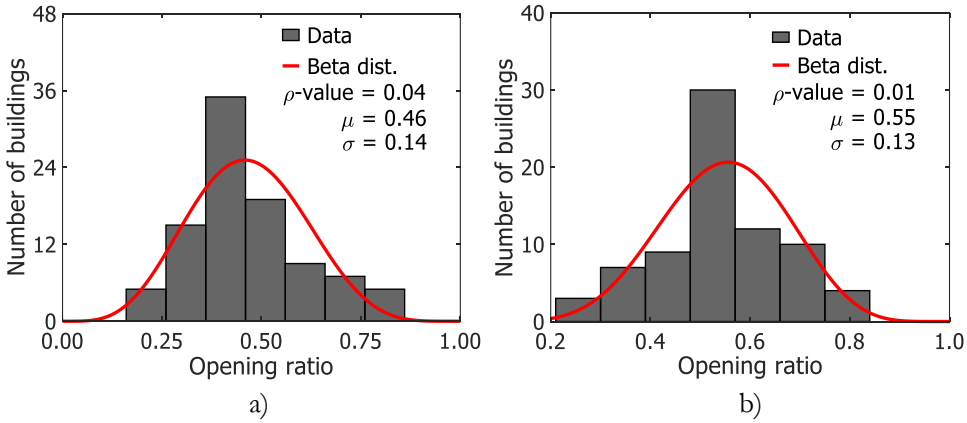

Figure 3.21 Histogram, fitted distribution and goodness-of-fit results for the percentage of openings for a) façade of the ground storey and b) façade of the upper storeys for the limestone masonry buildings

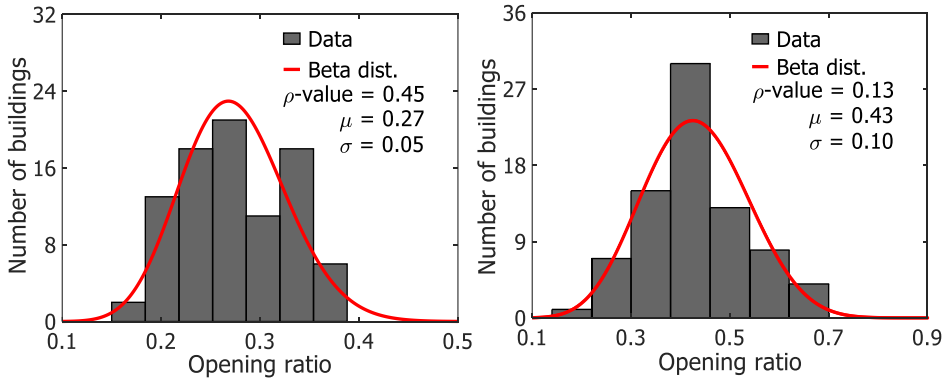

a) b)

Figure 3.22 Histogram, fitted distribution and goodness-of-fit results for the percentage of openings for a) façade of the ground storey and b) façade of the upper storeys for the granite masonry buildings

f) Average density of non-structural walls

This variable represents the ratio between the area of the non-structural walls in plan and the total plan area of the building. These walls can either present or not continuity in elevation in all floors, but do not contribute to the lateral load resisting system of the building. Accounting for these elements is relevant as they might affect the functionality of the building and contribute to the amount of debris in case of extensive damage (Jeon et al. [140], Domaneschi et al. [141]). Figure 3.23 presents the dispersion of the non-structural wall density for each building height category. Once again, the ANOVA tests did not reveal any statistical differences across these categories, and consequently, all buildings were analysed jointly. Figure 3.24 presents the fitted distributions for this variable.

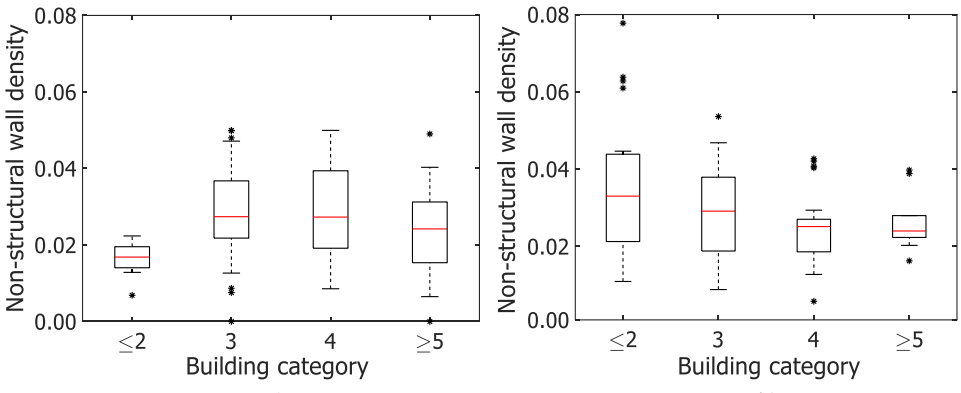

a) b)

Figure 3.23 Dispersion in the non-structural wall density for a) limestone and b) granite masonry buildings

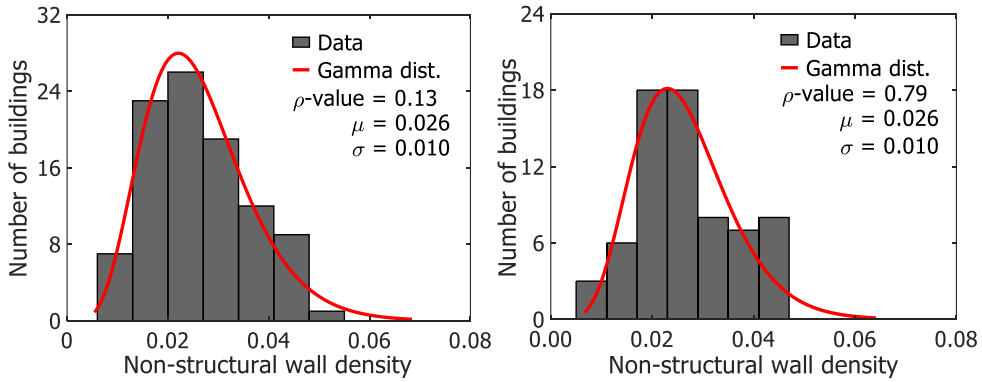

Figure 3.24 Histogram, fitted distribution and goodness-of-fit results for the non-structural wall density for a) limestone and b) granite masonry buildings

A summary of the geometric properties together with its probability density functions, and corresponding parameters are shown in Table 3-2.

Table 3-2 Random variables for limestone and granite masonry buildings

Random variable	Unit	Limestone			Granite		
		Function	Mean	Std. deviation	Function	Mean	Std. deviation
Ground floor height	m	Normal	2.98	0.46	Normal	3.60	0.39
Upper storeys height	m	Normal	2.90	0.31	Normal	3.30	0.39
Length X-direction	m	Lognormal	6.70	2.70	Lognormal	6.20	0.94
Length Y-direction	m	Normal	8.20	2.10	Normal	17.0	3.90
Wall thickness (≤3 storeys)	m	Weibull	0.66	0.07	Weibull	0.54	0.11
Wall thickness (>3 storeys)	m	Lognormal	0.69	0.08	Normal	0.61	0.11
Average wall thickness reduction	-	Gamma	0.15	0.09	Gamma	0.16	0.08
Opening ratio (ground)	-	Beta	0.46	0.14	Beta	0.55	0.13
Opening ratio (upper storeys)	-	Beta	0.27	0.05	Beta	0.43	0.10
Non-structural walls density	-	Gamma	0.026	0.010	Gamma	0.026	0.010

g) Wall thickness – Building height relationship

Increasing the wall thickness is a common engineering practice for taller buildings. However, the question remains in the sense of to what extent the wall thickness is associated with the building height relationship. A test was performed in the current work to plot the building's height of each observation against the wall thickness in the ground storey. The level of correlation was measured through the Pearson correlation coefficient for a linear relationship, as shown in Figure 3.25. Even when the correlation coefficient remains low, it is noticed a positive trend for wall thickness as building height increases.

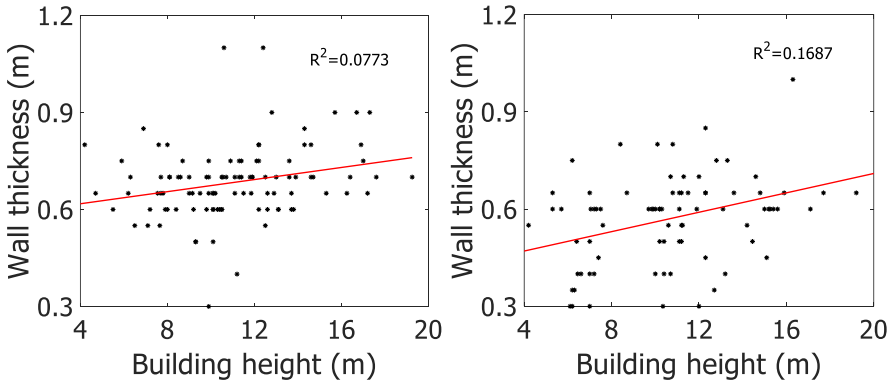

Figure 3.25 Wall thickness – Building height relationship for a) limestone and b) granite masonry buildings

3.3 Definition of typical archetypes and sampling

Based on the revision of the building drawings, technical specifications, existing literature and the statistical information presented in the previous section, typical archetypes for the masonry buildings in Portugal were identified, as presented in Table 3-3. These archetypes represent typical residential buildings as built originally (i.e. without considering any modifications due to commercial activities or retrofitting interventions), and their configuration depends mostly on the number of storeys. This information is relevant for the development of numerical models that are representative of these building classes in Portugal.

Table 3-3 Archetypes for masonry buildings in Portugal.

Nº	Archetype	Elevation view
1	Buildings with up to 2 storeys. Two or three entry doors and one window at the ground storey façade.	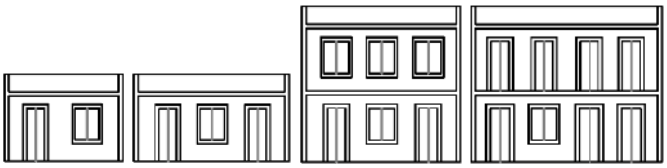
2	Buildings with 3-4 storeys. Two or three entry doors and one window at the ground storey façade. Doors and/or windows at all other upper levels.	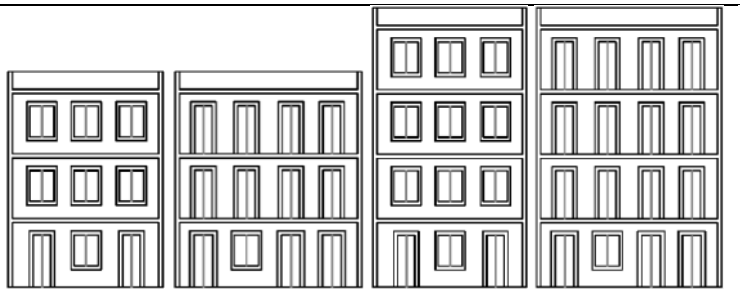
3	Buildings with 5 or more storeys. Two or three entry doors and one window at the ground storey façade. Doors and/or windows at all other upper levels.	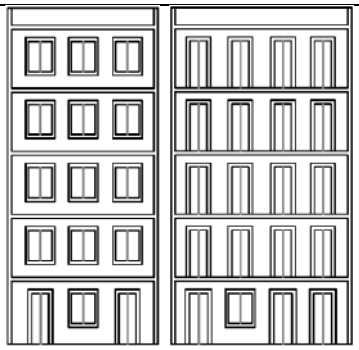

A full sampling of synthetic buildings can be achieved by using the aforementioned random variables and the archetypes shown in Table 3-3, allowing the analysis of building-to-building variability (Silva et al. [64]) of this portfolio.

Sampling facades can be a challenging task, in special in masonry buildings. This trouble arises from the vast diversity of arrangements observed in masonry building facades, which in some cases can have an irregular disposition. During the blueprints review, three main façade styles were identified both for limestone and granite buildings. The styles are defined according to the number of openings as DW, DWD, and DWDD, acronyms which stands for combination of doors (D) and windows (W). The identified archetypes can be seen in Figure 3.26a. The size of the openings was limited to certain values found during the data revision, then doors can have lengths from 1.0 to 1.8 m and heights from 2 to 2.4 m, while windows are limited to lengths between 0.8 to 1.4 m and heights from 1.0 to 1.8 m. Figure 3.26a shows the range of values for squared meters that can take place in each façade style, the latter values were calculated with basis on the number of openings per façade style and its minimum and maximum possible area. It can be noticed that overlapping is observed between façade styles, therefore ranges per façade style was limited to the middle point of the overlapping zone, leading to Figure 3.26b. This conditioning was made in order to dispose only one façade style per each area of opening.

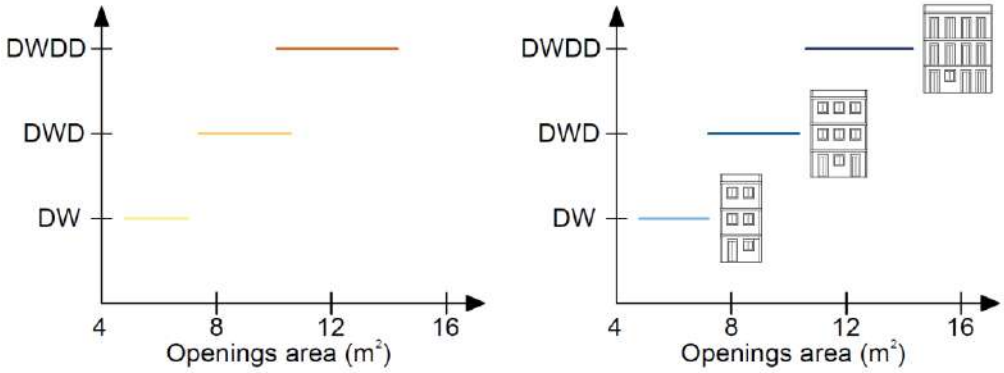

Figure 3.26 Range of openings area a) original, b) modified and archetypes

The first step of the procedure consists on sampling an opening ratio, height and façade length for the first storey. The area of openings is calculated with basis in the previous variables and a façade style is defined according ranges defined in Figure 3.26b. Once the façade style is defined, the best size of windows and facades is chosen giving privilege to the height of the openings in relation to its length. The best size is considered to be the closest one to the area of openings obtained by sampling. Upper storeys are assumed to have the same number of openings than the first storeys. Similarly, to first storey approach, the upper storeys are limited to be setup with 2-4 doors or windows. The length of the doors was limited between 0.8 and 1.8 m, and their height between 1.8 and 2.2 m. The size of the windows was limited from 0.6 to 1.2 m of length and 0.6 to 1.0 m of height. Correspondingly with the treatment of the first storey, the best size for openings was selected according to its closeness to the sampled value. The Monte Carlo method was adopted for the sampling procedure; all the process was performed in MATLAB [142] software.

3.4 Characterisation of the mechanical properties

Mechanical properties such as the elasticity modulus, compressive strength and shear strength of limestone and granite walls are fundamental for the assessment of the seismic vulnerability of this type of construction. These properties have been studied by several authors in the past through destructive, semi-destructive and non-destructive tests on masonry walls. For the sake of convenience, the main results from these studies have been summarised in Table 3-4 and Table 3-5 for limestone and granite masonry, respectively.

Significant differences were found across these studies due to the inherent uncertainty in the material properties of masonry walls, but also due to other factors such as the type of mortar and stone, the level of resemblance between units, state of conservation of the masonry specimens, and type of test to assess the mechanical properties (i.e. in-situ test versus laboratory conditions). These factors have been comprehensively studied by Drysdale et al. [143].

Table 3-4 Existing studies that addressed the mechanical properties of limestone masonry in Portugal

Source	Elasticity modulus (GPa)	Compressive strength (MPa)	Shear strength (MPa)	Type of test	Masonry description
Pagaimo [144]	0.30	1.00	-	In-situ flat-jack test	Irregular limestone masonry. Clay and lime mortar.
Pinho [54]	0.31	0.43	-	Laboratory compression test	Irregular limestone masonry. Lime and sand mortar
Vicente [145]	1.71	0.76	-	In-situ flat-jack test	Irregular limestone masonry. Lime, sand, pebble and clay mortar
Milosevic et al. [80]	1.64	8.01	0.45	Laboratory uniaxial compression, and triplet shear test	Irregular limestone masonry. Hydraulic lime and sand mortar
	0.56	7.41	0.22		Irregular limestone masonry. Air lime and sand mortar
Moreira [146]	1.02	1.70	0.29	Laboratory uniaxial, and diagonal compression test	Irregular limestone masonry. Hydraulic lime, sand, clay-rich sand and cement mortar
Simões [147]	2.00	1.89	0.19	In-situ flat-jack test	Irregular limestone masonry. Air lime mortar – Pombalino Building.
	0.39	0.63	0.13		Irregular limestone masonry. Air lime mortar – Gaioleiro Building.

Table 3-5 Existing studies that addressed the mechanical properties of granite masonry in Portugal

Source	Elasticity modulus (GPa)	Compressive strength (MPa)	Shear strength (MPa)	Type of test	Masonry description
Vasconcelos [84]	1.25	18.4	0.36	Laboratory uniaxial compression and cyclic shear wall test	Irregular granite masonry. Clay and sand mortar
Miranda [148]	0.55	0.50	-	In-situ flat-jack test	Irregular granite masonry. Non-reported mortar
Almeida [82]	0.34	4.14	-	Laboratory uniaxial compression test	Partially regular granite masonry. Air lime, sand and clay mortar
	0.29	3.93	-		Irregular granite masonry. Air lime, sand and clay mortar
Ferreira et al. [75]	0.49	-	-	Modal identification	Regular granite masonry
Domingues et al. [149]	0.83-1.99	-	-	In-situ flat-jack test	Roughly shaped granite stones. Lime mortar and earth

3.5 Final remarks

Geometric and mechanical properties of limestone and granite masonry buildings were defined based on the review of a large set of specifications and past studies, respectively. The results, which are presented in Table 3-4 and Table 3-5, demonstrate the high dispersion of the mechanical properties of limestone and granite buildings. Further experimental research is needed in order to construct a robust database of local URM buildings, but also to store and disseminate this type of data, as performed for other countries (e.g. Augenti et al. [67], Boschi et al. [68], Riahi et al. [69]).

Despite the reduced size of the number of buildings thoroughly analysed in this study, it is interesting to report some of the trends. On average, granite buildings were found to be taller than the limestone counterpart, with values of 20% and 14% higher for the ground floor and the average upper storeys, respectively. Similarly, the length in the Y-direction of granite buildings tends to be higher than in the limestone case. However, the length in the X-direction of both building classes is quite similar. For what concerns the thickness of the walls, limestone masonry presented on average 17% higher values than the granite walls. Moreover, in both classes, a clear trend in wall thickness reduction was observed with the total number of storeys of a building (i.e. lower storeys present thicker walls than upper storeys). Finally, regarding the percentage of openings, granite buildings presented higher percentages for the ground level (i.e. 20%) and upper level (i.e. 60%) storeys.

This information can be used as input information for the development of numerical models to assess the seismic vulnerability of this type of construction in Portugal. The authors recognise the need to expand the current database of building drawings to increase the reliability of the statistical models defined herein. For this reason, the data that has been compiled in this study is available in a public repository at GitHub (https://github.com/holgermlq/Limestone-and-granite-masonry-database-Portugal), thus allowing the broader scientific community to explore the datasets directly, as well as to add additional information that can be used to revise the current statistical models.

Chapter 4

Development of fragility functions

This chapter discusses the development of physical damage fragility functions for limestone and masonry buildings representative in Portugal. Two novel engineering demand parameters (EDPs) are proposed to measure the damage with a more accurate description of the damage in masonry buildings when subjected to earthquake loading.

Lovon H., Silva V., Vicente R., Ferreira T.M. (2022). Seismic Vulnerability Assessment of Portuguese Masonry Buildings (under review). *Engineering Structures*.

Also, the author participated in the implementation of the framework herein used for physical damage and fatality estimation to evaluate specific cases of adobe masonry buildings in Portugal. Outcomes of this research were published in doi: 10.3390/buildings11050200

Momin S., **Lovon H.**, Silva V., Ferreira T.M., Vicente R. (2021). Seismic vulnerability assessment of Portuguese adobe buildings. *MDPI – Buildings*, 11(5).

4.1 Numerical modelling strategy

Significant efforts regarding the computational analysis of masonry structures have been made in the last decades [94], [95], [150]. However, most of these efforts focused on the structural analysis of masonry buildings up to near-collapse state. The approach proposed herein is intended to model both, the collapse mechanism and the propagation of wall cracking, and use this information as EDPs. This strategy consists in uniformly discretizing the building into interlocked block elements connected by cohesive zero-thickness elements. Due to a large number of blocks per model, the complexity of the building geometry, and the number of analysed buildings, this procedure was implemented within a numerical framework that automatically uses the geometric and mechanical properties to define the characteristics of each building and generates the LS-Dyna input model, as depicted in Figure 4.1.

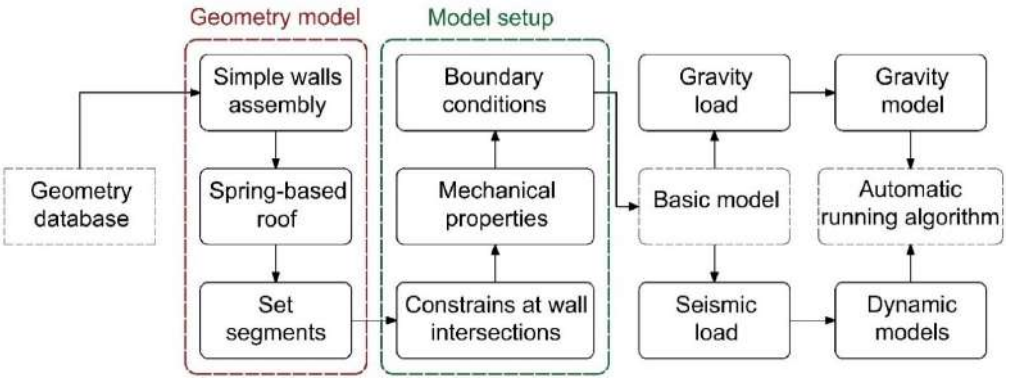

Figure 4.1 Procedure for the automatic generation of LS-Dyna input model

To reduce the computational effort and increase numerical stability, the blocks were assumed to have an elastic behaviour. The MAT_COHESIVE_MIXED_MODE element was used to model the cohesive material in the contact area between blocks. This numerical element displays a linear behaviour followed by a linear softening and quadratic mixed-mode damage formulation [30]. After

the failure of the cohesive elements, the blocks are released, and the software employs contact search algorithms to identify which blocks get into contact. The failure criterion can be expressed by equation Eq. 4.1

$$\left(\frac{\sigma_n}{\sigma_{n,u}}\right)^2+\left(\frac{\sigma_s}{\sigma_{s,u}}\right)^2\geq 1 \qquad \text{Eq. 4.1}$$

Where σ_n and σ_s are the shear and tensile stress in the interface, $\sigma_{n,u}$ and $\sigma_{s.u}$ are the shear and tensile maximum strength, respectively

The penalty stiffness approach is used for the treatment of elements in contact, as this modeling strategy has shown high numerical stability for the assessment of explicit collapse [30]. The method consists in verifying, at each time step, the projection distance of the slave node into the master segment. After that, if the slave went into the master segment, a spring is allocated in the corresponding node. The stiffness of the spring is calculated as a function of the elasticity modulus of the blocks, the size of the segments, and the penalty stiffness factor (Eq. 4.2). The spring has the intention to model the reaction forces generated from the contact between blocks. Finally, Coulomb friction was considered for slave nodes sliding above master segments.

$$k=\frac{f_s\cdot K\cdot A^2}{V} \qquad \text{Eq. 4.2}$$

Where K is the bulk modulus, A is the face area, V is the volume and f_s is the penalty stiffness factor, herein adopted as 1 according to Mendes et al [139]. All parameters are related to the element that contains the master segment.

The simulation of the effect of the floor diaphragm depends mainly on the stiffness and the quality of the connection with the walls. The timber slab was modeled as a set of only-compression linear springs in order to represent the most common inter-story configuration of this type of buildings. Figure 4.2 shows an example of a numerical model automatically generated. An interlocking effect is introduced by shifting the blocks in the horizontal plane.

Also, Figure 4.3 shows three different 3-storey buildings with different number of opening axis (2, 3 and 4), thus having different opening ratios. The same can be performed for buildings with 1 to 5 storeys.

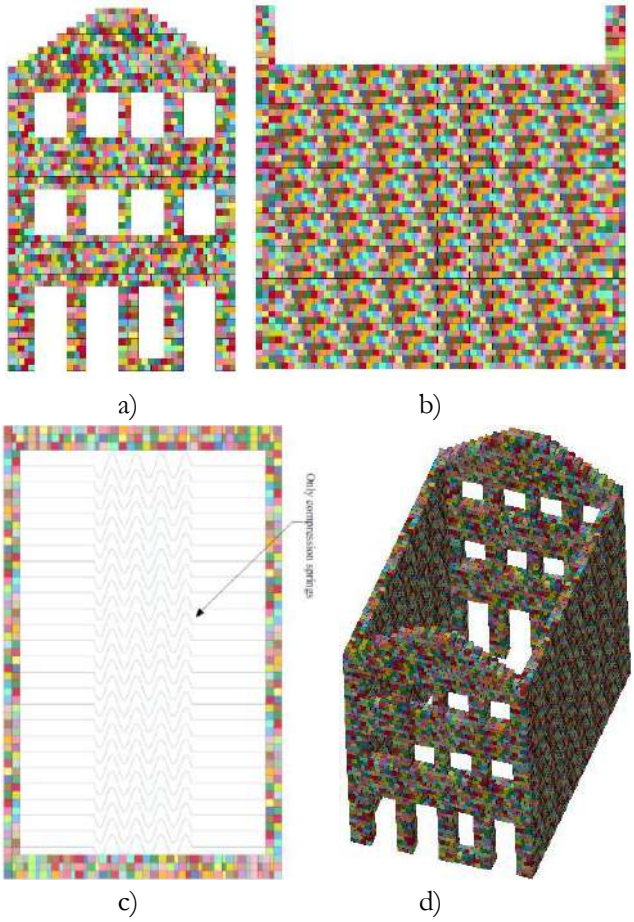

Figure 4.2 Numerical model of a 4-axis building type: a) front view, b) side view, c) plan view, and d) isometric view

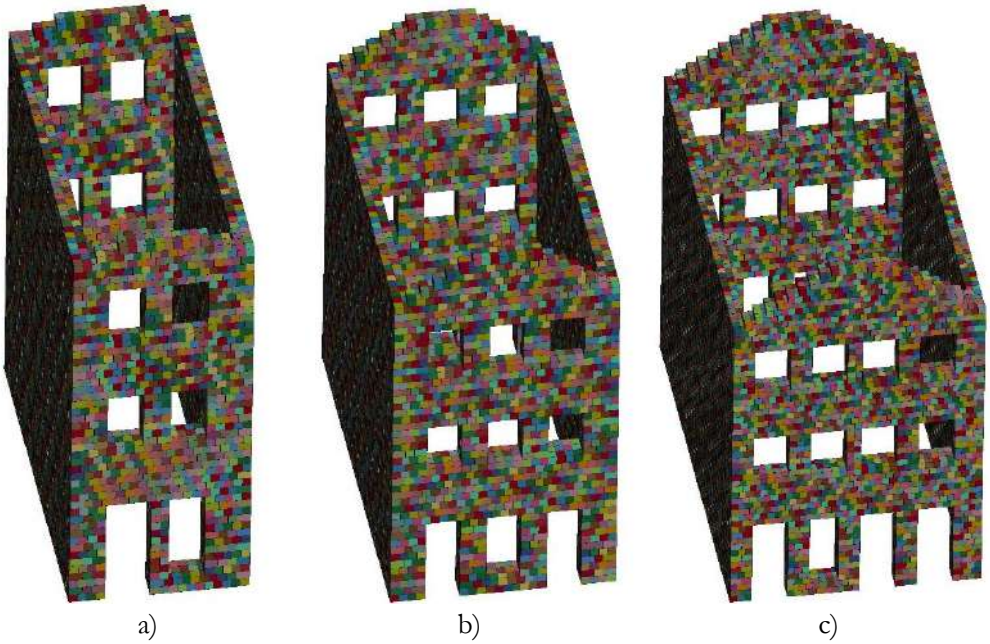

Figure 4.3. Sampled buildings exhibiting a) two, b) three, and c) four axis of openings.

Mechanical properties were defined according to the literature review performed in Section 3.4, a summary of the mechanical properties for limestone and granite masonry buildings is shown in Table 4-1.

Table 4-1 Mechanical properties for limestone and granite masonry buildings

Element	Description	Unit	Limestone	Granite	Source
Bricks (solid elements)	Elasticity modulus	GPa	0.76	0.93	Lovon et al. [151]
	Poison ratio	-	0.30		Alshawa et al. [32]
	Static coefficient of friction	-	0.80		Bakeer [152]
	Dynamic coefficient of friction	-	0.60		
	Penalty stiffness factor	-	1.00		Alshawa et al. [32]
Mortar (cohesive elements)	Normal failure stress	MPa	0.12	0.15	Lovon et al. [151]
	Shear failure stress	MPa	0.12	0.15	
	Normal energy release rate	N/m	30.00	36.00	Herein calibrated
	Shear energy release rate	N/m	30.00	36.00	
	Normal stiffness	GPa	0.76	0.93	Lovon et al. [151]
	Tangential stiffness	GPa	0.76	0.93	
Beams	Timber elasticity modulus	GPa	7.00		Moreira et al. [146]
	Design compressive strength	MPa	16.00		

4.2 Framework for fragility assessment

Fragility functions define the probability of exceeding a set of damage states conditional on a ground motion intensity measure (IM)[18]. The procedure adopted in this study for the derivation of fragility functions is illustrated in Figure 4.4. It consists of using the geometric and material parameters from Table 3-2 to generate either a single model, or a random population of buildings, thus allowing the propagation of the building-to-building variability. These models were assembled through an automatic process that generates the input models to the LS-Dyna software.

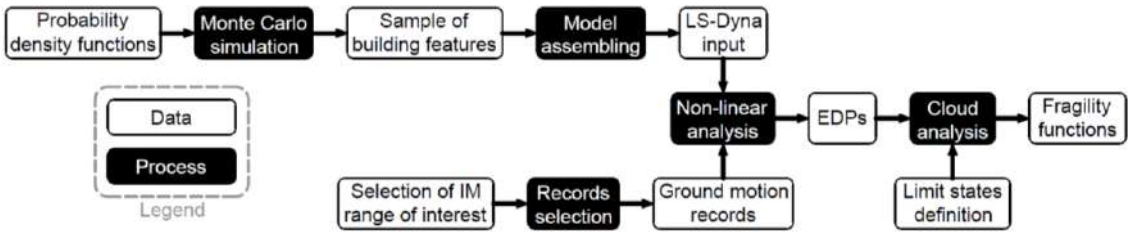

Figure 4.4 Representation of the procedure adopted for the derivation of fragility functions

A set of 48 ground motion records were selected from the European Strong Motion database, considering the tectonic environment of the country and the results from a seismic hazard disaggregation. Portugal is characterized by moderate-to-strong magnitude events located offshore (southwest of the country) and low-to-moderate magnitude events located mostly along the Tagus Valley (e.g., Vilanova & Fonseca [135]). Seismic hazard disaggregation analyses were performed for the most populous cities to identify the combinations of magnitude and site-to-source distances

affecting the country. Using this information, ground motion records from stable continental and active shallow regions were selected. Figure 4.5 shows the response spectrum of the selected ground motion records in both directions.

Finally, given the lack of empirical data to validate the numerical models and resulting fragility functions, our results were compared to some experimental results, and used to computed two seismic risk metrics. To this end, seismic hazard curves from the hazard model proposed by Vilanova and Fonseca [135] were computed. A similar approach for the generation of fragility functions has been proposed by Erberik [153], Silva et al. [14], and Villar et al. [5] for masonry buildings in Turkey, reinforced concrete structures in Portugal, and common building classes in South America, respectively.

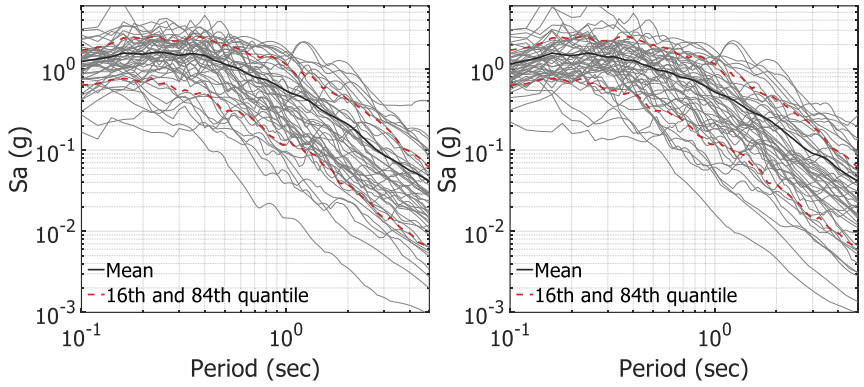

Figure 4.5 Response spectra in the a) N-S direction, b) E-W direction of records selected for fragility assessment

4.3 EDPs and damage criterion

The vast majority of the past vulnerability studies have used *EDPs* such as maximum inter-story drift ratio (e.g. [14], [59]) or the maximum global drift (e.g., [7], [14], [115]) to allocate buildings into damage states. Such an approach is particularly convenient when using simplified models to simulate the structural response of a building portfolio, such as single-degree-of-freedom oscillators (e.g. Villar et al. [5]) or mechanical models. However, the use of detailed 3D finite-elements models (such as those presented herein) enables the consideration of *EDPs* with a closer correlation to the actual damage. Moreover, the consideration of an *EDP* such as the maximum inter-story drift ratio could lead to biased results due to localized damage. Table 4-2 shows an example of predicted damage for a limestone masonry building of 3 storeys.

Table 4-2. Exampled of buildings per damage threshold, corresponding illustration and EDP

Damage state	EPD	Damage threshold	Illustrative damage	EDP value of the illustration
1	Cracked wall ratio	0.20	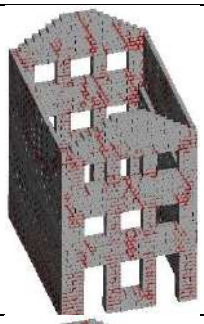	0.14
2		0.35	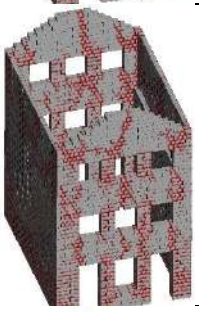	0.29
3		0.10		0.11
4	Volume loss ratio	0.25		0.26
5		0.60		0.41

4.4 Cloud Analysis

A cloud analysis procedure was used to calculate the statistical parameters of the fragility functions [108]. This method has been employed in several fragility assessment studies due to the low computational effort and the capability to incorporate a wide range of uncertainties such as the record-to-record and building-to-building variability [108], [113], [114]. The first step in the methodology consists of estimating a best-fit curve between log(IM) and log(EDP). We estimated this curve using the maximum likelihood method with a censored regression [115]. Homogeneity of variance is assumed for the IM-EDP relationship, and the expected value of log(EDP) and associated standard deviation can be described by the formulae below:

$$\begin{cases} E\left[\log\left(EDP|IM\right)\right] = \log\left(a\right) + b \cdot \log\left(IM\right) \\ \sigma_{\log\left(EDP|IM\right)} = \sqrt{\dfrac{\sum_{i=1}^{n}\left(\log\left(EDP_i\right) - E\left[\log\left(EDP_i|IM_i\right)\right]\right)^2}{n-2}} \end{cases} \quad \text{Eq. 4.3}$$

Where $\mathrm{E}[\log(EDP|IM)]$ is the expected logarithm of EDP given an IM, $\log(a)$ and b are the regression parameters of the best fit curve, $\sigma_{\log(EDP|IM)}$ is the logarithmic standard deviation of the distribution of log(EDP) given log(IM), and EDP_i corresponds to the i-th value obtained from the nonlinear dynamic analyses. If only one structure (i.e., numerical model) is used for the dynamic analysis, then the $\sigma_{\log(EDP|IM)}$ only represents the record-to-record variability (σ_{rtr}). If multiple structures are used, then the $\sigma_{\log(EDP|IM)}$ covers not only the variability due to the ground motion records but also the building-to-building variability (σ_{btb}). Since these two variables are not correlated, $\sigma_{\log(EDP|IM)}$ can be expressed as:

$$\sigma_{\log\left(EDP|IM\right)} = \sqrt{\sigma_{btb}^2 + \sigma_{rtr}^2} \quad \text{Eq. 4.4}$$

Considering both sources of variability in the fragility derivation process requires running hundreds of nonlinear dynamic analyses, whose computational burden might be cost-prohibitive when using complex 3D models. For this reason, it was decided to consider multiple structures for a single building class (3-story limestone buildings) to explicitly estimate both the σ_{rtr} and σ_{btb}. For the remaining typologies, we considered the full suite of ground motion records, but only one representative structural model. For these typologies, $\sigma_{\log(EDP|IM)}$ was estimated using the standard deviation from the best-fit curve and the σ_{btb} computed for the 3-story limestone building class, as further explained in this section.

The probability of exceeding a given damage state conditional on an IM ($P[EDP \geq ds_i | IM]$) can be computed using the statistical parameters defined by Eq. 1 and the following expression:

$$P\left[EDP \geq ds_i | IM\right] = 1 - \Phi\left(\frac{\log\left(EDP_{dsi}\right) - E\left[\log\left(EDP|IM\right)\right]}{\sigma_{\log\left(EDP|IM\right)}}\right) \quad \text{Eq. 4.5}$$

Where Φ is the cumulative standard normal distribution and EDP_{ds_i} is the EDP damage threshold for the respective damage state. This procedure is depicted in Figure 4.6a. The blue line represents the best fit curve in the log space. Three IMs are shown with their corresponding expected value

$\mathrm{E}[\log(EDP|IM)]$, assumed to be the mean of the Gaussian distributions with a constant standard deviation. The probabilities of exceedance are calculated as the shaded area above the damage threshold for each IM. These probabilities are plotted with their corresponding *IM* in Figure 4.6b. The parameters of a cumulative lognormal function can then be computed using these results.

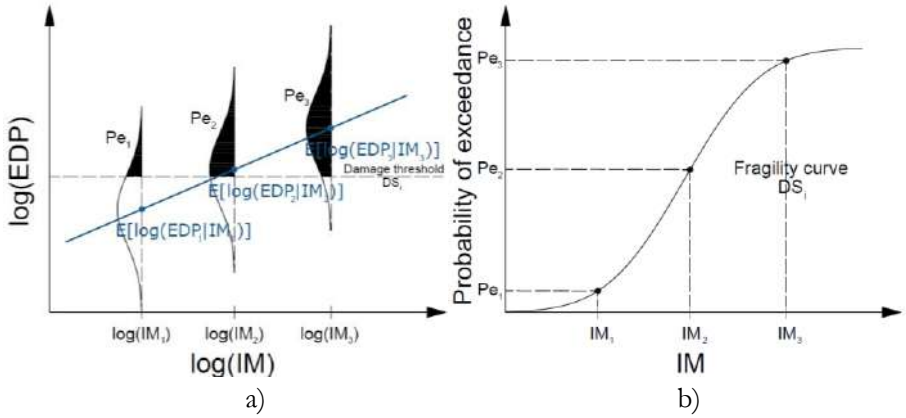

Figure 4.6 Schematic fragility assessment procedure a) probability of exceedance for 3 IMs for a damage state *i*, b) Fragility curves for damage state *i*.

4.5 Building-to-building and record-to-record variability

As previously described, the evaluation of the building-to-building variability can be performed by sampling several buildings. This analysis was carried out for 3-story limestone buildings with 20 randomly generated numerical models, sampled according to the procedure described in Section 3.1. Through cloud analysis, we calculated the record-to-record variability (σ_{rtr}) for each building (as indicated in Eq. 1). The best fit curve for each individual building according to the two *EDPs* is presented in Figure 4.7. Then, we performed the same calculation considering simultaneously the entire set of randomly sampled buildings. In this case, the resulting $\sigma_{\log(EDP|IM)}$ includes both the record-to-record and the building-to-building variability. The building-to-building standard deviation can be explicitly calculated by isolating the term σ_{btb} from Eq. 2. The resulting standard deviations for the 3-story limestone buildings are shown in Table 4-3.

For the selection of the IM, we tested PGA and Sa ranging between 0.1 and 1.5 secs. The IM exhibiting the higher *efficiency* (i.e., lower logarithmic standard deviation of the fragility function - σ) was chosen for the definition of the fragility functions. In addition to these common IMs, average spectral acceleration (AvgSA) was also considered. AvgSA is defined as the geometric mean of the spectral accelerations within a relevant interval of periods. It was considered an interval between 0.2T and 1.5T, as recommended by [87], [154], [155]. We assessed which central period, T, led to higher efficiency, considering a range between 0.1 to 1.5 sec. For most building classes SA at 0.4 sec and AvgSA with a central period of 0.5 sec led to a satisfactory *efficiency*. PGA led to higher efficiency for the 1-story typologies (characterized by a low elastic period of vibration).

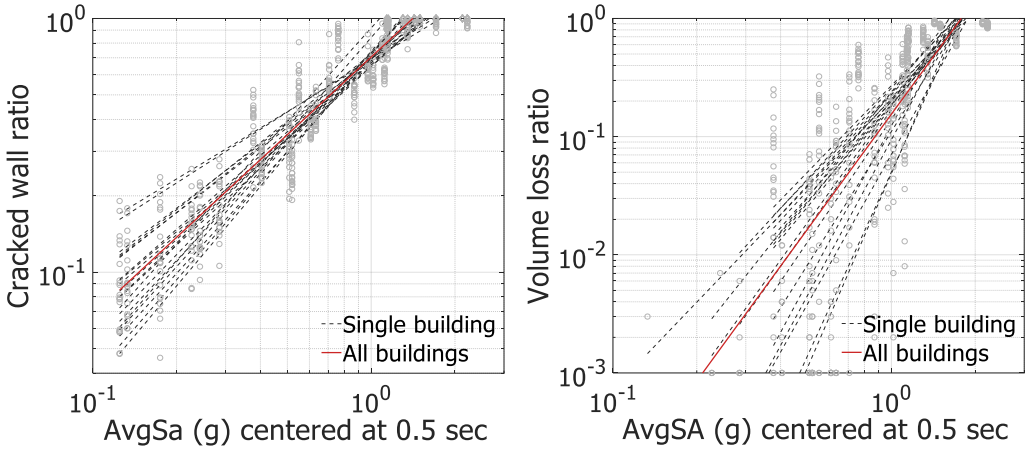

a) b)

Figure 4.7 Best linear fit for a) Crack propagation level and b) volume loss. The red dashed line is the best fit for the overall data, while the black-continuous line represents the best fit for each building.

Table 4-3 σ-values for 3-story building class

EDP	σ_{rtr}	σ_{btb}	σ_{total}
Cracked wall ratio	0.26	0.16	0.31
Volume loss ratio	1.28	0.74	1.48

These results indicate a higher contribution from the record-to-record variability to the total variability, which is in agreement with past studies that have assessed the impact of these sources of uncertainty in probabilistic risk metrics [116]. Moreover, the building-to-building variability estimated herein is identical to the values provided by Casotto et al. [156] and Silva et al. [14] for Italian and Portuguese RC buildings.

The progression of the regression parameters was recorded to investigate their convergence with the increase in the number of buildings analysed – Figure 4.8 shows the aforementioned progression. The average of the regression parameters was calculated each time one building was added, and the outcome was normalized to the total average considering all the buildings

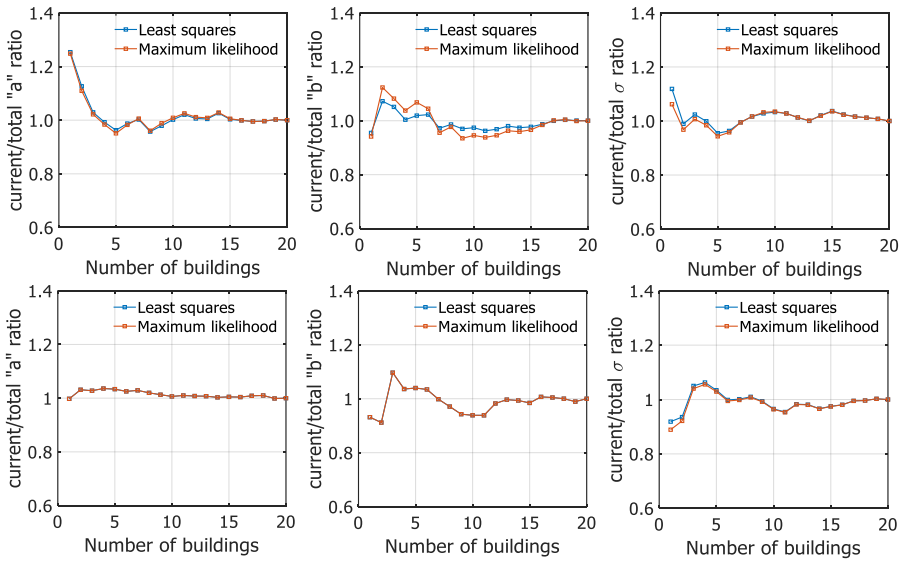

Figure 4.8 Progression of regression parameters along the number of sampled buildings

4.6 Fragility functions

The procedure described in section 4.2 was applied to each building class, considering the damage thresholds presented in Table 4-2. Figure 4.9 and Figure 4.10 present the fragility functions for the limestone and granite masonry buildings in terms of the conventional IMs, while Table 4-4 and Table 4-5 include the logarithmic mean (μ) and logarithmic standard deviation (σ). In order to compare our results with proposals from the literature, functions for similar building classes were included in Figure 4.9 and Figure 4.10. These include the fragility functions proposed by Borzi et al. [66] for Italian masonry buildings and the fragility functions developed by Martins & Silva [115] for global risk analysis. It should be noted that these existing models were not originally defined in terms of the IMs used herein.

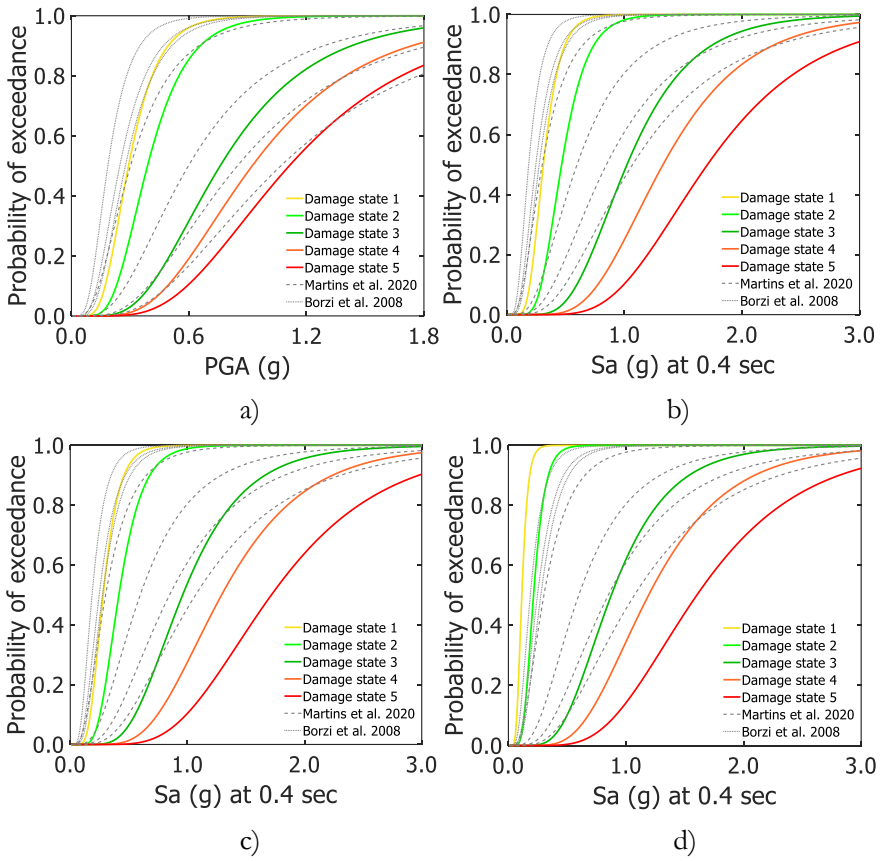

Figure 4.9 Fragility functions for a) 1-story, b) 2-story, c) 3-story, and d) 4-story limestone masonry buildings. Continuous lines show results from the present study and dashed lines curves from Borzi et al. [66] and Martins & Silva [115]

Table 4-4 Fragility function parameters for limestone masonry buildings

Building class	IM	Negligible to slight		Moderate		Substantial to heavy		Very heavy		Destruction	
		μ	σ	μ	σ	μ	σ	μ	σ	μ	σ
1-storey	PGA	-	0.411	-	0.411	-	0.494	-	0.494	0.107	0.494
2-storey	Sa (0.4)	-	0.364	-	0.364	0.022	0.422	0.284	0.422	0.535	0.422
3-storey	Sa (0.4)	-	0.385	-	0.385	-	0.429	0.256	0.429	0.541	0.429
4-storey	Sa (0.4)	-	0.362	-	0.362	-	0.440	0.175	0.440	0.470	0.440

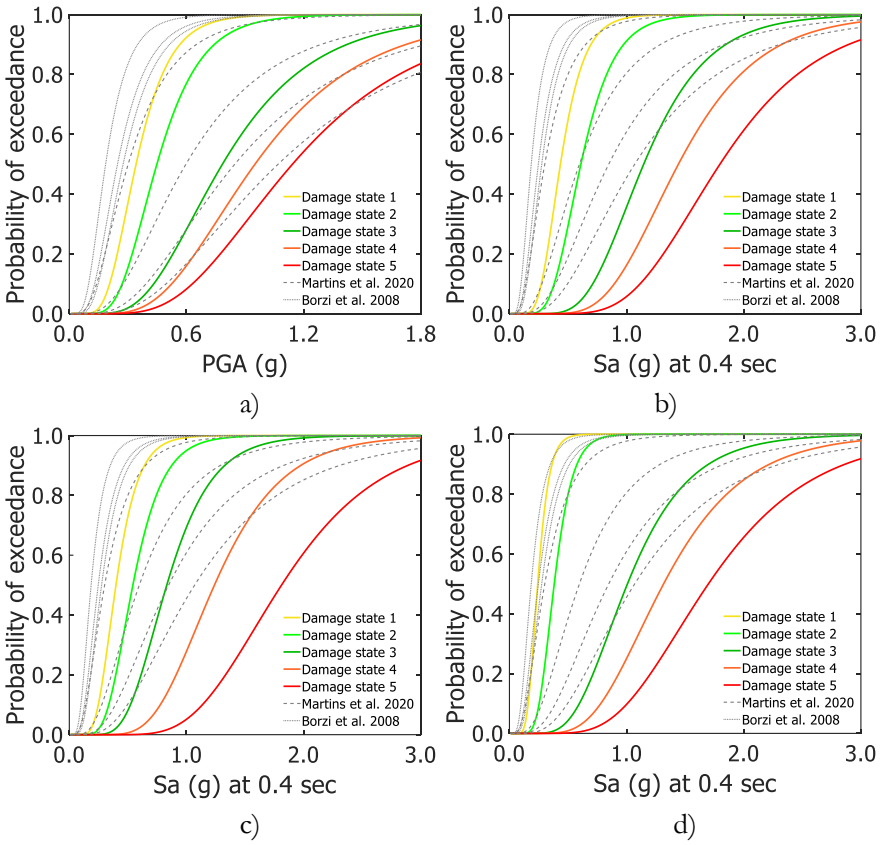

Figure 4.10 Fragility functions for a) 1-story, b) 2-story, c) 3-story, and d) 4-story granite masonry buildings. Continuous lines show results from the present study and dashed lines curves from Borzi et al. [66] and Martins & Silva [115].

Table 4-5 Fragility function parameters for granite masonry buildings

Building class	IM	Negligible to slight		Moderate		Substantial to heavy		Very heavy		Destruction	
		μ	σ	μ	σ	μ	σ	μ	σ	μ	σ
1-storey	PGA	-1.073	0.393	-0.802	0.393	-0.243	0.464	-0.050	0.464	0.134	0.464
2-storey	Sa (0.4)	-0.832	0.366	-0.495	0.366	0.136	0.372	0.366	0.372	0.586	0.372
3-storey	Sa (0.4)	-0.921	0.372	-0.612	0.372	-0.184	0.364	0.214	0.364	0.594	0.364
4-storey	Sa (0.4)	-1.422	0.320	-0.961	0.320	0.008	0.408	0.275	0.408	0.530	0.408

The validation, verification, and calibration of fragility models are one of the most challenging tasks in fragility assessment. Experimental and/or empirical data are scarce, and even when available, fragility models are ultimately probabilistic models that do not intend to provide exact predictions for all levels of ground shaking, but rather the expected damage on average. However, we can perform consistency checks to verify whether the numerical models lead to damage patterns in agreement with past experimental campaigns, as well as whether the resulting functions are comparable with models from the literature.

The fragility functions presented herein are slightly less vulnerable in comparison with the functions proposed by Martins & Silva [115]. Such results are expected given that the latter study used information regarding masonry structures typical from regions characterized by a high seismic

vulnerability (e.g., Turkey, Peru, Eastern Europe). In general, the comparison with experimental results and existing models indicates that the functions proposed herein are plausible.

4.7 Damage risk metrics

Finally, we estimated the expected annual probability of sustaining moderate damage or suffering collapse for three cities in Portugal with distinct levels of seismic hazard (Porto, Coimbra, and Lisbon). We considered the probabilistic seismic hazard model from Vilanova and Fonseca [135] to derive seismic hazard curves in terms of PGA and SA(0.4s), and computed the average annual probability of moderate damage (AAPM) and collapse (AAPC) following the procedure described in Lovon et al. [7]. Fragility functions for granite masonry buildings were used for Porto, while limestone was evaluated for the seismic hazard of Coimbra and Lisbon. The risk metrics for moderate damage and collapse are illustrated in Figure 4.11 for 1 to 4-story masonry buildings.

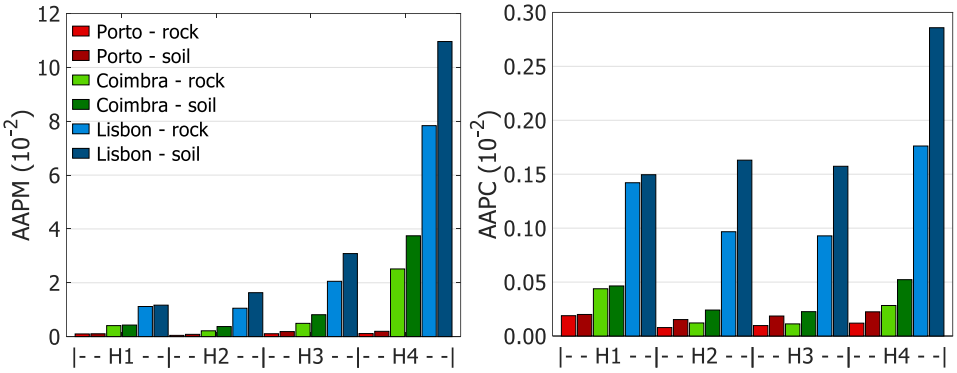

Figure 4.11 a) Average annual damage probability, and b) Average annual collapse probability for masonry buildings from 1 to 4 stories (H1-H4) in Porto, Coimbra, and Lisbon.

Both the annual probabilities of sustaining moderate damage and suffering collapse increase with the number of stories. Such a trend is expected given that the seismic demand increases with longer fundamental periods of vibrations (see response spectra in Figure 4.5), as well as the fact that P-delta effects were observed for the 3- and 4-story buildings. For what concerns the absolute values, some existing studies have suggested reasonable average annual collapse probabilities for modern construction (e.g. [157]–[159]). These past studies indicate annual collapse probabilities between 10^{-4} and 10^{-5}, depending on the level of seismic hazard of the region. The AACP presented herein is between 1 and 2 orders of magnitude above these values. These discrepancies are expected given that the building classes analysed herein are not code-compliant and have demonstrated a high vulnerability in past seismic events. Regarding the annual probability of sustaining moderate damage, Martins et al. [17] indicate values between 10^{-3} and 10^{-4} for code-compliant reinforced concrete buildings. The results from Figure 4.11 suggest a range between 10^{-1} and 10^{-2}; on average 2 orders of magnitude higher. This difference is considered reasonable, once again, because these building classes do not have any seismic provisions and masonry construction tends to have a much brittle behaviour than reinforced concrete (i.e., lower-yielding drifts) due to the low displacement capacity. These average annual probabilities also agree with the values Martins and Silva [17] proposed for similar building classes subjected to moderate and high seismic hazard.

4.8 Final remarks

A numerical strategy modelling for limestone and granite masonry buildings was implemented in the current chapter. The implementation of the aforementioned approach required the development of algorithms capable to automatize the generation of the blocks that shapes the building.

A damage threshold was defined with basis in past studies and the recommendations from EMS-98 scale using two novel EDPs. The Cracked wall ratio, defined as the ratio between the cracked area and the area of potential cracks, is used for the first two damage states. The volume loss ratio is defined as the ratio between the debris and the original volume of the structural elements. The model seems to predict accurately both EDPs.

The building-to-building variability was explored by sampling a set of 3-storey limestone masonry buildings and tracking the regression parameters. It was found that regression parameters remain stable after sampling around 20 buildings. The uncertainties associated to the building-to-building and record-to-record variability were separated for the two EDPs herein used. It was found that record-to-record variability is the main source of uncertainty, but building-to-building variability is still a significant proportion of the total variability.

A set of representative archetypes were selected and tested against the set of records for deriving fragility functions for the remaining building classes. EDPs were gathered for each realization and fragility functions were obtained. Verification checks were performed by comparing the results obtained with fragility models of other authors. The average annual moderate damage probability and collapse probability were obtained and compared with databases and past studies.

Chapter 5

Fatality vulnerability functions

This chapter addresses the framework proposed for fatality vulnerability assessment. Advanced numerical models developed in chapter 4 are improved and used to predict the Internal Volume Reduction (IVR), a good predictor of fatalities due to earthquakes. Two earthquake scenarios are developed to explore potential human losses in active seismic zones of the country. Results from this chapter were submitted as:

Lovon H., Silva V., Vicente R., Ferreira T.M. (2022). Analytical Vulnerability functions for the assessment of fatalities in masonry buildings (in preparation).

5.1 State-of-practice in seismic fatality vulnerability assessment

The estimation of fatalities and injured due to the impact of earthquakes is a fundamental metric for the development and implementation of risk reduction strategies (e.g. Jonkman et al. [160], Tsang and Wenzel [161], Sinković and Dolšek [162]). In fact, international agendas such as the Sendai Framework for Disaster Risk Reduction or the United Nations 17 Sustainable Development Goals ask specifically for the reduction in the human impact due to natural hazards. The assessment of the impact of earthquakes in livelihoods requires models that can relate directly the expected ratios of building occupants into different injured levels conditional on an intensity measure (IM) (i.e., fragility functions). Alternatively, a model that relates directly the probability of fatality conditional on an IM can also be used (i.e., vulnerability functions). However, the vast majority of the existing fragility studies focused on the assessment of structural damage (Yepes et al., [163]), or in the expected economic losses (e.g., ref. [164], [165]). This lack of fragility or vulnerability functions to evaluate the human impact hinders the availability, accuracy and reliability of fatality modelling studies.

Past efforts regarding the assessment of human losses followed mainly two approaches: 1) empirical functions based on databases of human losses, and 2) hybrid approaches that combine fragility functions with empirical (or expert judgement) fatality rates. The former approach consists on the development of statistical models that relate directly fatality rates with a magnitude or an IM (e.g., Moment magnitude - Mw or Modified Mercalli Intensity - MMI). For example, the PAGER group of the United States Geological Survey developed a set of global empirical vulnerability functions that allows estimating the fraction of population expected to perish based on MMI (Jaiswal et al. [121]). This model is used within the well-known PAGER Alerts to estimate first-order human losses, and are well-calibrated for regional analysis. Such models do not consider directly the local building stock nor the expected extend of damage. Similarly Samardjieva & Badal [120] proposed empirical relationships between Mw and number of casualties. In the second approach, the assessment of human losses or population left injured is performed through the application of ratios that convert the probability of complete damage into probability of structural collapse, which is then further converted into probability of fatality (or injured) based on empirical fatality/injured rates conditional on structural collapse (e.g., Spence [26], FEMA [21]). This approach has the advantage of allowing users to take advantage of the multitude of existing fragility functions originally derived for structural damage (e.g., ref. [13], [122]), but the employment of such rates might lead to unrealistic fatality rates, in particular for seismic events where extreme shaking is observed. This issue is illustrated in Figure

5.1. In this example, an existing fragility function (i.e., 2-storey unreinforced masonry) for complete damage (i.e., herein termed as DS4) is converted into probability of collapse using a collapse probability conditional on complete damage ($P[col|DS4]$), and then converted into probability of fatality using a fatality rate conditional on structural collapse ($P[F|col]$). The collapse and fatality rates (15% and 20%, respectively) were extracted from the HAZUS manual (FEMA 2004), and the expected fatality rate conditional on an IM ($E[FR|IM]$) can be described by the following equation:

$$E\left[F|IM\right] = P\left[F|col\right] \times E\left[col|DS4\right] \times E\left[DS4|IM\right] \quad \text{Eq. 5.1}$$

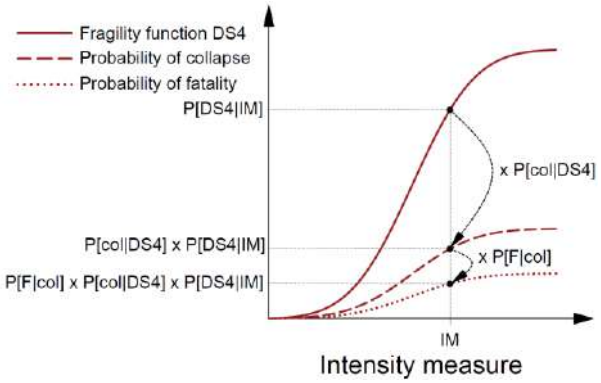

Figure 5.1 Procedure to derive a vulnerability function in terms of fatality rates, starting from an existing fragility function for structural damage.

This approach for the derivation of fatality vulnerability leads to a rapid saturation of the fatality rates, even for extremely high seismic intensities, and potentially to an underestimation of the expected losses for strong seismic events. For example, the average fatality rates for the collapsed buildings in the 2019 M6.4, Durres (Albania) and 2020 M6.7 Elazig (Turkey) earthquakes were 45% and 46%, respectively [22]. One of the limitations of this approach is the reliance on traditional damage states and conventional engineering demand parameters (EDPs – e.g., maximum interstorey drift ratio) which cover a wide range of building destruction (i.e., from damaged beyond repair to complete collapse), which will naturally influence the likelihood of fatal injuries (e.g., Crowley et al. [18]; Abeling and Ingham [118]).

It is thus important to consider alternative approaches to measure the level of damage in buildings exposed to strong ground shaking. So [24] did a thorough review of damage and fatality data from 25 fatal earthquakes between 1968 and 2011, and established a correlation between typical volume loss and fatality rates for several building classes. Lida et al. [28] proposed four parameters to characterize the extend of collapse of buildings (volume loss, plan loss, section loss and amount of dust), and defined fatality vulnerability function for wooden structures in Japan. Abeling & Ingham [118] used survey data from the M7.1 2010 Darfield and M6.2 2011 Christchurch earthquakes to evaluate the correlation between volume loss and fatality ratios. In all cases, a remarkable correlation between volume loss and fatality rates were observed. However, such metrics are difficult to obtain empirically, in particular for earthquakes with long sequences of events where damage accumulation is expected. Moreover, this approach is only possible to pursue in regions frequently affected by earthquakes. Alternatively, volume of loss or volume of survivable space can be estimated analytically, using advanced tree-dimensional numerical models.

5.2 Framework for fatality vulnerability assessment

The estimation of fatalities due to earthquakes has been the target of several past studies, which correlated different predictor variables with the likelihood of fatalities such as earthquake magnitude [120], macroseismic intensity [121] and physical damage [18]. With the significant advancements in numerical modelling of masonry buildings, it is possible to simulate explicitly structural collapse. For example, Grant et al. [166] modelled a 2-storey unreinforced masonry building typical from the Groningen region (Netherlands), and quantified the probability of explicit collapse through nonlinear time history analysis. This type of analysis allows taking advantage of engineering demand parameters (EDPs) that characterize explicitly the level of destruction. The framework for fatality vulnerability assessment followed in this study starts with the generation of a single or multiple 3D building models, based on existing geometric and mechanical models (see Table 3-2, Table 3-4and Table 3-5). These models are subjected to nonlinear dynamic analyses using a set of ground motion records, and an algorithm is used to estimate the volume loss resulting from each analysis. This framework is depicted in Figure 5.2, and each step is further described in the following sections.

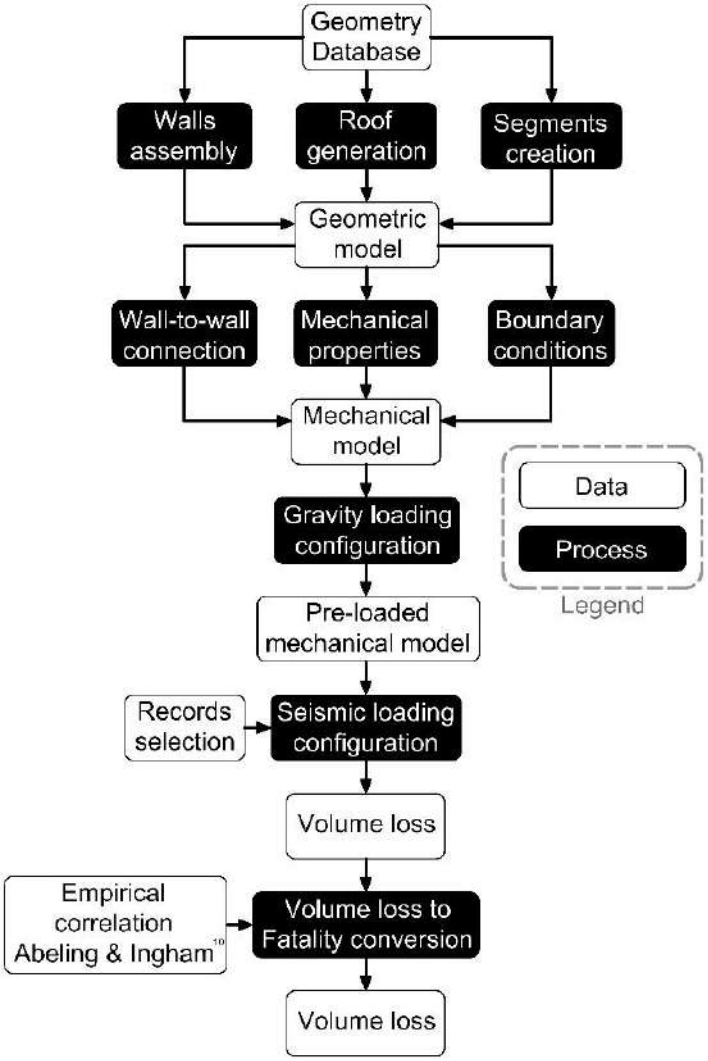

Figure 5.2 Algorithm flowchart for automatic models generation.

We created 3D numerical models for 1, 2, 3 and 4-storey limestone and granite buildings. A representative archetype was selected for each building class in order to keep low the computational effort. The 8 archetypes were tested against the 48 records previously gathered (review section).

As previously mentioned, the vast majority of the studies on fatality modelling use existing fragility functions (for complete or near-collapse damage states), which usually use engineering demand parameters (EDPs) such as maximum inter-storey or global drift. However, field data-based studies [22] indicate that the likelihood of mortality is strongly correlated with the level of destruction of buildings, which correlates well with the volume loss [24], [118]. This parameter is defined by Okada [123] as the reduction of "survival space" inside the building. The survival represents the volume of the plan area of the building in the first two meters, as illustrated in Figure 5.3.

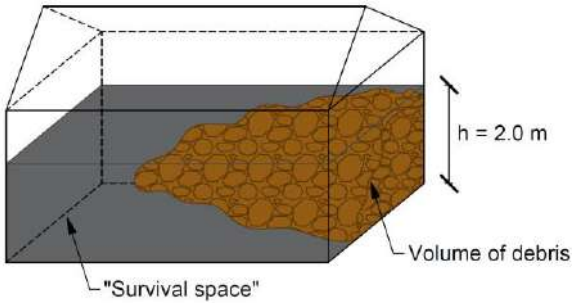

Figure 5.3 Volume loss (i.e. loss of survival space due to debris fall) [123].

An IVR is computed for each storey, and the average value across all storeys is used. For the cases where a particular storey collapsed (for example, the top floor), a value equal to 1 for the IVR was assumed. Moreover, collapse is assumed when the volume loss is higher than 60 % as proposed by So [24] for similar building classes. A routine was implemented in LS-Prepost [167] in order to calculate both the IVR and the volume loss of structural elements. The procedure to calculate the fatality ratio based on the IVR is depicted in Figure 5.4, and it consists of three steps. First, the IVR is calculated from structural analysis, leading to pairs of IM versus IVR. Second, the IVR is associated to a fatality ratio (FR), resulting in pairs of IM versus FR. Then, the fatality vulnerability functions are obtained using the scatter of pairs between IMs and FRs.

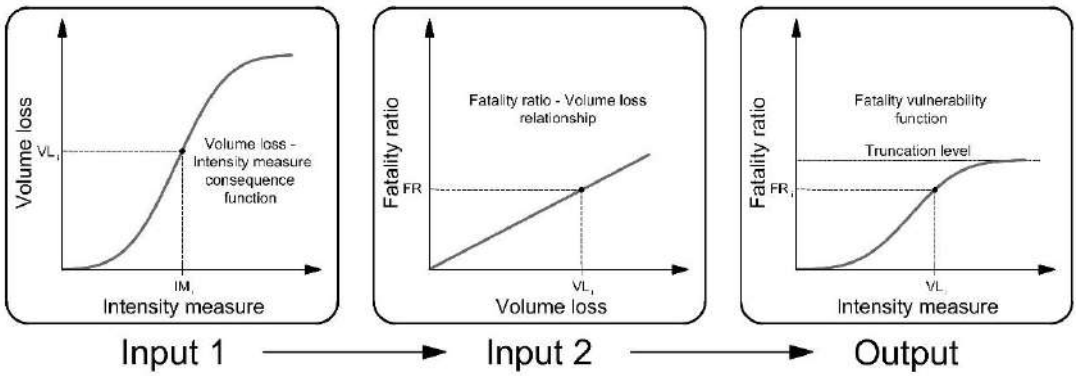

Figure 5.4 Procedure for fatality vulnerability assessment.

The IVR – FR relationship is a key input for the model. Past studies have explored this relationship for fatality modelling [25], [118], [168]. In this study, two options for the IVR – FR relationship are

used: the Abeling and Ingham [118] linear correlation, and an equation fitted to the IVR – FR data shown in the work of Spence and So[25], with the following expression:

$$FR = e^{0.932 \cdot IVR} - 0.867 \cdot IVR - 1 \qquad \text{Eq. 5.2}$$

Where the IVR and the FR are both expressed as fractions. The data presented by Spence and So[25] considered damage and fatality observations from 47 seismic events that occurred in regions such as Europe, Latin America, United States and Asia. These models are depicted in Figure 5.5, and both approaches were used for the development of earthquake scenarios for Portugal, as described in Section 5.

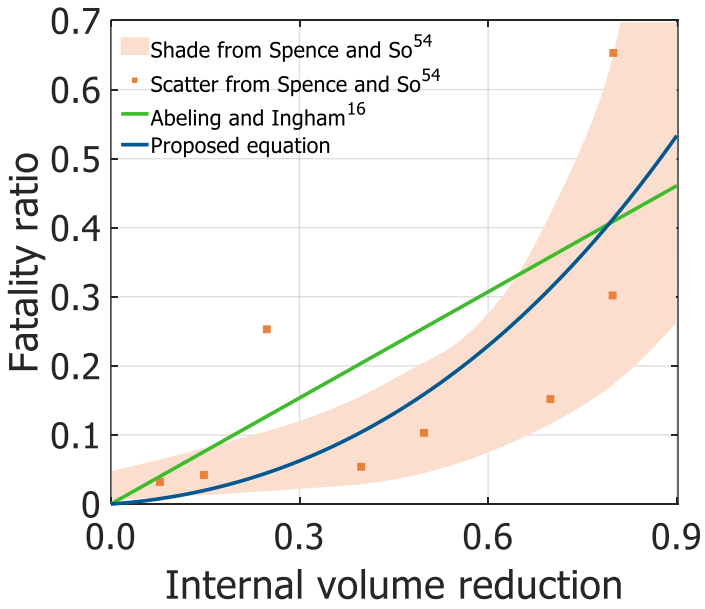

Figure 5.5 Fatality ratio – Internal volume loss relationships.

The FR – IM pairs are fitted to a truncated lognormal cumulative density function, as shown in equation 5.

$$FR = a \cdot \Phi\left(\frac{\ln(x) - \theta}{\beta}\right) \qquad \text{Eq. 5.3}$$

Where a is the maximum FR obtained from all the analyses, θ is the logarithmic mean, and β is the logarithmic standard deviation, both obtained using the least squares method.

5.3 Failure mechanisms

The evaluation of the most likely failure mechanism is fundamental to ensure that numerical models depict adequately the expected seismic behaviour of the targeted building typologies. Due to the absence of destructive events in the last decades in continental Portugal, there is a lack of damage data for these building typologies. Thus, the expected damage patterns must be inferred from similar types of construction, or from experimental campaigns. From these data sources [11], [169]–[171], we identified two main expected failure mechanisms. The first failure type is the so called "zero" mechanism [119] and it is one of the primary cause of collapse. It consists in the disaggregation of masonry elements due to the poor quality and lack of capacity to resist horizontal forces, as depicted

in Figure 5.6a. The second failure type is the out-of-plane mechanism, which consists in the total or partial overturning of a façade. This mechanism depends on the height/thickness relationship and the quality of the connection between perpendicular walls and floors. An example of out-of-plane mechanism can be seen in Figure 5.6b.

a) b)

Figure 5.6 a) "Zero" collapse mechanism, b) out-of-plane failure mechanism [172] observed in the Mw 5.9 L'Aquila Earthquake

Wall vertical instability, bending rupture, corner overturning and roof pounding are other important mechanisms regarding residential buildings that have been reported in past earthquakes. Further information related to failure mechanisms and their contribution to damage levels can be found in [119].

These numerical models allowed the simulation of several common collapse mechanisms, including the two main mechanisms previously described (i.e. "zero" and out-of-plane collapse mechanisms), as depicted in Figure 5.7.

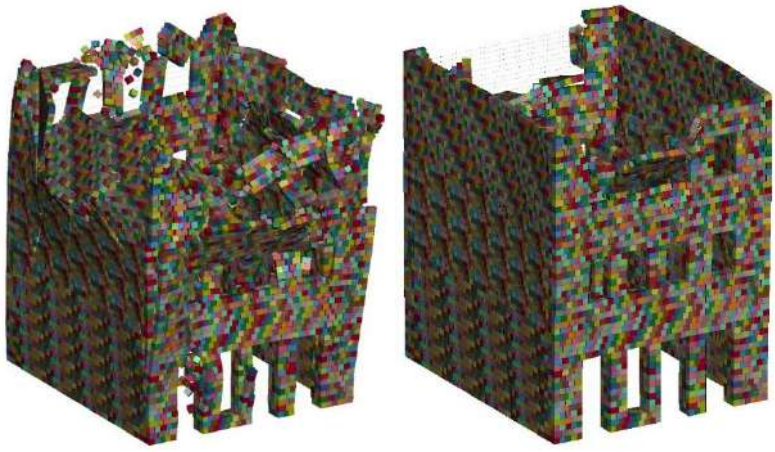

a) b)

Figure 5.7 Prints of structural analysis in hidden mesh, a) "zero" collapse mechanism, and b) Out-of-plane collapse mechanisms in the upper storey of the front façade.

5.4 Results and comparison with conventional models

In this section we present the results of the vulnerability functions developed herein, considering four methods. Approaches A and B use the relationships in terms of IM versus IVR derived in this study, but Method A uses the model to convert IVR to FR from Abeling and Ingham [118], while Method B uses the equation fitted to the data shown by Spence and So[25]. For approaches C and D, we used the fragility functions for complete damage and collapse proposed by Lovon et al. [173] for the same building typologies, which were then converted into probability of fatality using the ratios proposed by HAZUS. Approaches A and B aim at demonstrating the value in using an EDP (i.e. IVR) that has a strong correlation with fatalities, while methods C and D represent the conventional approach to fatality modelling, in which existing fragility functions for structural damage are adjusted. For the sake of clarity, these four methods are summarized in Table 5-1. All of the fatality vulnerability functions are presented in Figure 5.8 and Figure 5.9.

Table 5-1 Summary of the fatality vulnerability assessment approaches.

Approach	Estimation of IVR or probability of collapse	Estimation of fatality rates
A	IVR computed based on the nonlinear time-history analysis in LS-Dyna within this study.	Fatality rates estimated using the IVR-FR model proposed by Abeling and Ingham [118]
B		Fatality rates estimated using Equation 4, which was derived using the data from Spence and So [25].
C	Probability of collapse provided directly by the fragility functions derived by Lovon et al. [173]	Fatality rates estimated using rates proposed by HAZUS (i.e., 10%).
D	Probability of collapse estimated using the complete damage fragility functions derived by Lovon et al. [173], and the collapse rate given complete damage proposed by HAZUS (i.e., 15%)	

In general, all methods agree on the minimum level of ground shaking after which fatality rates start to increase. This is mostly due to the fact that before ground shaking values between 0.5g and 0.8g of Sa at 0.4 sec, structural damage is limited. Approach A is more conservative than approach B, a trend that was expected given that the linear regression proposed by Abeling and Ingham [118] leads to higher fatality rates for most of the IVR values, as shown in Figure 5.5. The same occurs when comparing approach C with D, however in this case the difference can be explained by the use of the collapse rates from HAZUS in approach D (which limits the probability of collapse to a maximum value of 15%), while approach C uses directly the collapse fragility curves from Lovon et al. [173], which can go up to 100% probability. It is interesting to note that for 1-storey masonry buildings, approach B and D lead to similar results. The IVR computed in approach B for this building class is relatively low, given that even if most of the external walls collapse, some survival space still remains. Moreover, due to the lack of upper floors, there is a lower likelihood of a catastrophic collapse. Likewise, the collapse rates proposed by HAZUS are equally low (i.e., 15%), potentially due to the fact that such rates were defined based on observations from earthquakes that occurred in the United States, in regions whose built environment is predominantly characterized by low-rise wooden buildings.

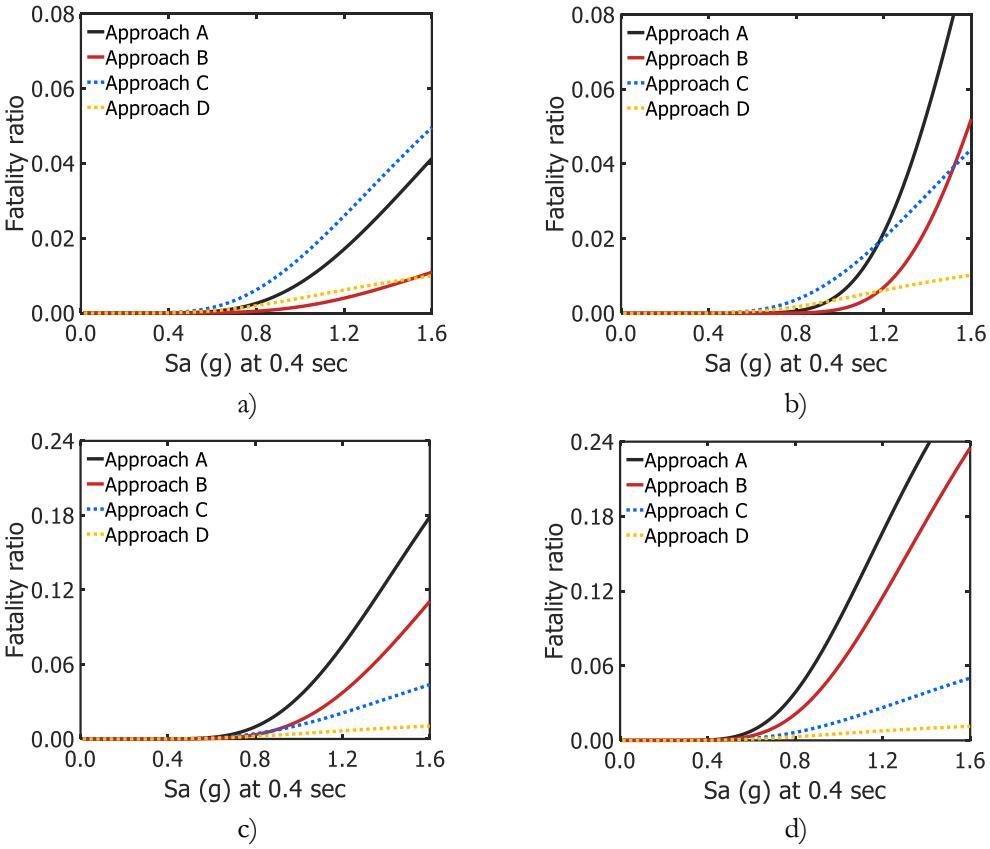

Figure 5.8 Fatality vulnerability functions for limestone masonry buildings of a) 1-storey, b) 2-storeys, c) 3-storeys, d) 4-storeys.

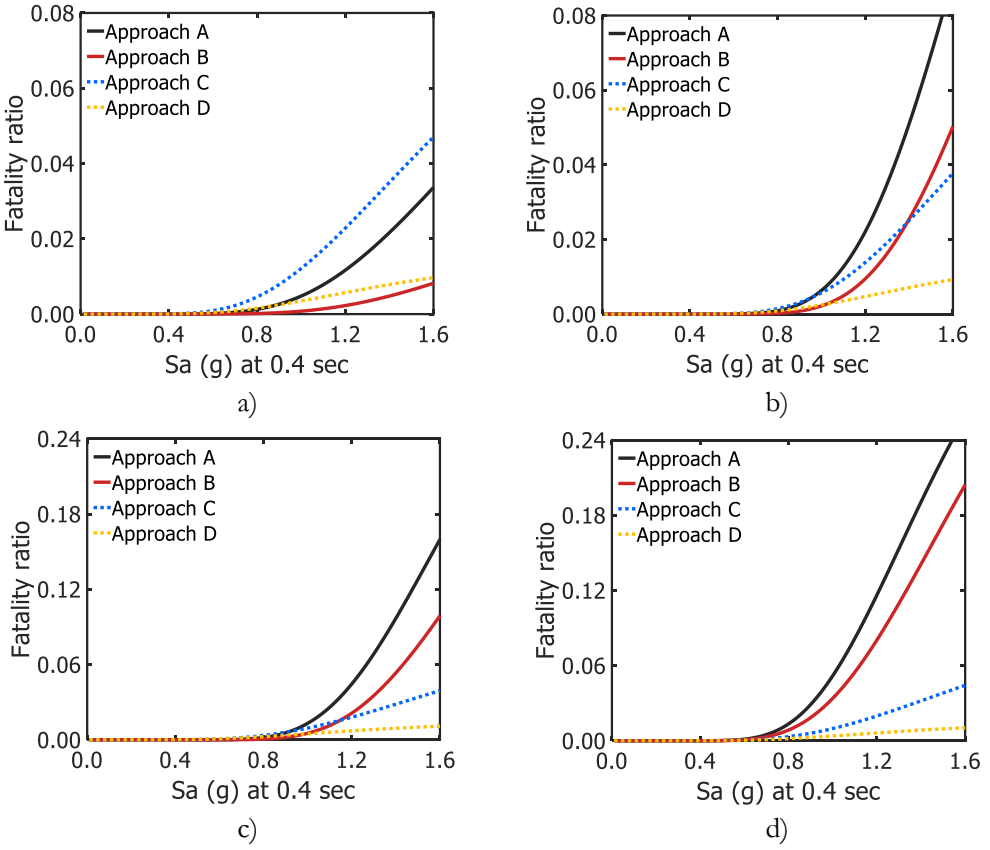

Figure 5.9 Fatality vulnerability functions for granite masonry buildings of a) 1-storey, b) 2-storeys, c) 3-storeys, d) 4-storeys.

From these results, we argue that approach B is the most balanced and suitable method for the assessment of fatalities. This approach uses the IVR as the EDP which has a stronger correlation with fatalities, and Equation 4 for the conversion of IVR into FR, which despite the limited data, leads to a better fit (see Figure 5.5). Table 5-2 summarizes the parameters for the fatality vulnerability functions (according to equation 5) using approach B. These functions are used in Section 5 to estimate average annual fatalities for selected Portuguese cities and the number of fatalities for two earthquake scenarios.

Table 5-2 Parameters of the fatality vulnerability functions

Type of stone	Number of storeys	Fatality vulnerability function parameters		
		a	θ	β
Limestone	1	0.038	0.707	0.417
Limestone	2	0.233	0.666	0.256
Limestone	3	0.340	0.638	0.370
Limestone	4	0.432	0.426	0.392
Granite	1	0.040	0.781	0.379
Granite	2	0.233	0.706	0.300
Granite	3	0.340	0.631	0.292
Granite	4	0.430	0.492	0.348

5.5 Fatality risk metrics and earthquake scenarios

Risk metrics are compared in this section in order to perform a consistency check against the outcomes of other fatality modelling studies. The individual annual fatality risk inside of a building is herein calculated by a convolution process between the hazard curves computed using the model from Vilanova and Fonseca [135], and the fatality vulnerability functions shown in Figure 5.8 and Figure 5.9 (using Approach B). The hazard curves were calculated for three densely populated cities in Portugal with distinct hazard levels: Porto (low hazard), Coimbra (moderate hazard), and Lisbon (high hazard). Vulnerability functions for granite buildings were used for Porto, and while functions for limestone buildings were applied to the cases of Coimbra and Lisbon. The average annual fatality rates for the three cities are presented in Figure 5.10.

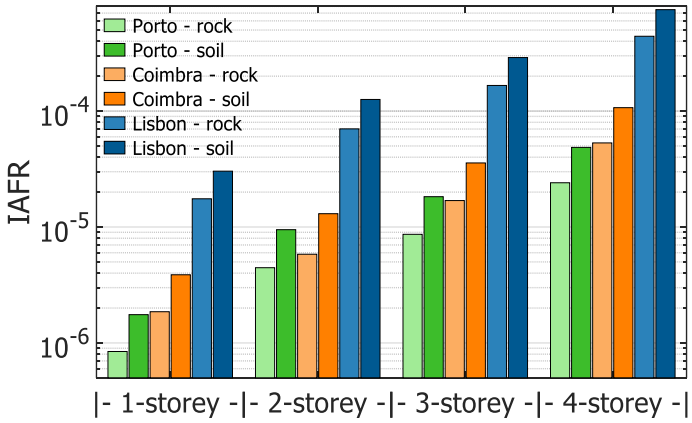

Figure 5.10 Individual annual fatality risk for 1 to 4-storey masonry buildings in Porto, Coimbra, and Lisbon considering rock and soft soil conditions.

Individual annual fatality risk (IAFR) is a common risk measure that indicates the probability of loss of life of a single unprotected person inside of a building. Several past studies [161], [174], [175] indicate that IAFR may vary depending on the type of activity and potential benefits. Some existing literature and standards (e.g., ISO [176] standard, Ale [177]) agree on an acceptable IAFR equal to 10^{-6}. Despite the fact that such studies do not specify the reason associated to collapse, the proposed tolerated IAFR has been widely used for the calibration of the probability of collapse in risk-targeted seismic hazard assessment [161], [162], [178], [179]. Other studies addressing events more closely related to earthquakes (e.g., Diamantidis et al. [180]) propose an acceptable IAFR of 10^{-5} for structures subjected to geohazards. Similarly, Silva et al. [159] proposes an acceptable IAFR of $5x10^{-6}$ for risk-targeted hazard maps in Europe. Liel and Deierlein [164] calculated the IAFR for RC code-compliant buildings with 1 to 4 storeys in California, and indicated a range for this metric between $2x10^{-6}$ to 10^{-5}. In the present study, values ranging between $2x10^{-5}$ to $2x10^{-3}$ are shown, which are clearly higher than the aforementioned thresholds. However, the building classes covered herein are vulnerable typologies, whose associated risk will obviously be much higher than that of recent buildings designed according to modern seismic codes. According to damage observations from X and Y earthquakes, the collapse rate of masonry buildings was A times greater than that of modern reinforced concrete buildings. If adjusted to the values presented herein by this ratio, then they match the range of IAFR for modern construction.

The assessment of earthquake scenarios is an extremely useful tool for disaster preparedness (e.g. Mendes et al. [181], Sousa [182]) and long-term risk management (e.g. Sengezer and Koç [183]). The development of earthquake scenarios has been widely used in Portugal for disaster preparedness, earthquake drills, and risk awareness campaigns. Carvalho et al. [184], and Oliveira [185] proposed two earthquake scenarios covering the southwest region of the country, which is characterized by a higher concentration of population and seismic hazard. These studies agree in proposing two hypothetical earthquake scenarios corresponding to: a) a moderate magnitude event associated to shallow crustal faults located near the Metropolitan Area of Lisbon (MAL), and b) a strong magnitude event produced near the "Marques de Pombal" fault. One must note that the stronger event is not meant to replicate the consequences of the well-known Great Lisbon Earthquake of 1755, that devasted the capital and the Southwest of the country. In fact, the location of the event and the ground motion model adopted herein (see Table 5-3) lead to a distribution of ground shaking in the country that is relatively low (i.e., PGA < 0.15g). Nonetheless, such event allows demonstrating the potential use of such scenarios.

It is well known that occupancy rates change significantly for residential buildings during the day, and therefore the time of occurrence of the event plays an important role in the assessment of fatalities. In this study, we considered that seismic events can happen during the day or the night, and the loss calculations were performed at the municipality level according to the European exposure model developed for Portugal [48]. The calculation of ground motion fields and losses was performed using the OpenQuake-engine (Pagani et al. [186]), and the four approaches presented in Section 4. Site effects were considered as proposed by Silva et al. [187]. The seismogenic properties of the earthquake scenarios and a summary of the results are shown in Table 4 and Table 5, respectively. The distribution of losses per municipality are shown in Figure 5.11 and Figure 5.12 for the onshore and offshore events, respectively.

Table 5-3 Earthquake rupture features

Earthquake scenario	Epicentre		Strike	Dip	Rake	GMPE
	Latitude	Longitude				
Onshore 5.5 Mw	38.72	-8.88	220°	55°	0°	Atkinson and Boore [188]
Offshore 8.6 Mw	36.50	-10.00	35°	40°	90°	Akkar and Bommer [189]

Table 5-4 Average human losses for the two earthquake scenarios.

Earthquake scenario	Daytime	Approach A		Approach B		Approach C		Approach D	
		Mean	Std	Mean	Std	Mean	Std	Mean	Std
Onshore 5.5 Mw	Day	106	88	61	57	132	47	28	8
	Night	488	404	280	264	609	218	131	37
Offshore 8.6 Mw	Day	45	68	22	38	18	19	7	7
	Night	207	315	103	174	85	89	34	30

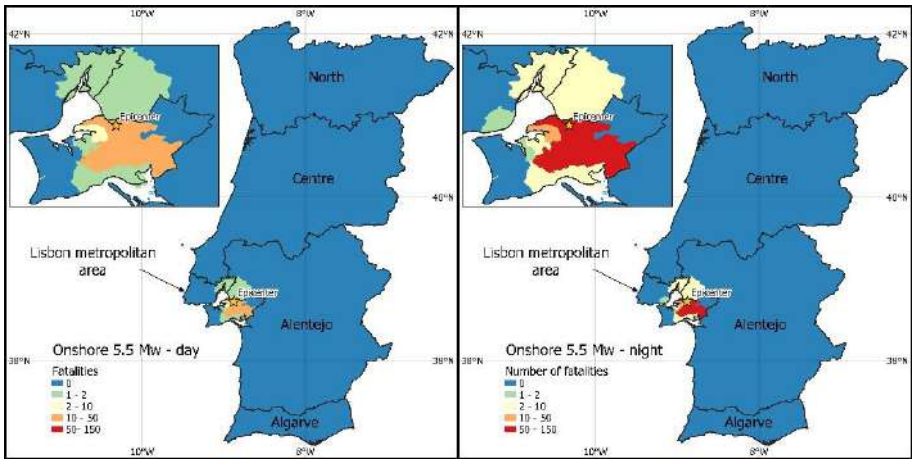

Figure 5.11 Fatality loss map for Onshore 5.5 Mw earthquake scenario occurred during a) day, and b) night using Eq. 4. Portuguese regions according to NUTS-II

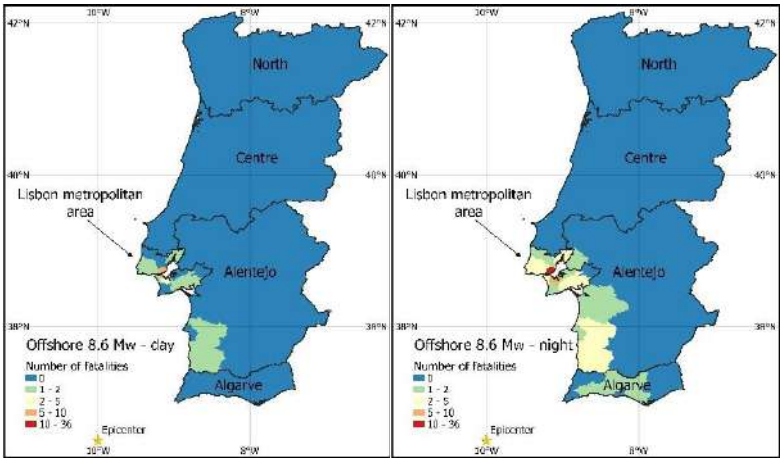

Figure 5.12 Fatality loss map for Offshore 8.6 Mw earthquake scenario occurred during a) day, and b) night using Eq.4. Portuguese regions according to NUTS-II

The results from the earthquake scenarios indicate that for most of the combinations, Approach A (IVR + Abeling and Ingham [118] regression) leads to the highest fatalities, while Approach D (HAZUS collapse and fatality rates) leads to the lowest. These results indicate that the Metropolitan Area of Lisbon (MAL) has the highest number of fatalities. Based on post-earthquake data, Samardjieva and Badal [120] proposed an empirical procedure for the estimation of the expected number of casualties conditional on the magnitude of the event. The latter approach suggests a death toll for an event with a M_w of 5.5 of approximately 300 people for densely populated areas ≥200/km, such as the MAL. The results obtained herein cover only unreinforced masonry, which host about 50% of the population. Considering this fraction, the values proposed by Approach B (an average of 171 fatalities considering both day and night periods) are close to the adjusted empirical value (i.e., 150 fatalities). The same exercise could not be performed for the offshore event, given that the large-magnitude events considered by Samardjieva and Badal [120] were mostly located close to populated areas, and thus their estimates are in the other of the tens of thousands of casualties.

5.6 Final remarks

This chapter discusses the implementation of a framework for fatality vulnerability assessment based on advanced numerical modelling. The current framework overcomes some issues of the current state-of-practice in fatality vulnerability assessment, such its dependence from damage and its fast saturation for moderate-to-high intensities. The framework uses advanced numerical modelling to obtain a relationship between IM and IVR, latter IVR is transformed into FR by using a correlations based on field data observations. Outcomes are fitted to a truncated lognormal cumulative probability density function for the sake of simplicity.

Collapse mechanisms obtained in numerical analysis were checked to correspond with most common collapse mechanisms from earthquake observations. Hence leading to a good representation of the masonry analysed. As a consistency check, the procedure was compared against HAZUS procedure, which is widely used for risk analysis. In general terms, it was found that HAZUS approach overestimate losses for low intensity, while the proposed framework overestimate losses for high intensities. Also, the IAFR was calculated for three important cities in Portugal with different levels of hazard. It was found that in most cases the IAFR overcomes the umbral of acceptable risk.

Earthquake scenarios were developed for the two most common sources of seismic events in Portugal, an onshore 5.5 Mw and an offshore 8.6 Mw events to occur in the day and night time. Average losses predicted for each approach are shown in Table 5-4. It should be noticed that HAZUS approach tends to underestimate losses for the Mw 5.5 scenario. The latter can be explained by two reasons: the high intensity of the event because the closeness of the epicentre and the asset and the small depth of the event, and the underestimating trend of the HAZUS fatality vulnerability functions shown in Figure 5.8 and 5.9. Similarly, HAZUS approach tends to overestimate damage for the 8.6 Mw offshore event, which can be explained as the same effect of the previous scenario for low-intensity events. Between all the approaches herein evaluated, a maximum of 488 and 207 fatalities are expected in average for the onshore and offshore events respectively, both occurring during the night.

Chapter 6

Vulnerability assessment of retrofitted masonry building

The feasibility of two seismic retrofitting techniques is evaluated in the present chapter through a cost-benefit analysis. Those techniques were selected based on compatibility, applicability, and low-cost criteria. Each technique is implemented within the numerical framework described in Chapters 4 and 5, thus allowing the estimation of the structural performance but also the structural safety in fatality terms. Outcomes of the current chapter were prepared for submission to a journal as:

Lovon H., Silva V., Vicente R., Ferreira T.M. (2022). Fatality reduction effectiveness of seismic retrofitting techniques for URM buildings in Portugal.

6.1 Introduction

It is well known that seismic risk is a combination of exposure, hazard and vulnerability. In this regard, vulnerability is the unique component that can be reduced through risk mitigation strategies. Those usually consist in retrofitting interventions, but the large variety of such procedures makes necessary to perform cost-benefit analysis in order to evaluate its feasibility and effectiveness. Significant efforts have been made to assess the impact of large scale retrofitting interventions [39], as well as performing cost-benefit analysis of traditional retrofitting techniques in Portugal [13]. The current research attempts to analyse cost-effective solutions of some retrofitted techniques, applied to the masonry building stock in Portugal.

Retrofitting techniques can prevent buildings from collapse, even when physical damage enforces the demolition of the entire building. Hence, even when structural damage is not reduced, life loss is prevented, which implies a revenue as result of the intervention. In this respect, the inclusion of human losses as part of the cost-benefit analysis of retrofitting interventions are a key contribution. The inclusion of casualties may be polemic from an ethical perspective, however not considering them may lead to an underestimation of the risk.

Seismic vulnerability of stone masonry buildings in Portugal has been widely addressed in past studies (e.g. [46], [47], [62]). Nevertheless, most of the studies focused only in structural damage of buildings, but not in human losses. In addition, traditional procedures [22], [27], [122] propose to calculate fatalities with basis on physical damage. The latter proposition has been refuted in past studies [118], [168] due to the fact that most extreme damage states do not disclosure the level of destruction and the loss of volume, which is closely related to the fatality ratio as shown in Crowley et al. [18], as well as in Abeling and Ingham [118]. The novel procedure attempting to assess human losses described in Chapter 5 is herein adopted to predict fatalities of retrofitted masonry buildings. It leverages advanced numerical modelling with the purpose of assess the extent of collapse, after that the reduction of survival space is transformed into fatality ratios based on post-earthquake data studies [18], [118].

The selection of an appropriate retrofitting technique relies in a wide range of approaches such as traditional practice, cost-effectiveness, the employment of modern materials or the aesthetical

preservation. From an engineering perspective, some retrofitting techniques are mainly devoted to the improvement of the strength, ductility, stiffness or stability improvement. Hence, different techniques might result depending on the current state of the building to intervene.

The current study focusses in two retrofitting approaches that well known to reduce the damage and stability, and have been largely used in similar building portfolios (e.g. [190]–[193]). The set of representative buildings are selected for retrofitting in the current study. Fragility and vulnerability functions are derived for comparison. In this study, it was decided to analyse the application of each technique individually. However it is possible to apply more than one as has been proposed in past studies (e.g. [13], [39]).

6.2 Walls grouting

Grout injection consist in the introduction of a binder material in either the face of a wall, the inner voids, or ultimately in visible cracks if the walls present some level of damage. The injection allows the homogenization of the masonry behaviour by saturating the cavities. The grout injection practice has been employed for several years, and its use has been standardized (e.g. [194], [195]). This technique can be performed either with or without induced pressure. The procedure is not only used for strengthening but also for repairing masonry walls (e.g. [196], [197]).

The grout composition plays an important role for the efficiency and durability of the grouting. It should be capable to infiltrate along the voids of the masonry, be compatible with the materials that compound the masonry, and exhibit a high resistance itself. A wide range of mortars have been tested for injection in masonry walls. These can be classified into cementitious, hydraulic, lime, or resins-based [190], [198].

The percentage of voids susceptible to be fulfilled by grout plays an important role in this procedure. Penazzi et al. [199] suggest to perform injection only when the percentage of voids overcomes 4%. Other studies associate the percentage of voids to a better improvement of the mechanical properties. Also, the technique may not have a significant effect on well-constructed masonry walls, especially if the failure is dominated by the resistance of the units, or if the percentage of voids is low.

Grout injection gains special relevance for retrofitting of masonry walls covered with mosaics, or paintings. In the latter case, it is important to keep the original outer appearance of the walls, as allowed by this technique. In some cases, grout injection is accompanied by repointing. This technique consists in cleaning degraded bonds in masonry and fulfilling them with new mortar. Other imperfections shown in the outer masonry are also repaired. Besides, transversal tying may be included as part of retrofitting programs using grouting. However, this technique is significantly more intrusive and costlier. There are several studies devoted to the mechanical characterisation of masonry walls with this kind of strengthening (e.g. [129], [200]).

The effectiveness of the procedure is still a matter of research, and it is often attributed to the effectiveness of the injection, the type of grout, the material of the mortar/units, or the state of the wall at the rehabilitation time. Uranjek et al. [190] employed non-destructive tests like sonic, and radar explorations to measure the effectiveness of the injection by measuring the success of filling voids on the masonry. The author also performed surface and in-depth probing and coring to confirm its

findings. Grout injection has proved to be effective not only by means of cyclic and statics tests, but also by shaking table tests on scaled specimens (e.g. [201], [202]).

6.2.1 Implementation

In this work, a literature review was performed regarding mechanical properties of masonry walls. Elasticity modulus and tensile strength were gathered for strengthened masonry assemblies. The improvement ratio was calculated for each mechanical property considering the baseline specimen. Table 6-1summarizes the reviewed studies. Only studies addressing the strengthening of undamaged specimens were considered. Figure 6.1 shows the dispersion of the elasticity modulus and tensile strength from the reviewed studies.

Table 6-1 Review of mechanical properties for masonry assemblies strengthened by grouting.

Nº	Study	Unstrengthen			Strengthened			Ratios	
		Specimen	Elasticity modulus (GPa)	Tensile strength (Mpa)	Specimen	Elasticity modulus (GPa)	Tensile strength (Mpa)	E	ft
1	Toumbakari [203]				13b-10	-	-	2.25	1.06
2					Cb-0	-	-	1.37	1.97
3					13b-0	-	-	0.7	2.07
4	Corradi et al. [204]	B-C-04-OR, P-C-15-OR	0.835	-	V-C-07-IN	1.703	-	2.04	
5	Valluzzi [205]	5I1-6I1	2.210	-	13I1	3.992	-	1.81	
6		1I2-8I2	1.505	-	16I2	1.223	-	0.81	
7	Vintzileou and Miltiadou-Fezans [206]	-	1000	0.1	1	1200	0.21	1.20	2.10
8		-	1440	0.1	2	1550	0.33	1.08	3.30
9		-	1500	0.1	3	1300	0.22	0.87	2.20
10	Almeida et al. [207]	PP1-PP2	0.36	-	PP3	1	-	2.78	
11	Oliveira et al. [208]	1W1-1W2-2W1-3W1	1.183	-	3W2	1.604	-	1.36	
12		1W1-1W2-2W1-3W1	1.183	-	3W3	1.114	-	0.94	
13	Uranjek et al. [190]	U	0.785	0.07	C1	1.52	0.29	1.94	4.14
14		U	0.785	0.07	C2	1.507	0.3	1.92	4.29
15		U	0.785	0.07	CL1	1.347	0.21	1.72	3.00
16		U	0.785	0.07	CL2	1.164	0.21	1.48	3.00
17	Silva et al. [209]	SCF_1.00NI	2531	0.07	SCF_1.00I	4966	0.15	1.96	2.14
18		SCF_1.25NI	2531	0.05	SCF_1.50I	4966	0.16	1.96	3.20
19		SCF_0.75NI	2531	0.04	SCF_1.25I	4966	0.18	1.96	4.50
20		SCF_0.50NI	2531	0.06	SCF_2.00I	4966	0.18	1.96	3.00
21		SCS_0.50NI	2959	0.04	SCS_1.25I	5125	0.17	1.73	4.25
22		SCS_1.00NI	2959	0.02	SCS_1.00I	5125	0.16	1.73	8.00
23		SCS_0.75NI	2959	0.08	SCS_1.50I	5125	0.14	1.73	1.75
24		SCS_1.25NI	2959	0.09	SCS_2.00I	5125	0.14	1.73	1.56
25	Luso and Lourenco [210]	P4 nI	297	-	P2 IA	2500	-	8.42	
26		P4 nI	297	-	P6 IA	533.3	-	1.80	
27		P5 nI	263	-	P1 IB	597	-	2.27	
28		P5 nI	263	-	P3 IB	1053	-	4.00	

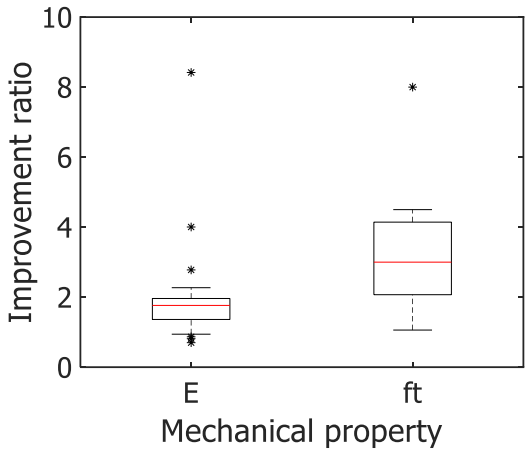

Figure 6.1 Dispersion of elasticity modulus and tensile strength from review studies.

6.2.2 Results

The mechanical properties of the strengthened models were calculated by applying the improvement ratio to the original mechanical properties defined in Table 4-1. Those are roughly 1.72 and 2.80 for the elasticity modulus and tensile strength, respectively. For the sake of readability, the mechanical properties of the unstrengthen buildings are repeated in Table 6-2 accompanied by the updated mechanical properties.

Table 6-2 Mechanical properties of unstrengthen and strengthened masonry buildings.

Element	Description	Unit	Unstrengthen		Strengthen	
			Limestone	Granite	Limestone	Granite
Bricks (solid elements)	Elasticity modulus	GPa	0.78	0.93	1.34	1.60
	Poison ratio	-	0.30		0.30	
	Static coefficient of friction	-	0.80		0.80	
	Dynamic coefficient of friction	-	0.60		0.60	
	Penalty stiffness factor	-	1.00		1.00	
Mortar (cohesive elements)	Normal failure stress	MPa	0.12	0.15	0.34	0.42
	Shear failure stress	MPa	0.12	0.15	0.34	0.42
	Normal energy release rate	N/m	30.00	36.00	84.00	100.80
	Shear energy release rate	N/m	30.00	36.00	84.00	100.80
	Normal stiffness	GPa	0.78	0.93	1.34	1.60
	Tangential stiffness	GPa	0.78	0.93	1.34	1.60

The procedure followed in Section 4.2 and 5.2 was implemented to develop fragility and vulnerability functions. The same archetypes were used for a proper comparison with the strengthened counterpart. Fragility functions are shown in Figure 6.2 and Figure 6.3, while their parameters are shown in Table 6-3 and Table 6-4.

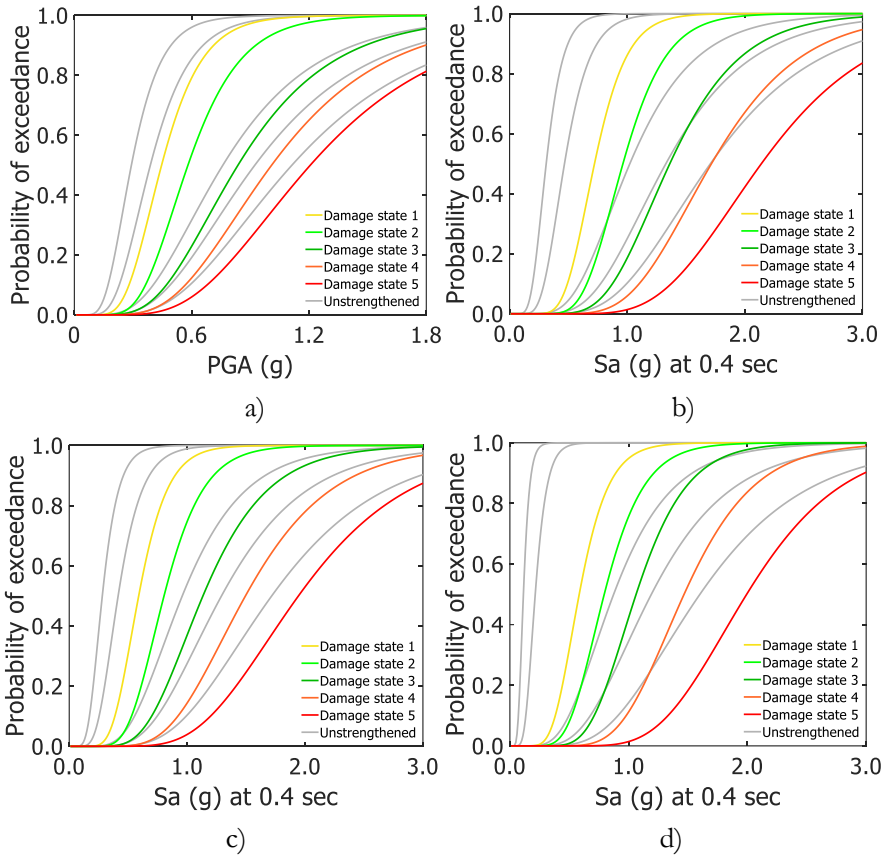

Figure 6.2 Fragility functions for a) 1-story, b) 2-story, c) 3-story, and d) 4-story original and grouted limestone masonry buildings.

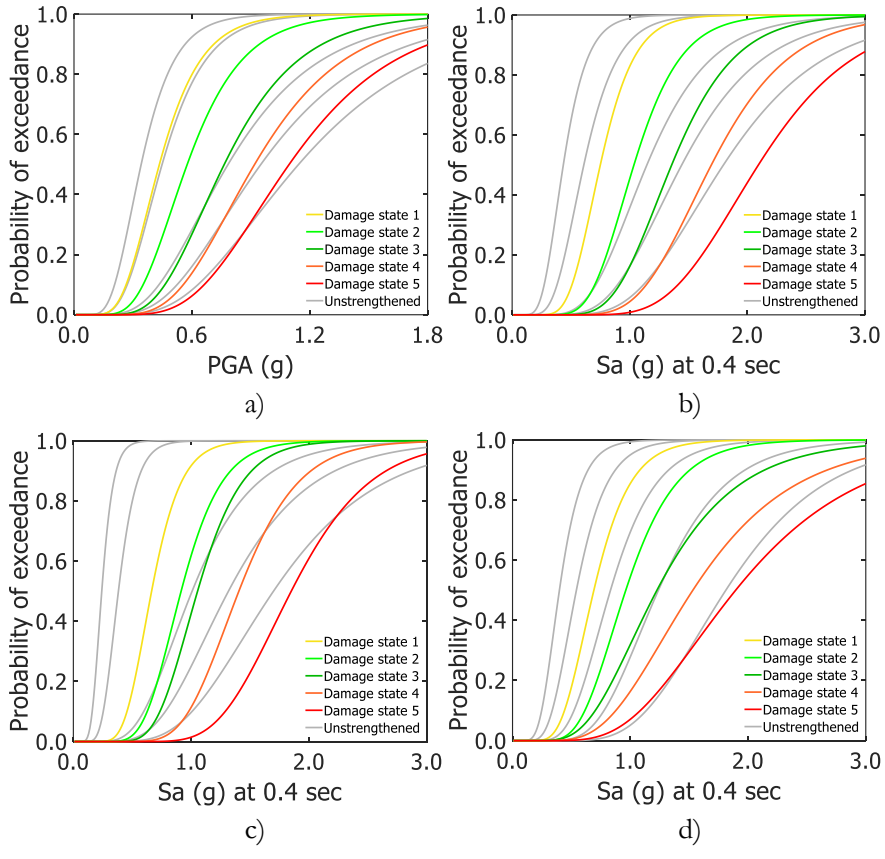

Figure 6.3 Fragility functions for a) 1-story, b) 2-story, c) 3-story, and d) 4-story original and grouted granite masonry buildings.

Table 6-3 Fragility function parameters for grouted limestone masonry buildings

Building class	IM	Negligible to slight		Moderate		Substantial to heavy		Very heavy		Destruction	
		μ	σ	μ	σ	μ	σ	μ	σ	μ	σ
1-storey	PGA	-0.807	0.365	-0.543	0.365	-0.178	0.449	0.009	0.449	0.188	0.449
2-storey	Sa (0.4)	-0.326	0.300	-0.037	0.300	0.309	0.346	0.540	0.346	0.761	0.346
3-storey	Sa (0.4)	-0.529	0.328	-0.218	0.328	0.126	0.378	0.402	0.378	0.665	0.378
4-storey	Sa (0.4)	-0.538	0.330	-0.230	0.330	0.061	0.315	0.383	0.315	0.690	0.315

Table 6-4 Fragility function parameters for grouted granite masonry buildings

Building class	IM	Negligible to slight		Moderate		Substantial to heavy		Very heavy		Destruction	
		μ	σ	μ	σ	μ	σ	μ	σ	μ	σ
1-storey	PGA	-0.833	0.385	-0.551	0.385	-	0.392	-0.084	0.392	0.091	0.392
2-storey	Sa (0.4)	-0.288	0.303	0.035	0.303	0.305	0.309	0.527	0.309	0.739	0.309
3-storey	Sa (0.4)	-0.370	0.350	-0.039	0.350	0.204	0.435	0.426	0.435	0.639	0.435
4-storey	Sa (0.4)	-0.409	0.295	-0.089	0.295	0.053	0.282	0.340	0.282	0.615	0.282

The framework proposed for fatality vulnerability assessment was implemented for the grouted masonry buildings. For the sake of simplicity, only Approach B was used for comparison between unstrengthen and strengthened masonry buildings. Resultant fatality vulnerability functions are shown in Figure 6.4 and Figure 6.5, and their parameters are shown in Table 6-5.

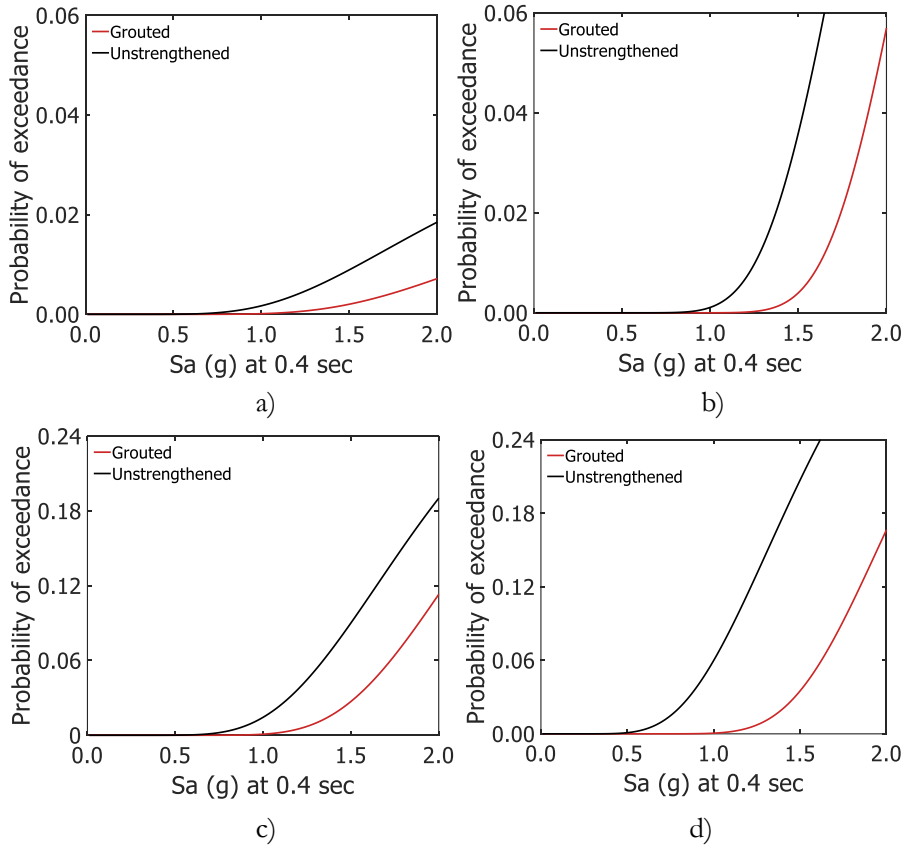

Figure 6.4 Fatality vulnerability functions for limestone masonry buildings of a) 1-storey, b) 2-storeys, c) 3-storeys, d) 4-storeys retrofitted by grouting.

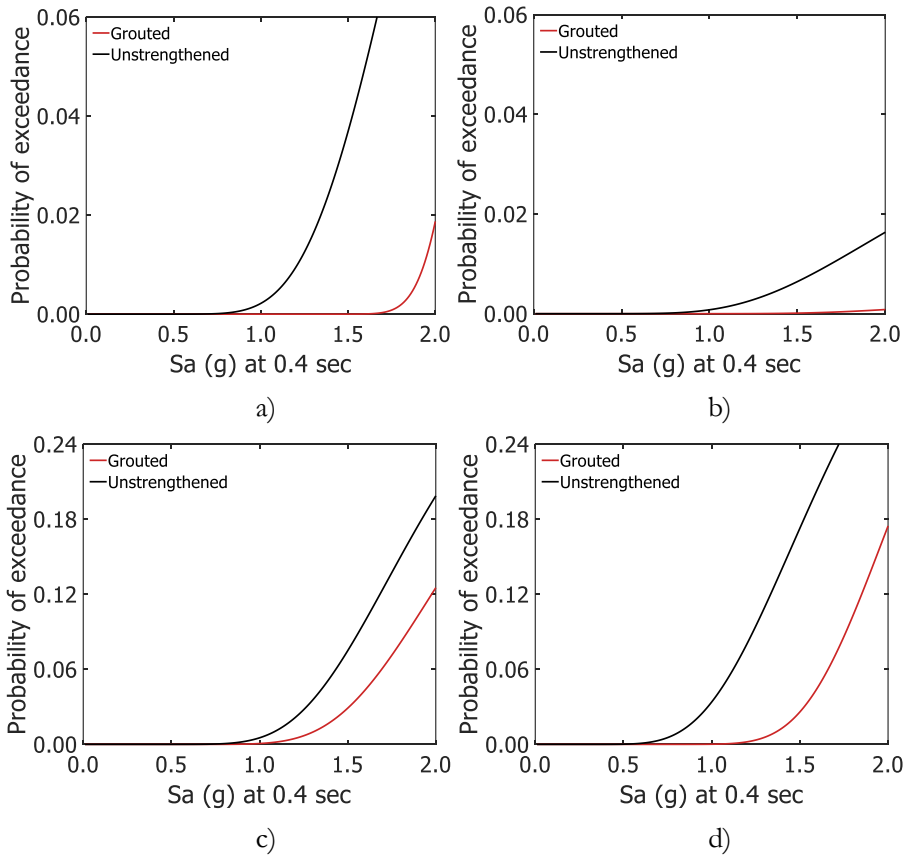

Figure 6.5 Fatality vulnerability functions for granite masonry buildings of a) 1-storey, b) 2-storeys, c) 3-storeys, d) 4-storeys retrofitted by grouting.

Table 6-5 Parameters of the fatality vulnerability functions

Type of stone	Number of storeys	Fatality vulnerability function parameters		
		a	θ	β
Limestone	1	0.026	0.898	0.349
Limestone	2	0.192	0.795	0.191
Limestone	3	0.312	0.794	0.285
Limestone	4	0.375	0.728	0.244
Granite	1	0.003	0.854	0.248
Granite	2	0.190	0.822	0.100
Granite	3	0.296	0.744	0.261
Granite	4	0.390	0.721	0.210

6.3 Walls coating

Amongst all of the retrofitting procedures available, the ones consisting in the surface's wall treatment have been largely tested. These techniques include reinforced mortar coating, shotcrete, and reinforced fibbers. The so called "Modern materials" have also been used for surface treatment, such is the case of Steel Fibber Reinforced Mortar (SFRM). The latter consists in a thin layer of mortar covering the sides of the masonry panel. The mortar contains short steel fibbers homogeneously

distributed in the mortar without following a specific pattern. SFRM can be applied in only one side of the wall in order to preserve the aesthetical appearance of the building, or to reduce disruption. This technique can be easily accompanied by thermal retrofitting as studied by Facconi et al. [193]. Sevil et al. [211] studied the retrofitting of masonry infill panels in RC buildings, application effort, low price and effectiveness of the retrofitted technique.

The fibbers enhance the tensile behaviour of the mortar, thus allowing a better control of crack propagation. A higher volume fraction of steel fibbers leads to a more stable behaviour of mortar in terms of post-cracking strength and ductility according to Facconi et al. [212]. Also, a minimum rebar cover is not needed, hence allowing thinner layers of covering. In general, in-plane and out-of-plane behaviour of masonry buildings is improved. The technique can be accompanied by other retrofitting techniques like grouting, tie-rods, steel rings, among others.

Some studies investigated characterisation of SFRM, focusing either in the dosage of the mortar (e.g. [213]), mechanical properties of the mortar (e.g. [214]), uniaxial and diagonal compression tests of masonry panels (e.g. [193]), or cyclic test of masonry walls (e.g. [212]). The literature addressing the SFRM retrofitting technique is still scarce, but all studies available highlight its effectiveness, low price, and relatively easy application.

6.3.1 Implementation

Mechanical properties of SFRM were gathered (see Table 6-6). These properties were defined according to the study performed by Lucchini et al. [193]. In this study, the matrix is a cement-based mortar mixed at 24 % (in weight) of water with a fibbers volume fraction equal to 0.76 %. Fibbers have a double hooked-end with a length of 32 mm, 0.4 mm of diameter, and 2800 MPa of tensile strength.

Table 6-6 Mechanical properties of the SFRM layers

Description	Unit	Value	Study
Elasticity modulus	GPa	20.40	Lucchini et al. [193]
Compressive strength	MPa	30.20	
Tensile strength	MPa	3.60	
Poisson coefficient	-	0.20	
Compressive maximum strain	-	0.010	Herein derived
Tensile maximum strain	-	0.0025	Herein derived

Despite the efforts performed towards the mechanical characterisation of SFRM, some properties still require more experimental research. This is the case of the compressive and tensile maximum strain, whose values are still unclear and might depend of the proposed dosage. Hence, these values have been defined based on the results from experimental tests reported by Lucchini et al. [193] and Sevil et al. [211].

The application of mortar layers (25 mm thickness) was limited to walls located in facades of the archetypes selected for limestone and granite masonry buildings. Only piers were covered to reduce associated costs, and the application was performed on both sides of the walls, as illustrated in Figure 6.6.

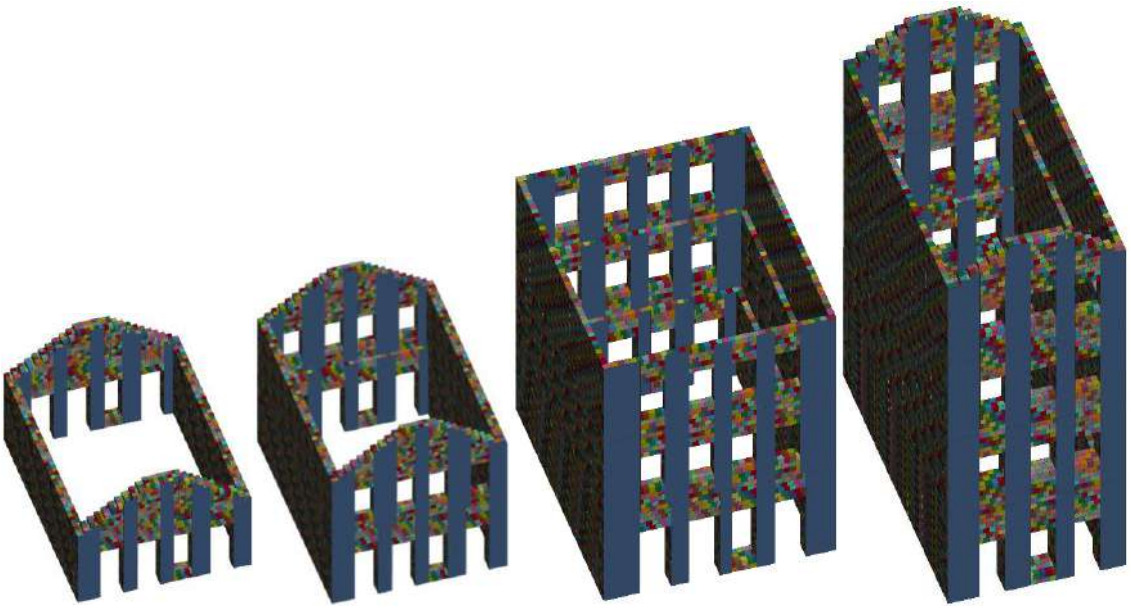

Figure 6.6 Retrofitted building archetypes selected for fragility analysis.

Due to the small thickness of the mortar layers, these elements were included in the structural model using shell elements with the Belystschko-Tsay formulation [30]. Shell nodes are tied to solid element's nodes using the TIED_NODES algorithm available in LS-Dyna. An erosion criterion was necessary in order to avoid numerical issues and to permit the detachment of solid blocks by the deletion of the shell elements. The deletion criterion limits the minimum principal strain at -2E-3 and the maximum at 2E-4.

The model herein implemented is substantially heavier than its original counterpart. This is because the inclusion of new nodes (those belonging to the shell elements), but mainly because of the reduction of the minimum time-step. The latter has been reduced to around one eighth of its original value. Therefore, limestone and granite masonry buildings were merged into a single building class with the purpose to reduce the computational effort.

6.3.2 Results

Fragility and vulnerability functions were calculated following the procedures described in Section 4.2 and 5.2. Archetypes used for the as-built fragility assessment were also used for this retrofitting procedure. Figure 6.7 shows the fragility functions and the associated parameters are shown in Table 6-7 for reproducibility.

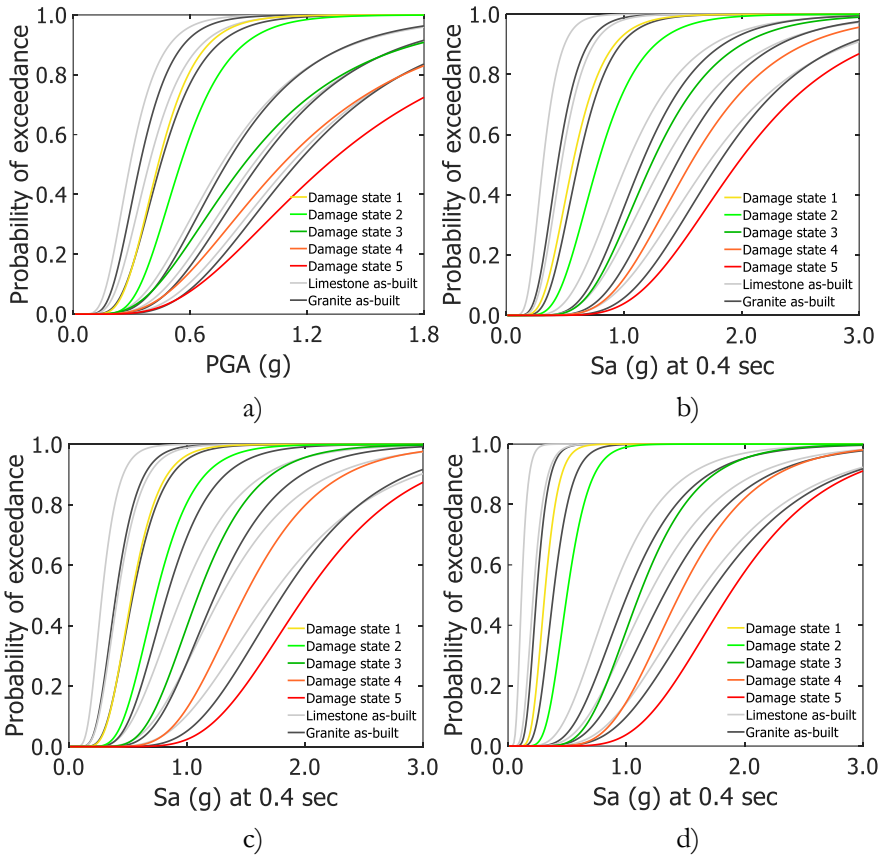

Figure 6.7 Fragility functions for a) 1-story, b) 2-story, c) 3-story, and d) 4-story original and grouted limestone masonry buildings.

Table 6-7 Fragility function parameters for masonry buildings retrofitted through coating.

Building class	IM	Negligible to slight		Moderate		Substantial to heavy		Very heavy		Destruction	
		μ	σ	μ	σ	μ	σ	μ	σ	μ	σ
1-storey	PGA	-0.831	0.362	-0.598	0.362	-0.134	0.542	0.070	0.542	0.265	0.542
2-storey	Sa (0.4)	-0.574	0.385	-0.255	0.385	0.208	0.381	0.445	0.381	0.672	0.381
3-storey	Sa (0.4)	-0.631	0.351	-0.304	0.351	0.091	0.351	0.400	0.351	0.695	0.351
4-storey	Sa (0.4)	-1.173	0.299	-0.697	0.299	0.104	0.352	0.370	0.352	0.625	0.352

The framework proposed for fatality vulnerability assessment was implemented for the masonry buildings with wall coating. For the sake of simplicity, only Approach B was used for comparison between unstrengthen and strengthened masonry buildings. Resultant fatality vulnerability functions are shown in Figure 6.8, and their parameters are shown in Table 6-8.

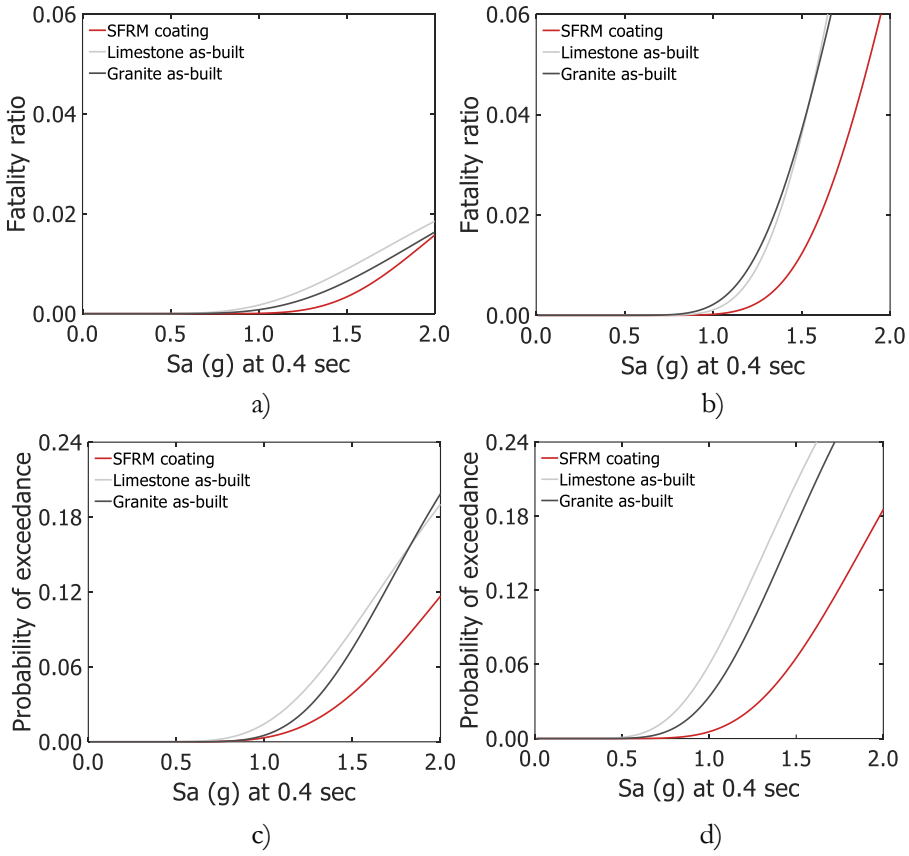

Figure 6.8 Fatality vulnerability functions for limestone masonry buildings of a) 1-storey, b) 2-storeys, c) 3-storeys, d) 4-storeys.

Table 6-8 Parameters of the fatality vulnerability functions for masonry buildings retrofitted through coating

Type of stone	Number of storeys	Fatality vulnerability function parameters		
		a	θ	β
Limestone/Granite	1	0.037	0.738	0.250
Limestone/Granite	2	0.226	0.834	0.267
Limestone/Granite	3	0.338	0.835	0.357
Limestone/Granite	4	0.431	0.753	0.337

6.4 Final remarks

In the present chapter, two retrofitting techniques were evaluated by means of physical damage and fatality vulnerability functions. Retrofitting techniques were selected with basis on a set of criteria as: the applicability to the masonry building stock in Portugal, the low cost, the level of intrusiveness. Literature provides a large range of possible retrofitting techniques. However, they can be massively applied only when they represent a small proportion of the building cost. In this regard, walls grouting and coating were selected for this case of study.

A literature review was necessary to assess the improvement of mechanical properties induced by the injection of grout. Around 30 studies were reviewed gathering information about laboratory test performed on grouted masonry assemblies. The improvement ratio was measured as the quotient between the mechanical properties of the baseline and the retrofitted specimen, giving around 1.72 and 2.80 for elasticity modulus and tensile strength, respectively. The latter ratios, were used to update the mechanical properties originally used to for as-built building's modelling.

Modern materials are being progressively introduced in the retrofitting and rehabilitation of masonry buildings. Literature presents a vast set of materials testing for walls coating, such as the SFRM. This material was selected because of its easy preparation and application. Literature regarding its mechanical properties is still scarce, but existent. In this chapter, mechanical properties were defined according to Lucchini et al. [193]. A strategy was developed to include explicitly the SFRM layers within the numerical framework explained in Chapter 4.

Results show that coating might exhibit a better performance than grout injection. Nonetheless, coating results heavily invasive for the aesthetical appearance of masonry buildings, while coating is used specially when it is necessary to preserve patrimonial structures.

Chapter 7

Seismic risk evaluation at national scale

In this chapter, a nationwide seismic risk evaluation is carried out to estimate direct losses associated with physical damages, as well as average annual losses associated with human casualties. Fragility and fatality vulnerability functions developed in Chapter 4 are used herein to evaluate the current seismic risk, and the retrofitting techniques studied in Chapter 6 are used to perform cost-benefit analyses and identify the most attractive geographic zones for retrofitting implementation. Outcomes of this chapter will be part of a future journal article tentatively entitled:

Lovon H., Silva V., Vicente R., Ferreira T.M. (2022). Cost-benefit analysis for seismic retrofitting interventions of masonry buildings in Portugal.

7.1 Introduction

Risk analysis is defined as "the combination of the consequences of an event or hazard and the associated likelihood of its occurrence" (ISO [215]). Seismic risk can be performed either within a deterministic or probabilistic framework, both having pros and cons in different aspects. However, probabilistic-based assessment is more advantageous when uncertainties can potentially play a meaningful role in the analysis, as is the case here, and this is why a probabilistic assessment was adopted in the analysis discussed in the present chapter. Those uncertainties range from the location and magnitude of the event, the rupture's features, the ground shaking, and the performance of the structures affected by the shaking. All these uncertainties must be considered by a stakeholder wanting to manage risks and investments. It should be noted that a deterministic framework allows evaluating scenarios of potential events, hence providing valuable information for preparedness and contingency plans. However, the main difficulty within the deterministic approach is the definition of a "worst-case" scenario and its connection with the performance objective of the evaluated system. Vast literature can be found discussing the usage, advantages, and comparison between both approaches (e.g. [216], [217]).

Probabilistic risk has been progressively adopted in the engineering practice either for the design of new buildings as well as for its safety assessment, all with the objective to achieve societally acceptable risk [218]. For example, the majority of the modern design codes specify a design response spectrum based on probabilistic seismic hazard analysis (e.g. [219], [220]). Similarly, risk-based behaviour factors can be specified as proposed by Baltzopoulos et al. [221]. Likewise, other performance objectives can be defined, such as collapse probability and individual fatality risk, among others (e.g. [162], [222]). In the assessment of structures, the probabilistic field has been extensively implemented for the evaluation of the overall economic and social impact, the identification of the best alternatives and locations for retrofitting programmes, and the prioritization of risk mitigation programmes. Finally, risk studies are also valuable tools for risk communication, enhancing the awareness of the citizens and their willingness to take decisions towards risk mitigation.

From the literature (e.g. [162], [222]), the three main components of seismic risk are 'exposure', 'hazard' and 'vulnerability'. The exposure contains data from the assets such as building class, number of buildings and location. The hazard describes the intensity and frequency of events at a given location, and it can be fully described by a hazard curve which indicates the annual probability of

exceeding certain IMs. The vulnerability expresses the likelihood of a building to suffer damage given a certain IM, and it can be fully defined by means of fragility and vulnerability functions.

The present study performs a probabilistic risk assessment using the exposure model developed by Crowley et al. [48], which covers all European countries. The seismic source models proposed in Vilanova and Fonseca [135] are used for the hazard definition. The vulnerability of masonry buildings is represented by the functions developed in Chapter 4, and the cost ratios proposed by HAZUS [27]. Despite the effort performed in the past to assess risk assessment in the Portuguese territory (e.g. [46], [223], [224]), innovatively, the present work provides detailed modelling of masonry buildings, and assesses human losses through new analytical fatality vulnerability functions, developed in Chapter 5. Additionally, a cost-benefit analysis is performed for the two retrofitting techniques explored in Section Chapter 6.

7.2 Components of the probabilistic risk model

7.2.1 Exposure model

As previously explained, the exposure describes the location and number of exposed assets classified according to their seismic performance. Masonry buildings represent around 50 % of the masonry building stock and host around 40 % of the population. Nowadays, masonry buildings have been progressively replaced by RC structures. As observed in Figure 7.1, the construction of masonry buildings is decreasing in the whole Portugal territory, regardless of the seismic hazard.

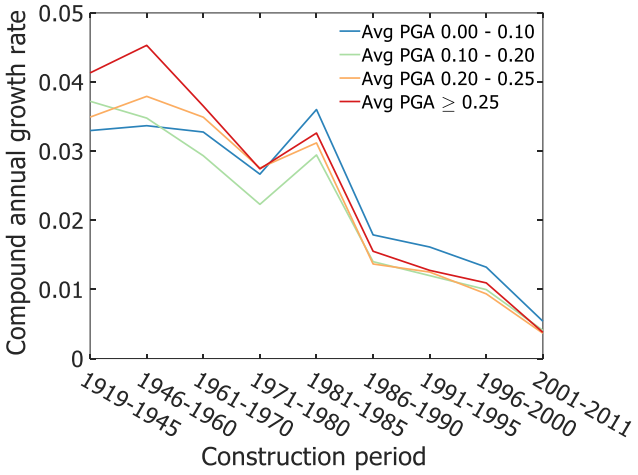

Figure 7.1 Compound annual growth rate of the masonry buildings.

The exposure model developed by Crowley et al. [48] for application in Europe was used for the risk calculations presented here. Only masonry buildings were considered though, since the objective here is to apply the fragility and vulnerability functions developed in the previous sections. Likewise, only residential buildings were included the exposure model, and the overall model was divided into limestone and granite models for assets located in the southern and northern regions, respectively. Buildings with four or more storeys were all merged, as they represent a small proportion of the overall building stock. The dataset provides information at the smallest administrative level, building class, the aggregated replacement cost, and the aggregated number of occupants. Assets are assumed to be lumped at the centroid of each municipality.

7.2.2 Seismic source model

The seismic source model allows for performing probabilistic seismic hazard analysis, commonly known as PSHA. In general, the seismic source model describes the geometry of the seismic sources and all of the parameters necessary to describe the recurrence law (magnitude – frequency relationship). The work presented herein makes use of the seismic source models developed by Vilanova and Fonseca [135] and the updating proposed by Silva et al. [187]. The source model considers two seismic zones (SA and SB) to account for different views of the distribution of seismicity in the country – such zones are depicted in Figure 7.2.

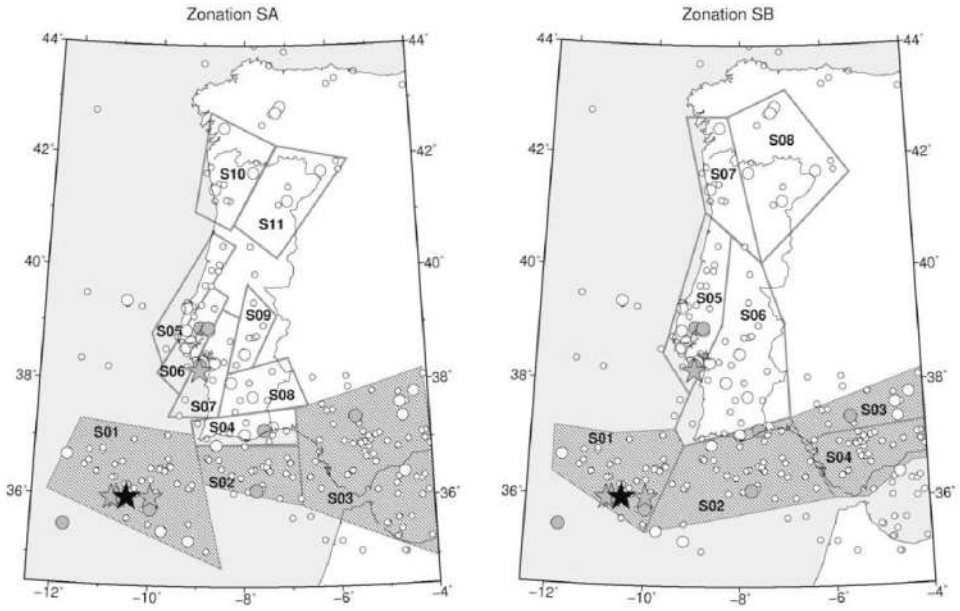

Figure 7.2 Seismic sources proposed by Vilanova and Fonseca [135]

The earthquake catalogue constructed by Vilanova and Fonseca [135] is constituted by data from IGN [225] and the work from Sousa [226]. However, two sets of parameters were derived for two hypothetical catalogues with distinct levels of error in the magnitude definition, CA and CB, being the latter more precise for the magnitude quantification. The same approach was followed for the procedure proposed for the computation of the recurrence rates, where Stepp [227] and Albarello et al. [228] are considered, as RA and RB, respectively. Two possibilities of truncation of the recurrence law were considered, using a minimum moment magnitude equal to a(M>4.0) and a(M>4.6), and an additional one considering the maximum moment magnitude found in the source Max(source) and Max (source)+0.5. All the aforementioned uncertainties regarding the source geometry, parameters and recurrence calculations were implemented resorting to a logic-tree approach, schematised in Figure 7.3.

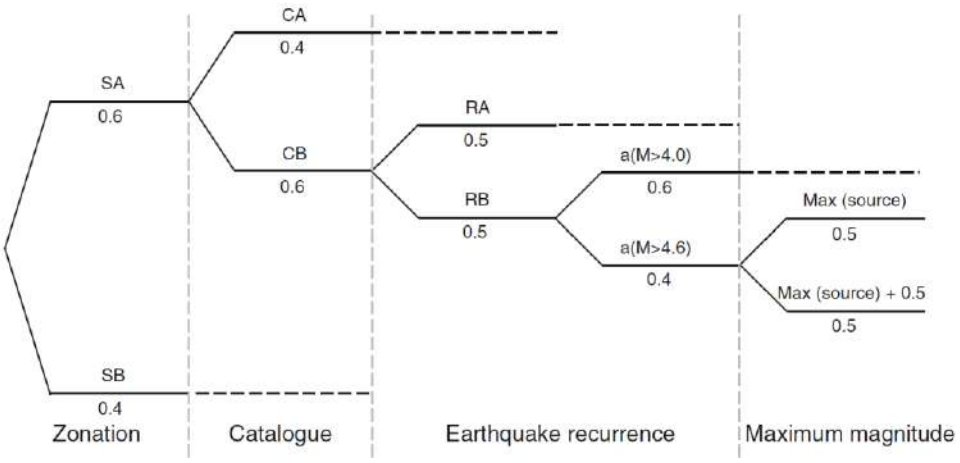

Figure 7.3 Logic tree approach for seismic hazard assessment from Silva et al. [187]

7.2.3 The Ground Motion Prediction Equations (GMPE) and site conditions

The GMPE establish a relationship between the location and magnitude of an event and the ground shaking intensity at a given site. In addition to the distance and magnitude, the attenuation law should also consider other aspects like the nature of the fault, the rupture's features, and the site conditions. The selection of the GMPE is a key factor in PSHA, as highlighted by Pelaez and Casado [224] and Crowley et al. [229]. Table 7-1 summarizes the GMPEs that will be implemented herein to model the propagation of shaking and perform PSHA, which were proposed by Delavaud et al. [230].

Table 7-1 GMPEs proposed by Delavaud et al. [230]

Stable continental region		Active shallow crustal region	
GMPE	Weight	GMPE	Weight
Campbell [231]	0.2	Akkar and Bommer [189]	0.35
Toro [232]	0.2	Cauzzi and Faccioli [233]	0.35
Akkar and Bommer [189]	0.2	Zhao et al. [234]	0.10
Cauzzi and Faccioli [233]	0.2	Chiou and Youngs [235]	0.20
Chiou and Youngs [235]	0.2		

Site conditions refer to the potential amplification of the ground shaking due to the characteristics of the site, such as soil stiffness and topography. Its influence has been largely reported in past studies (e.g. [236]), which have evidenced the importance of considering site conditions for PSHA calculations. A softer soil tends to amplify the ground shaking; hence amplification factors are calculated based on the Vs30 (average velocity of a wave propagating in the upper 30 m of soil). The site conditions can also be considered within the GMPE. In this work, the Vs30 map proposed by Silva et al. [187] was considered for all calculations.

7.3 Seismic risk

All risk components were implemented in the OpenQuake engine [186] developed by the Global Earthquake Model (GEM) initiative. Seismic hazard was calculated using the classical PSHA approach [218]. Hazard curves were calculated at each site under analysis and convoluted with the corresponding consequence function following the methodology presented by Field et al. [237]. Damage factors are assigned as suggested in HAZUS [27], meaning 1.0, 1.0, 0.6, 0.2, 0.05 for damage

states from DS5 to DS1, respectively. The replacement cost is calculated as the product of the average area per dwelling, the number of dwellings, and the average price per square meter given by Crowley et al. [48].

Economic losses were computed for the 475-year return period. Mean, 16th, and 84th percentile maps are shown in Figure 7.4 and Figure 7.5, respectively. Significant higher damage is shown in the western coastal regions and the Algarve region. This is expectable due to the high density of buildings and the moderate seismic hazard. The latter is particularly high in the metropolitan area of Lisbon, where the highest losses are observed.

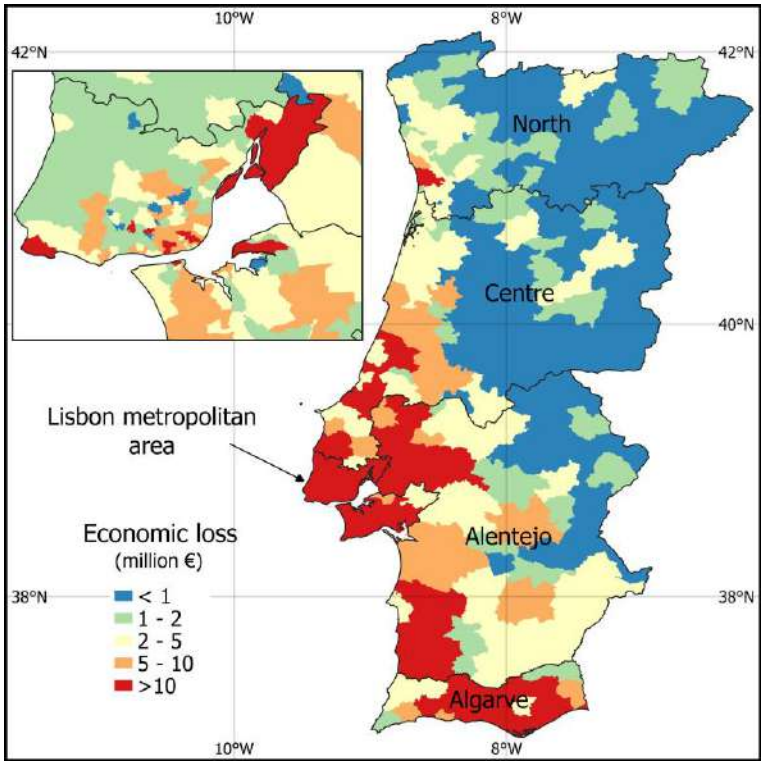

Figure 7.4 Average economic loss map for a probability of exceedance of 10 % in 50 years

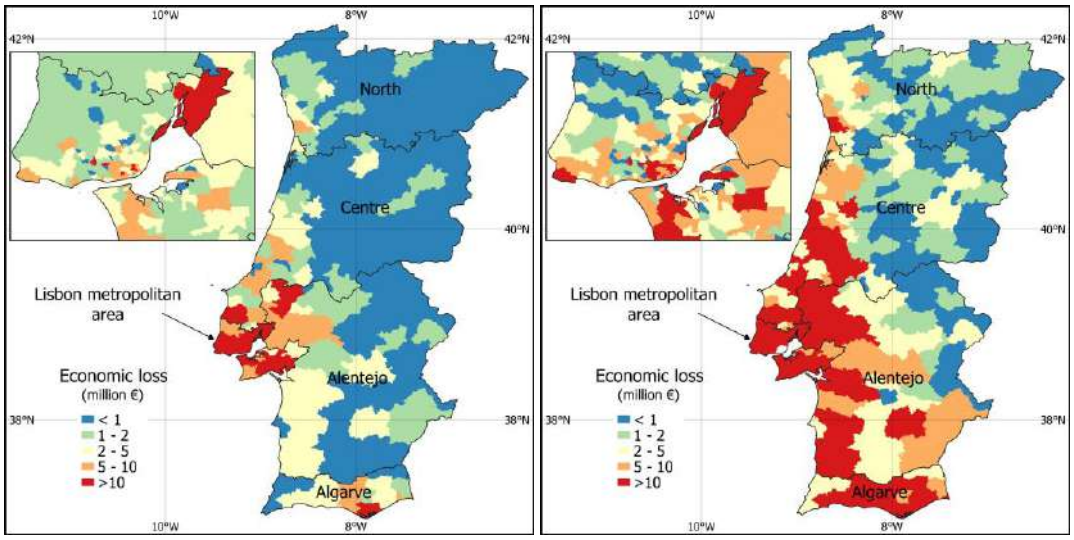

a) b)

Figure 7.5 Quantiles a) 16th, and b) 84th of economic loss map for a probability of exceedance of 10 % in 50 years in

7.4 Cost-benefit analysis

The poor performance of masonry buildings has been extensively documented throughout recent decades, which supports the need for the study of effective seismic retrofitting techniques able to mitigate the intrinsic vulnerability of these buildings. Chapter 6, and Section 6.1 in particular, aimed to contribute to that by discussing a few retrofitting techniques. The selection of the appropriate retrofitting technique should be made within a rational framework of optimization of resources. In this context, a cost-benefit analysis represents a viable, extensively used financial analysis technique capable of evaluating different alternatives of investment. The cost-benefit analysis consists of comparing the benefits to the investment required at the present time. Benefits come from the reduction of average annual losses of retrofitted buildings in comparison to their as-built counterpart, and costs are those associated with the price of implementing the retrofitting technique.

The present value theory is used to translate the benefits of the future to the present in order to perform a proper comparison with the investment (which is supposed to be made in the present). The translation consists in calculating the present value that produces the income in the future, using a simple interest rate, which considers inflation and changes in the consumer indices.

Present value is obtained through Eq. 7.1 for each asset in the building stock. The analysis considers that the building's lifespan will be extended up to 50 years after retrofitting. The latter period is usually considered (e.g. [13], [133], [164], [238]–[240]) as the time that the building will be used before being replaced or further upgraded.

$$CBR = \frac{\left(\sum_{t=1}^{T} \frac{L - L_{ret}}{(1+r)^t} \right)}{C_{ret}} \qquad \text{Eq. 7.1}$$

Where CBR is the cost-benefit ratio, T is the lifespan under analysis, L_{ret} is the average annual loss of the retrofitted assets, L is the average annual loss of the as-built asset, r is the rate of return, C_{ret} is the cost of the intervention. A constant value of the rate of return equal to 2 % was used for the calculations, the latter was defined based on past studies (e.g [239], [240]).

The cost of retrofitting was calculated for each building archetype and normalized to the replacement cost of each building. After that, the same ratio was assigned for each building in all assets of the building portfolio. The costs of grouting were calculated by getting the volume of grout per masonry volume according to Uranjek et al. [190]. The mortar costs were defined conservatively according to Luso and Lourenço [210], while activities associated with the mortar injection itself were defined based on commercial standards and time associated with infiltration of grout, resulting in a total of 470 €/m³. Table 7-2 summarizes the costs associated with this kind of retrofitting for masonry archetypes used in this study.

Table 7-2 Retrofitting and replacement costs for grouting in building archetypes

Building class	Retrofitting cost (€)	Replacement cost (€)	Ratio retrofitting/replacement

1	13872	63773	0.22
2	23047	127545	0.18
3	27410	168810	0.16
4	41679	191647	0.22

The grouting technique seems to be more expensive than others. However, it allows to preserve the aesthetical appearance of the buildings, which is a critical issue for buildings allocated in city centres.

Costs associated with the retrofitting of masonry buildings with SRFM were defined per building archetype by assuming costs per square meter of wall based on Diz et al. [133] as 128 €/m². Table 7-3 summarizes the prices obtained for the building classes used in the present study.

Table 7-3 Retrofitting and replacement costs for SRFM in building archetypes

Building class	Retrofitting cost (€)	Replacement cost (€)	Ratio retrofitting/replacement
1	4269	63773	0.08
2	7805	127545	0.08
3	9818	168810	0.07
4	10078	191647	0.07

Cost-benefit ratios were calculated according to Eq. 7.1 per building class considering only the structural damage. The results are shown in Figure 7.6 for masonry buildings from one to four storeys.

The losses associated with the as-built and retrofitted states of the assets consider not just the direct physical damage of the buildings but also the equivalent economic losses due to fatalities. Including fatalities as part of the economic loss is of great importance, otherwise the losses would be underestimated, and retrofitting programs would become less attractive than other types of public investments. Considering an economic loss equivalent to human losses is thus imperative in order to protect users from possible seismic events.

Human losses are quantified by means of the value of a statistical life (VSL), which is frequently used in the insurance industry and risk regulations [241]. This parameter represents the willingness of the people or governments to pay for fatality risk reduction in a certain local context. The parameter considers socio-economic aspects like income level, life expectancy and risk regulations, among others. Viscusi et al. [241] studied the income elasticity of the VSL, and proposed VSLs values for many countries around the world by taking as a baseline the United States VSL value. The latter study established a VSL value of 3.532 million dollars for Portugal. This value was used in the present study for fatalities losses estimation.

Cost-benefit ratios were obtained at the NUTS-II spatial resolution for both grouting and coating interventions. The zones in which 4-storey masonry buildings are inexistent were filled with grey colour. Figure 7.6 shows the cost-benefit ratios for masonry buildings from one to four storeys, retrofitted with grout injection. It can be easily verified that this retrofitting technique does not lead to profitable outcomes, even for the regions with higher seismic hazards in Portugal. Its high cost (20 % of the total replacement cost on average) is the main reason for that.

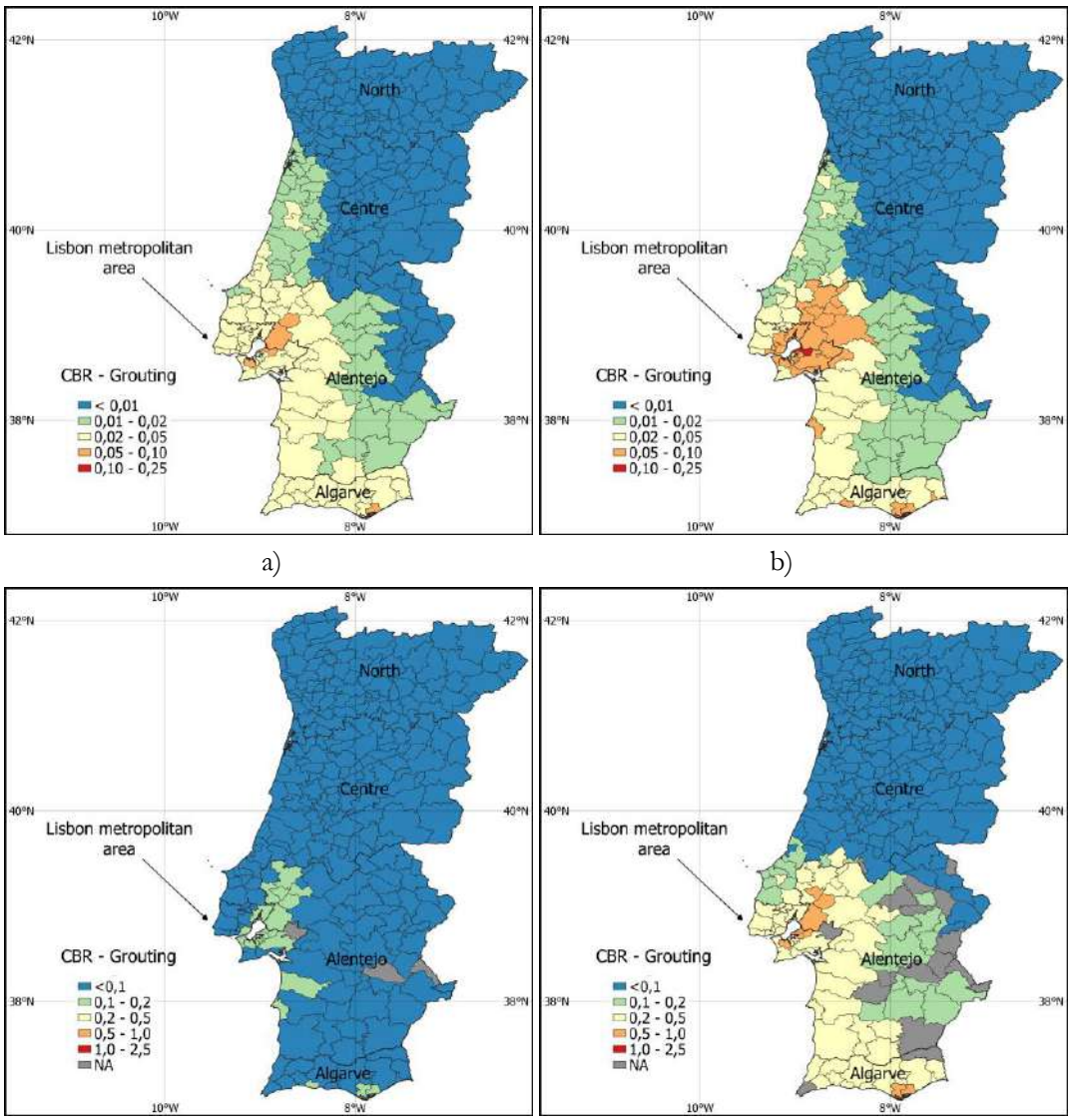

Figure 7.6 Cost-benefit ratios for buildings from one to four storeys retrofitted with grout injection.

The cost-benefit ratios obtained for SFRM coating are shown in Figure 7.7 for masonry buildings from one to four storeys. It was found that retrofitting investment becomes profitable for 4-storey masonry buildings located near the Metropolitan Area of Lisbon, as well as the Algarve region. It should be noted that the current study covers the building stock up to four storeys, so retrofitting buildings with five or more storeys should be assumed as profitable as well. The SFRM coating is financial advantageous due to its low cost (7 % of the total replacement cost on average). Also, the high vulnerability of 4-storey masonry buildings contributes to the benefits obtained from structural interventions.

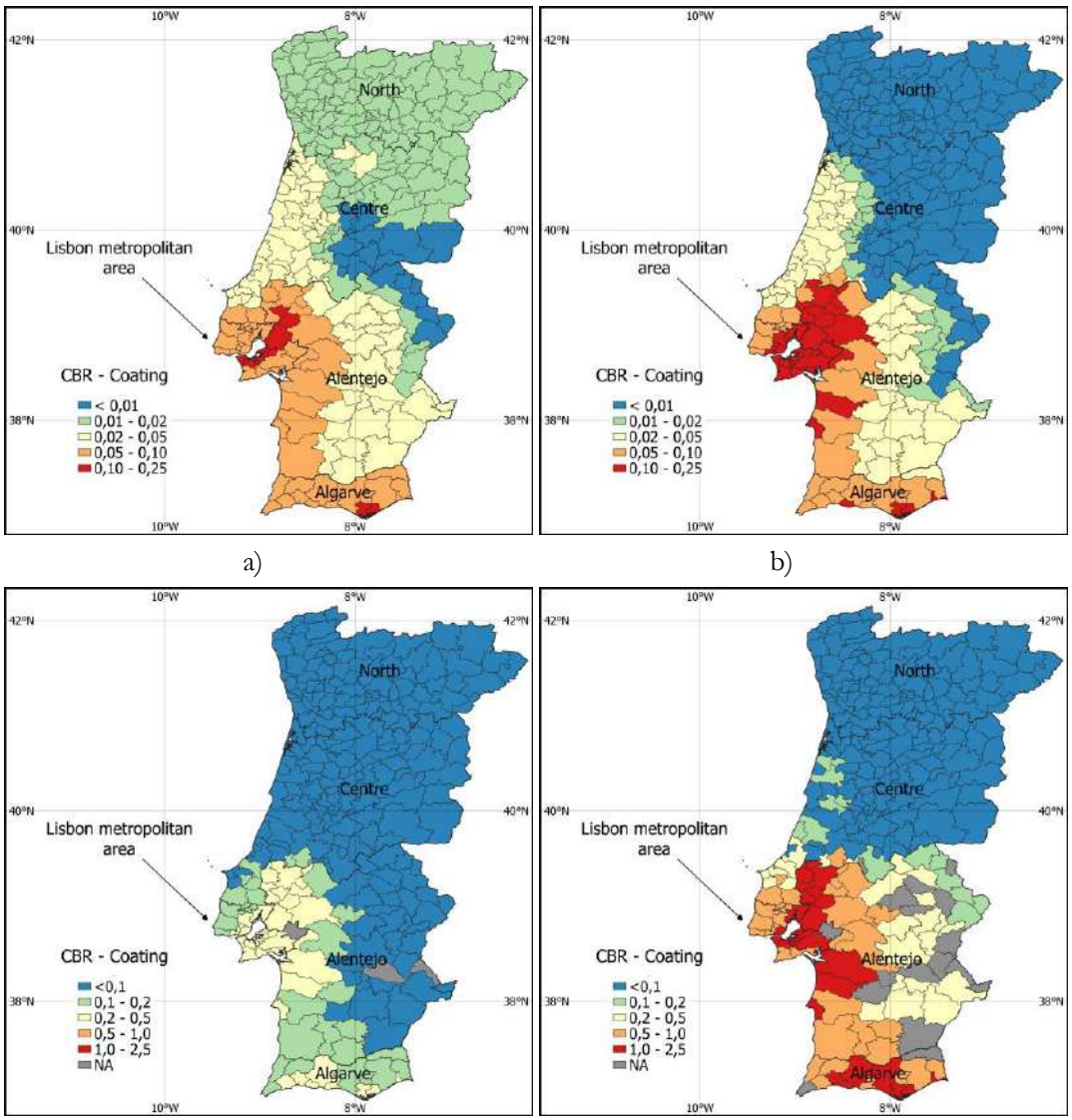

Figure 7.7 Cost-benefit ratios for buildings with one to four storeys retrofitted by SRFM coating

7.5 Final remarks

In this chapter a seismic risk model was implemented for the cost-benefit analysis of the retrofitting techniques proposed in Chapter 6. The exposure model developed by Crowley et al. [48] for Europe was used for residential masonry building assets in Portugal. The hazard model proposed by Silva et al. [187] was used for hazard modelling, and fragility and vulnerability functions were used from the Chapter 4 and 5 of this work.

Average economic loss map for a probability of exceedance of 10 % in 50 years were calculated. The most affected areas seem to be the Metropolitan Area of Lisbon, the coastal areas of Alentejo, and Algarve.

Cost-benefit analysis was performed following the present net value approach. Retrofitting costs were obtained from the analysis of past studies. Grouting and coating costs approximately 20 and 8 % of the replacement cost of the building. Results indicate that retrofitting masonry buildings is only profitable for 4-storey masonry buildings located in the surroundings of the Lisbon Metropolitan Area.

Chapter 8

Conclusions and future developments

8.1 Conclusions

The main conclusions are summarized in the following subsections on the most important topics addressed in the scope of this dissertation.

8.1.1 Characterisation of masonry buildings in Portugal

The characterisation of masonry buildings can be an overwhelming task because of the enormous diversity and heterogeneity with a building class. Some of the most important features that allow the characterisation of masonry buildings are the type of stone, the type of arrangement, the masonry joint mortar, the number of leaves, the type of roofing system, and the type of connection between walls and roofs, among other factors. Such a diversity traduces into large uncertainties regarding its mechanical and geometric properties, which are necessary to analyse in order to consider the building-to-building variability within a probabilistic risk assessment.

It was presented in Section 2.1 statistical distributions for geometric features for limestone and granite masonry buildings based on the information gathered of around 200 buildings located in two cities , Porto and Coimbra. Some of the important geometric features studied herein were the inter-storey height, the wall thickness, the reduction of the wall thickness, the ratio of openings, the length of the building, and the gable wall when available. This work included the identification of masonry archetypes, through which a strong correlation between the ratio of openings and the number of vertical axes of openings was found. The latter was important in order to implement a sampling procedure that allows us to calculate the building-to-building variability.

The territorial evaluation of masonry buildings and the seismic hazard proposed by Vilanova and Fonseca [135] allowed to estimate the percentage of buildings and population exposed to certain levels of hazard. It was found that around 50 % of the masonry building stock is exposed to a minimum PGA of 0.1g for a probability of exceedance of 10 % in the 50 years (measured in rock). Moreover, it was found that the wall thickness of limestone masonry buildings is around 17 % higher than the granite counterpart. For what concerns the inter-storey height, it was found that ground floors in granite masonry buildings are on average 20% higher, while the height of the regular (or upper) floors is on average 14 % higher.

8.1.2 Fragility assessment of masonry buildings

Within the scope of this dissertation, fragility functions were developed for limestone and granite masonry buildings in Portugal through an analytical approach. A sampling procedure was implemented in order to generate a random sample of masonry buildings and to find the uncertainty associated with the building-to-building variability for 3-storey limestone masonry buildings. By following the sampling procedure described in this dissertation, it was possible to find stable parameters of the cloud analysis after analysing around 20 buildings with 30 records each.

The structural capacity of each building class was simulated using a 3D numerical model, which was tested previously in other studies (e.g. [31], [242]). The numerical models were developed using the LS-DYNA software, thus allowing the consideration of EDPs with a strong correlation to structural damage (i.e., cracked walls ratio and the volume of loss ratio). The record-to-record variability was considered using a suite of 48 ground motion records in the nonlinear dynamic analysis and one archetype per building class.

Fragility functions were derived for each building class, testing the IMs that lead to the highest efficiency PGA and Sa for spectral ordinates from 0.1 to 1.0 s. Those can be easily combined with the outputs from probabilistic seismic hazard analysis to compute earthquake risk. The resulting fragility functions indicate that limestone masonry is slightly more vulnerable to earthquakes than granite masonry. This higher vulnerability is partially due to the mechanical properties, in particular the lower stiffness modulus. An increase in vulnerability was also observed with the increase in the number of stories. This trend is due to the changes in the dynamic properties (i.e., larger fundamental period of vibration) and the more substantial influence of P-delta effects.

These fragility functions were tested following different approaches. We evaluated the damage patterns observed in the numerical analysis and the thresholds for the initiation of damage and collapse and compared this information with past experimental campaigns. Considering the results available for one and 2-story buildings, it is possible to conclude that despite the limited sample, the results obtained herein were plausible. We also compared the fragility functions and associated risk metrics with other proposals. Our results are less conservative than other proposals, partially because other models have considered masonry construction from countries with high seismic vulnerability. It is also important to mention that according to the average annual probabilities of sustaining moderate damage or collapse, masonry construction in Portugal is on average 1-2 order(s) of magnitude more vulnerable than code-compliant reinforced concrete structures.

8.1.3 Fatality vulnerability assessment

For the fatality vulnerability functions, the number of records was increased to 48. The IVR was calculated for each record and transformed into fatality ratios using post-earthquake data from So [24]. The approach was compared with other procedures available in the literature in which the fatality vulnerability functions are calculated using fragility functions combined with collapse and fatality rates. Results suggest that conventional procedures overestimate losses for low intensities but underestimate losses for high ground shaking intensities. The latter is of great importance, especially when the event takes place close to densely populated areas near active faults.

The results presented herein clearly show that there is still a large uncertainty in the estimation of vulnerability functions for the assessment of fatalities, at least in comparison with its economic counterpart. Such observation is rather disappointing, given that risk mitigation measures should ultimately reduce the impact on human losses. The fatality vulnerability functions developed herein were used to calculate the IAFR, a common risk metric used in the legislation and insurance industry. It was found that for all building classes located in the southern regions, the IAFR overcomes the standardized values (e.g. 10^{-5} [176]). The latter means that the existing risk exceeds the tolerable thresholds in some regions, meaning that further measures should be taken to reduce the risk to the building occupants.

Earthquake scenarios were developed for hypothetical onshore and offshore events according to the seismicity in Portugal, and potential fatalities were calculated for those scenarios. Between 100 to 500 fatalities on average were estimated for events occurring during the night, depending on the methodology. However, the standard deviation is also quite large, which means that our measurements cannot be taken as exact predictions.

8.1.4 Seismic retrofitting of masonry buildings in Portugal

Two seismic retrofitting techniques, grout injection and wall coating, were explored for masonry buildings in Portugal. Grout injection was considered by tuning the mechanical properties of the masonry; therefore, it was not necessary to add additional numerical elements to the previously created numerical models. For this purpose, a set of improvement ratios were gathered from past studies addressing different types of masonry, grout and testing. It was found that there is strong evidence that grout injection improves the mechanical properties of masonry assemblies, but there is not enough testing information regarding the level of improvement and the conventional grout that can be used for this purpose. The improvement was calculated at the fragility level exhibiting good results. For example, for 1-storey limestone masonry buildings, it was found that given a PGA of 0.6g, the collapse rates decrease from 12 to 7 %. Similar trends were found for other building classes.

Wall coating was considered explicitly within the numerical framework by including shell elements to both sides of the walls. The approach was successful in terms of compatibility with the technique herein adopted to model the collapse. In general, a better performance was observed throughout all the ground shaking intensities. For example, it was found that for a PGA of 0.6g the collapse rates decrease from 12 to 8 % for 1-storey limestone masonry buildings.

8.1.5 Cost-benefit analysis of masonry buildings in Portugal

Seismic risk assessment was performed at the national level using the OpenQuake engine [186]. These analyses allow identifying the regions where losses are expected to be higher. In this process, losses for the 475-year return period (10 % of probability of exceedance in 50 years) were also calculated. The Metropolitan Area of Lisbon seems to be the most affected region in the country, followed by the southern coast of the country. The total average annual loss was calculated at 37 million EUR, considering only the masonry building stock. The latter finding is a significant contribution to the seismic risk assessment of masonry building stock in Portugal.

A cost-benefit analysis was performed for the two retrofitting techniques herein studied. It was found that retrofitting techniques might not be profitable for 1 to 3-storey masonry buildings. However, 4-storey masonry buildings show good CBR in the Metropolitan Area of Lisbon and the Algarve region. Buildings with five or more storeys were not part of this study. However, since a higher risk is expected for those buildings, a similar result is also expected. In this regard, other measures of risk management should be taken to transfer the risk associated with housing in masonry buildings.

8.2 Future developments

The current subsection highlights some important topics that require further effort and can be part of future studies. All those were identified throughout the development of the current work.

Despite the large effort made toward the characterisation of masonry buildings in Portugal, some gaps still exist. The number of leaves of masonry walls was found to be important according to past research. This aspect might result in out-of-plane instability of the walls during an earthquake. Expand on the building databases still necessary to characterize the mechanical properties and to implement numerical models capable of predicting their behaviour. Also, it was noted during the mechanical characterisation that further efforts should be devoted to obtain mechanical properties through either laboratory or in-situ tests.

Features associated with the roofing system, such as its configuration, the connections, and the materials, also play an important role in the seismic behaviour of masonry buildings. As highlighted by Moreira et al. [146], the roof-to-wall connection can be the difference between the development of local mechanisms or the box-like behaviour of the overall building. Further research should be devoted to the characterisation of roofing systems and connections.

The present work enabled the quantification of the variability of the EDPs associated with the building-to-building variability. However, due to its high computational effort, it was possible to perform these analyses only for limestone masonry buildings with 3-storeys. It is expected that this uncertainty can differ significantly according to the number of storeys. Further research can be conducted to explore the variability of more building classes but also include other sources of variabilities like the uncertainties in the mechanical properties and the roof configuration.

The introduction of novel EDPs to characterize the damage in masonry buildings was an important concept introduced herein in the fragility assessment field. However, it was noticed that additional efforts should be devoted to determining the damage factors associated with these damage states. The latter is because traditional damage factors are usually thought for damage quantified using traditional EDPs (e.g. inter-storey drift).

So [24] highlighted the importance of the roof in the collapse mechanism and the number of fatalities from building collapse. This architectural feature can be part of future investigation aiming at refining the fatality vulnerability functions herein developed. Something similar occurs for physical damage fragility assessment, where damage thresholds for collapse differ from 40 to 60 % for masonry buildings with heavy and light roofs, respectively, according to So [24].

For what concerns the retrofitting of masonry buildings, it was found that more experimental tests for mechanical characterisation are still needed. These parameters should be considered as a reference only since the effectiveness of the retrofitting might vary according to the type of masonry. Full-scale tests are still scarce in the literature and can be thus an important part of future investigations. Also, more retrofitting techniques should be assessed, namely tie-rods and the use of compatible modern retrofitting techniques, such as FRP meshes.

Some of the retrofitting techniques do not seem to be financially viable. However, cost-benefit analysis is not the only decision technique that should be evaluated for decision-making. Further research should introduce more innovative practices for seismic risk management (e.g., well-being). The retrofitting technique was solely analysed, but when combined with energy efficiency aspects, the structural interventions coupled to thermal improvement of the building envelope might become more advantageous form the cost-benefit point of view. Also, other sources of hazard, like tsunamis, landslides, should be considered in future investigations.

References

[1] C Oliveira."A simicidade historica e a revisao do catalogo sismico," Lisbon, 1986.

[2] M Correia, P Lourenco, and H Varum.*Seismic retrofitting: Learning from vernacular architecture*, 1st Editio. Lisbon: Taylor & Francis group, 2015.

[3] M Valente, G Barbieri, and L Biolzi."Damage assessment of three medieval churches after the 2012 Emilia earthquake," *Bull. Earthq. Eng.*, vol. 15, no. 7, pp. 2939–2980, 2017, doi: 10.1007/s10518-016-0073-7.

[4] P Candeias."Avaliação da vulnerabilidade sísmica de edifícios de alvenaria," University of Minho, 2008.PhD thesis

[5] M Villar-Vega *et al.*"Development of a Fragility Model for the Residential Building Stock in South America," *Earthq. Spectra*, vol. 33, no. 2, pp. 581–604, 2017, doi: 10.1193/010716EQS005M.

[6] G Sumerente, H Lovon, N Tarque, and C Chácara."Assessment of Combined In-Plane and Out-of-Plane Fragility Functions for Adobe Masonry Buildings in the Peruvian Andes," *Front. Built Environ.*, vol. 6, p. 52, 2020, doi: 10.3389/fbuil.2020.00052.

[7] H Lovon, N Tarque, V Silva, and C Yepes-Estrada."Development of Fragility Curves for Confined Masonry Buildings in Lima, Peru," *Earthq. Spectra*, vol. 34, no. 3, pp. 1339–1361, 2018, doi: 10.1193/090517EQS174M.

[8] T M Ferreira, R Vicente, J A R Mendes da Silva, H Varum, and A Costa."Seismic vulnerability assessment of historical urban centres: Case study of the old city centre in Seixal, Portugal," *Bull. Earthq. Eng.*, vol. 11, no. 5, pp. 1753–1773, 2013, doi: 10.1007/s10518-013-9447-2.

[9] H Kaplan, H Bilgin, S Yilmaz, H Binici, and A Öztas."Structural damages of L'Aquila (Italy) earthquake," *Nat. Hazards Earth Syst. Sci.*, vol. 10, no. 3, pp. 499–507, 2010, doi: 10.5194/nhess-10-499-2010.

[10] R Oyguc and E Oyguc."2011 Van Earthquakes: Lessons from Damaged Masonry Structures," *J. Perform. Constr. Facil.*, vol. 31, no. 5, p. 04017062, 2017, doi: 10.1061/(asce)cf.1943-5509.0001057.

[11] G Fiorentino *et al.*"Damage patterns in the town of Amatrice after August 24th 2016 Central Italy earthquakes," *Bull. Earthq. Eng.*, vol. 16, no. 3, pp. 1399–1423, 2018, doi: 10.1007/s10518-017-0254-z.

[12] I N de Estatística."Census data 2011," Lisbon, 2011.

[13] R Maio, J M C Estêvão, T M Ferreira, and R Vicente."Cost-benefit analysis of traditional seismic retrofitting strategies integrated in the renovation of stone masonry buildings," *Eng. Struct.*, vol. 206, p. 110050, 2020, doi: 10.1016/j.engstruct.2019.110050.

[14] V Silva, H Crowley, H Varum, R Pinho, and L Sousa."Investigation of the characteristics of Portuguese regular moment-frame RC buildings and development of a vulnerability model," *Bull. Earthq. Eng.*, vol. 13, no. 5, pp. 1455–1490, 2015, doi: 10.1007/s10518-014-9669-y.

[15] T Rossetto, I Ioannou, D Grant, and T Maqsood."Guidelines for empirical vulnerability assessment," Pavia, 2014.

[16] D D'Ayala, A Meslem, D Vamvatsikos, K Porter, T Rossetto, and V Silva."Guidelines for Analytical Vulnerability Assessment of Low/Mid-Rise Buildings, Vulnerability Global

Component Project.," 2015.

[17] L Martins, V Silva, H Crowley, P Bazzurro, and M Marques."Investigation of Structural Fragility for Risk-targeted Hazard Assessment," 2015.

[18] H Crowley, B Polidoro, R Pinho, and J Van Elk."Framework for developing fragility and consequence models for local personal risk," *Earthq. Spectra*, vol. 33, no. 4, pp. 1325–1345, 2017, doi: 10.1193/083116EQS140M.

[19] F Jalayer, R De Risi, and G Manfredi."Bayesian Cloud Analysis: Efficient structural fragility assessment using linear regression," *Bull. Earthq. Eng.*, vol. 13, no. 4, pp. 1183–1203, 2015, doi: 10.1007/s10518-014-9692-z.

[20] G Loa, A Muñoz, and S Santa-Cruz."Seismic evaluation of incremental seismic retrofitting techniques for typical Peruvian schools," in *Structures Congress 2017: Buildings and Special Structures - Selected Papers from the Structures Congress 2017*, 2017, pp. 101–110. doi: 10.1061/9780784480410.009.

[21] F P-58."FEMA P-58-1: Seismic Performance Assessment of Buildings. Volume 1 – Methodology," 2018.

[22] A Coburn, R Spence, and A Pomonis."Factors determining casualty levels in earthquakes: Mortality prediction in building collapse," 1992.

[23] Coburn Andrew and Robin Spence.*Earthquake Protection, 2nd Edition | Wiley*. 2003.

[24] E So.*Estimating Fatality Rates for Earthquake Loss Models*. Cham: Springer International Publishing, 2016. doi: 10.1007/978-3-319-26838-5.

[25] R Spence and E So.*Why do buildings collapse in earthquakes?*, 1st ed. Chichester: John Wiley & Sons, Ltd, 2021.

[26] R Spence."LESSLOSS Report 2007/07 - Earthquake Disaster Scenario Predictions & Loss Modelling for Urban Areas," 2007.

[27] FEMA."Hazus –MH 2.1 User Manual," 2012.

[28] A Iida, S Okada, T Nakashima, and M Kitahara."Volumetric Loss Estimation for Collapsed Buildings during Earthquakes," 2017, vol. 3589, no. Abstract ID.

[29] J Hallquist."LS-DYNA." Livermore Software Technology Corporation, Livermore, California, 2006.

[30] LSTC."LS-DYNA keyword User's Manual," Livermore, California, 2019.

[31] W Jäger, T Bakeer, and P Schöps."Simulation of Masonry in ANSYS and LS-DYNA The Features and Challenges," 2009.

[32] O AlShawa, L Sorrentino, and D Liberatore."Simulation Of Shake Table Tests on Out-of-Plane Masonry Buildings. Part (II): Combined Finite-Discrete Elements," *Int. J. Archit. Herit.*, vol. 11, no. 1, pp. 79–93, 2017, doi: 10.1080/15583058.2016.1237588.

[33] I E Bal, H Crowley, and R Pinho."Displacement-based earthquake loss assessment for an earthquake scenario in Istanbul," in *Journal of Earthquake Engineering*, 2008, vol. 12, no. SUPPL. 2, pp. 12–22. doi: 10.1080/13632460802013388.

[34] N Pereira and X Romao."Seismic Resistance of Portuguese Vernacular Architecture : A Critical Review," Lisbon, 2016.

[35] J Milosevic, M Lopes, A S Gago, and R Bento."Testing and modeling the diagonal tension strength of rubble stone masonry panels," *Eng. Struct.*, vol. 52, pp. 581–591, 2013, doi: 10.1016/j.engstruct.2013.03.019.

[36] F F S Pinho and V J G Lúcio."Rubble Stone Masonry Walls in Portugal: Material Properties, Carbonation Depth and Mechanical Characterization," *Int. J. Archit. Herit.*, vol. 11, no. 5, pp. 685–702, 2017, doi: 10.1080/15583058.2017.1289424.

[37] A A Costa, A Arêde, A C Costa, A Penna, and A Costa."Out-of-plane behaviour of a full scale stone masonry façade. Part 2: shaking table tests," *Earthq. Eng. Struct. Dyn.*, vol. 42, no. 14, p. n/a-n/a, 2013, doi: 10.1002/eqe.2314.

[38] P X Candeias, A Campos Costa, N Mendes, A A Costa, and P B Lourenço."Experimental Assessment of the Out-of-Plane Performance of Masonry Buildings Through Shaking Table Tests," *Int. J. Archit. Herit.*, vol. 11, no. 1, pp. 31–58, 2017, doi: 10.1080/15583058.2016.1238975.

[39] T M Ferreira, R Maio, and R Vicente."Analysis of the impact of large scale seismic retrofitting strategies through the application of a vulnerability-based approach on traditional masonry buildings," *Earthq. Eng. Eng. Vib.*, vol. 16, no. 2, pp. 329–348, 2017, doi: 10.1007/s11803-017-0385-x.

[40] A Meslem and D H Lang."Physical Vulnerability in Earthquake Risk Assessment," in *Oxford Research Encyclopedia of Natural Hazard Science*, Oxford University Press, 2017. doi: 10.1093/acrefore/9780199389407.013.71.

[41] F E Agency."Estimating Losses from Future Earthquakes," National Academies Press, 1989.

[42] S Brzev *et al.*"GEM Building Taxonomy (Version 2.0)," *GEM Tech. Rep.*, 2013.

[43] K Jaiswal and D J Wald."Creating a Global Building Inventory for Earthquake Loss Assessment and Risk Management," 2008.

[44] P Mouroux and B Le Brun."Risk-Ue Project: An Advanced Approach to Earthquake Risk Scenarios With Application to Different European Towns," in *Assessing and Managing Earthquake Risk*, Springer Netherlands, 2007, pp. 479–508. doi: 10.1007/978-1-4020-3608-8_23.

[45] U Hancilar and F Taucer."Guidelines for typology definition of European physical assets for earthquake risk assessment," Luxembourg, 2013.

[46] M Sousa."Risco sísmico em Portugal continental," Instituto Superior Técnico, 2006.PhD thesis

[47] A C Costa, M L Sousa, A Carvalho, and E Coelho."Evaluation of seismic risk and mitigation strategies for the existing building stock: Application of LNECloss to the metropolitan area of Lisbon," *Bull. Earthq. Eng.*, vol. 8, no. 1, pp. 119–134, 2010, doi: 10.1007/s10518-009-9160-3.

[48] H Crowley *et al.*"Exposure model for European seismic risk assessment," *Earthq. Spectra*, vol. 36, no. 1_suppl, pp. 252–273, 2020, doi: 10.1177/8755293020919429.

[49] BU-KOERI."Earthquake loss estimation routine-ELER V3.0," Zurich, 2010.

[50] J Appleton.*Reabilitação de edifícios antigos – patologias e tecnologias de intervenção*, 1st ed. Lisbon: Edições Orion, 2003.

[51] M Lopes.*Sismos e Edifícios*. Lisbon, 2008.

[52] P Lamego."Reforço sísmico de edifícios de habitação," University of Minho, 2014.PhD thesis

[53] N Mendes and P B Lourenco."Seismic assessment of masonry Gaioleiro buildings in Lisbon, Portugal," *J. Earthq. Eng.*, vol. 14, no. 1, pp. 80–101, 2010, doi: 10.1080/13632460902977474.

[54] Pinho."Paredes de alvenaria ordinária: Estudo experimental com modelos simples e reforçados," Universidade Nova de Lisboa, 2007.PhD thesis

[55] J Appleton."Contribuição para o estudo do seu comportamento e das acções de reabilitação a empreender de Edifícios Antigos em Portugal," Lisbon, 1991.

[56] F Neves, A Costa, R Vicente, C S Oliveira, and H Varum."Seismic vulnerability assessment and characterisation of the buildings on Faial Island, Azores," *Bull. Earthq. Eng.*, vol. 10, no. 1, pp. 27–44, 2012, doi: 10.1007/s10518-011-9276-0.

[57] M Da Rosa."Viabilidade do reforço sísmico de um edifício de pequeno porte em alvenaria de pedra ordinária," Instituto Superior de Engenharia de Lisboa, 2015.PhD thesis

[58] LNEC."Informações de interesse geral, edifícios com estrutura de alvenaria," 2005. http://www-ext.lnec.pt

[59] A Simões."Evaluation of the seismic vulnerability of the unreinforced masonry buildings constructed in the transition between the 19th and 20th centuries in Lisbon, Portugal," Instituto Superior Técnico, 2018.PhD thesis

[60] J Milosevic, R Bento, and S Cattari."Seismic behavior of lisbon mixed masonry-rc buildings with historical value: A contribution for the practical assessment," *Front. Built Environ.*, vol. 4, no. August, pp. 1–19, 2018, doi: 10.3389/fbuil.2018.00043.

[61] G Correia Lopes, R Vicente, T M Ferreira, and M Azenha."Intervened URM buildings with RC elements: typological characterisation and associated challenges," *Bull. Earthq. Eng.*, vol. 17, no. 9, pp. 4987–5019, 2019, doi: 10.1007/s10518-019-00651-y.

[62] A Simões, R Bento, S Cattari, and S Lagomarsino."Seismic performance-based assessment of 'Gaioleiro' buildings," *Eng. Struct.*, vol. 80, pp. 486–500, 2014, doi: 10.1016/j.engstruct.2014.09.025.

[63] A Alegre, J Appleton, and T Heitor."A reabilitação das casas de rendas económicas das células I e II do bairro de Alvalade," Lisbon, 1999.

[64] V Silva *et al.*"Current Challenges and Future Trends in Analytical Fragility and Vulnerability Modeling," *Earthq. Spectra*, vol. 35, no. 4, pp. 1927–1952, 2019, doi: 10.1193/042418EQS101O.

[65] A Furtado, C Costa, A Arêde, and H Rodrigues."Geometric characterisation of Portuguese RC buildings with masonry infill walls," *Eur. J. Environ. Civ. Eng.*, vol. 20, no. 4, pp. 396–411, 2016, doi: 10.1080/19648189.2015.1039660.

[66] B Borzi, H Crowley, and R Pinho."Simplified pushover-based earthquake loss assessment (SP-BELA) method for masonry buildings," *Int. J. Archit. Herit.*, vol. 2, no. 4, pp. 353–376, 2008, doi: 10.1080/15583050701828178.

[67] N Augenti, F Parisi, and E Acconci."MADA: online experimental database for mechanical modelling of existing masonry assemblages," 2012.

[68] S Boschi, L Galano, and A Vignoli."Mechanical characterisation of Tuscany masonry typologies by in situ tests," *Bull. Earthq. Eng.*, vol. 17, no. 1, pp. 413–438, 2019, doi: 10.1007/s10518-018-0451-4.

[69] Z Riahi, K J Elwood, and S M Alcocer."Backbone Model for Confined Masonry Walls for Performance-Based Seismic Design," *J. Struct. Eng.*, vol. 135, no. 6, pp. 644–654, 2009, doi: 10.1061/(asce)st.1943-541x.0000012.

[70] A Hussain and S Akhtar."Review of Non-Destructive Tests for Evaluation of Historic Masonry and Concrete Structures," *Arabian Journal for Science and Engineering*, vol. 42, no. 3. Springer Verlag, pp. 925–940, 2017. doi: 10.1007/s13369-017-2437-y.

[71] E Manning, L Ramos, and F Fernandes."Direct sonic and ultrasonic wave velocity in masonry under compressive stress," 2014.

[72] A American Society for Testing Materials."Standard test method for laboratory determination of pulse velocities and ultrasonic elastic constants of rock," Washington, 1995.

[73] B S I (BSI)."Testing concrete: recommendations for measurement of velocity of ultrasonic pulse in concrete," London, 1986.

[74] R Martini, J Carvalho, N Barraca, A Arêde, and H Varum."Advances on the use of non-destructive techniques for mechanical characterization of stone masonry: GPR and sonic tests," in *Procedia Structural Integrity*, 2017, vol. 5, pp. 1108–1115. doi: 10.1016/j.prostr.2017.07.096.

[75] T M Ferreira, A A Costa, A Arêde, A Gomes, and A Costa."Experimental characterization of the out-of-plane performance of regular stone masonry walls, including test setups and axial load influence," *Bull. Earthq. Eng.*, vol. 13, no. 9, pp. 2667–2692, 2015, doi: 10.1007/s10518-015-9742-1.

[76] R Vicente, T M Ferreira, J A R Mendes da Silva, and H Varum."In Situ Flat-Jack Testing of Traditional Masonry Walls: Case Study of the Old City Center of Coimbra, Portugal," *Int. J. Archit. Herit.*, vol. 9, no. 7, pp. 794–810, 2015, doi: 10.1080/15583058.2013.855840.

[77] ASTM."Standard test method for in-situ compressive stress within solid unit masonry estimated using flatjack measurements," West Conshohocken, 2020.

[78] RILEM."RILEM recommendation MDT. D. 4: in-situ stress tests based on the flat jack," 2004.

[79] A Brignola, S Frumento, S Lagomarsino, and S Podestá."Identification of shear parameters of masonry panels through the in-situ diagonal compression test," *International Journal of Architectural Heritage*, vol. 3, no. 1. Routledge, pp. 52–73, 2008. doi: 10.1080/15583050802138634.

[80] J Milosevic, A S Gago, M Lopes, and R Bento."Experimental assessment of shear strength parameters on rubble stone masonry specimens," *Constr. Build. Mater.*, vol. 47, pp. 1372–1380, 2013, doi: 10.1016/j.conbuildmat.2013.06.036.

[81] ASTM."Standard test method for diagonal tension (Shear) in masonry assemblages," West Conshohocken, 2002.

[82] C Almeida."Paredes de alvenaria do Porto: Tipificação e caraterização experimental," University of Porto, 2013.PhD thesis

[83] ASTM."Standard test method for compressive strength of laboratory constructed masonry prisms," West Conshohocken, 1997.

[84] G Vasconcelos."Experimental investigations on the mechanics of stone masonry: Characterization of granites and behavior of ancient masonry shear walls," University of Minho, 2005.PhD thesis

[85] M Tomazevic.*Earthquake-resistant design of masonry buildings*, 1st editio. London: Imperial College Press, 1999.

[86] J W Baker."Efficient Analytical Fragility Function Fitting Using Dynamic Structural Analysis," *Earthq. Spectra*, vol. 31, no. 1, pp. 579–599, 2015, doi: 10.1193/021113EQS025M.

[87] M Kohrangi, P Bazzurro, D Vamvatsikos, and A Spillatura."Conditional spectrum-based ground motion record selection using average spectral acceleration," *Earthq. Eng. Struct. Dyn.*, vol. 46, no. 10, pp. 1667–1685, 2017, doi: 10.1002/eqe.2876.

[88] H Shakib and V Jahangiri."Intensity measures for the assessment of the seismic response of buried steel pipelines," *Bull. Earthq. Eng.*, vol. 14, no. 4, pp. 1265–1284, 2016, doi: 10.1007/s10518-015-9863-6.

[89] C A Cornell, F Jalayer, R O Hamburger, and D A Foutch."Probabilistic Basis for 2000 SAC Federal Emergency Management Agency Steel Moment Frame Guidelines," *J. Struct. Eng.*, vol. 128, no. 4, pp. 526–533, 2002, doi: 10.1061/(ASCE)0733-9445(2002)128:4(526).

[90] N Luco and C A Cornell."Structure-Specific Scalar Intensity Measures for Near-Source and Ordinary Earthquake Ground Motions," *Earthq. Spectra*, vol. 23, no. 2, pp. 357–392, 2007, doi: 10.1193/1.2723158.

[91] K Mackie and B Stojadinovic."Fragility basis for california highway overpass bridge seismic decision making," Berkeley, 2005.

[92] D D Nguyen, B Thusa, T S Han, and T H Lee."Identifying significant earthquake intensity measures for evaluating seismic damage and fragility of nuclear power plant structures," *Nucl. Eng. Technol.*, vol. 52, no. 1, pp. 192–205, 2020, doi: 10.1016/j.net.2019.06.013.

[93] D Cardone and G Perrone."Developing fragility curves and loss functions for masonry infill walls," *Earthq. Struct.*, vol. 9, no. 1, pp. 257–279, 2015, doi: 10.12989/eas.2015.9.1.257.

[94] A M D'Altri *et al.*"Modeling Strategies for the Computational Analysis of Unreinforced Masonry Structures: Review and Classification," *Arch. Comput. Methods Eng.*, vol. 27, no. 4, pp. 1153–1185, 2020, doi: 10.1007/s11831-019-09351-x.

[95] P Roca, M Cervera, G Gariup, and L Pela'."Structural analysis of masonry historical constructions. Classical and advanced approaches," *Arch. Comput. Methods Eng.*, vol. 17, no. 3, pp. 299–325, 2010, doi: 10.1007/s11831-010-9046-1.

[96] D D'Ayala."Assessing the seismic vulnerability of masonry buildings," in *Handbook of Seismic Risk Analysis and Management of Civil Infrastructure Systems*, Elsevier Inc., 2013, pp. 334–365. doi: 10.1533/9780857098986.3.334.

[97] N Tarque, H Crowley, R Pinho, and H Varum."Displacement-Based Fragility Curves for Seismic Assessment of Adobe Buildings in Cusco, Peru," *Earthq. Spectra*, vol. 28, no. 2, pp. 759–794, 2012, doi: 10.1193/1.4000001.

[98] R Sousa, N Batalha, V Silva, and H Rodrigues."Seismic fragility functions for Portuguese RC precast buildings," *Bull. Earthq. Eng.*, pp. 1–18, 2020, doi: 10.1007/s10518-020-01007-7.

[99] S Lagomarsino, A Penna, A Galasco, and S Cattari."TREMURI program: An equivalent frame model for the nonlinear seismic analysis of masonry buildings," *Eng. Struct.*, vol. 56, pp. 1787–1799, 2013, doi: 10.1016/j.engstruct.2013.08.002.

[100] L Battaglia, T M Ferreira, and P B Lourenço."Seismic fragility assessment of masonry building aggregates: A case study in the old city Centre of Seixal, Portugal," *Earthq. Eng. Struct. Dyn.*, vol. 50, no. 5, pp. 1358–1377, 2021, doi: 10.1002/eqe.3405.

[101] A Karbassi and P Lestuzzi."Fragility Analysis of Existing Unreinforced Masonry Buildings through a Numerical-based Methodology," *Open Civ. Eng. J.*, vol. 6, no. 1, pp. 121–130, 2012, doi: 10.2174/1874149501206010121.

[102] A S International."Extreme Loading for structures," Raleigh, 2010.

[103] T Bakeer.*Collapse analysis of masonry structures under earthquake actions*, 1st ed. Dresde, Germany, 2009.

[104] T Bakeer and W Jger."Collapse analysis of reinforced and unreinforced adobe masonry structures under earthquake actions - case study: Bam Citadel," in *WIT Transactions on the Built Environment*, 2007, vol. 95, pp. 577–586. doi: 10.2495/STR070541.

[105] "OpenSEES." http://opensees.berkeley.edu/ (accessed Jun. 28, 2011).

[106] V Silva, H Crowley, R Pinho, and H Varum."Extending displacement-based earthquake loss assessment (DBELA) for the computation of fragility curves," *Eng. Struct.*, vol. 56, pp. 343–356, 2013, doi: 10.1016/j.engstruct.2013.04.023.

[107] N Ahmad, Q Ali, H Crowley, and R Pinho."Earthquake loss estimation of residential buildings in Pakistan," *Nat. Hazards*, vol. 73, no. 3, pp. 1889–1955, 2014, doi: 10.1007/s11069-014-1174-8.

[108] F Jalayer."Direct Probabilistic Seismic Analysis : Implementing Non-Linear Dynamic Assessments," University of Stanford, 2014.PhD thesis

[109] D Lallemant, A Kiremidjian, and H Burton."Statistical procedures for developing earthquake damage fragility curves," *Earthq. Eng. Struct. Dyn.*, vol. 44, no. 9, pp. 1373–1389, 2015, doi: 10.1002/eqe.2522.

[110] K Porter, R Kennedy, and R Bachman."Creating Fragility Functions for Performance-Based Earthquake Engineering," *Earthq. Spectra*, vol. 23, no. 2, pp. 471–489, 2007, doi: 10.1193/1.2720892.

[111] D Vamvatsikos and C A Cornell."Incremental dynamic analysis," *Earthq. Eng. Struct. Dyn.*, vol. 31, no. 3, pp. 491–514, 2002, doi: 10.1002/eqe.141.

[112] I Iervolino, M Giorgio, C Galasso, and G Manfredi."Conditional hazard maps for secondary intensity measures," *Bull. Seismol. Soc. Am.*, vol. 100, no. 6, pp. 3312–3319, 2010, doi: 10.1785/0120090383.

[113] F Jalayer, P Franchin, and P E Pinto."A scalar damage measure for seismic reliability analysis of RC frames," *Earthq. Eng. Struct. Dyn.*, vol. 36, no. 13, pp. 2059–2079, 2007, doi: 10.1002/eqe.704.

[114] F Jalayer, L Elefante, I Iervolino, and G Manfredi."Knowledge-based performance assessment of existing rc buildings," *J. Earthq. Eng.*, vol. 15, no. 3, pp. 362–389, 2011, doi: 10.1080/13632469.2010.501193.

[115] L Martins and V Silva."Development of a fragility and vulnerability model for global seismic risk analyses," *Bull. Earthq. Eng.*, no. 0123456789, 2020, doi: 10.1007/s10518-020-00885-1.

[116] V Silva."Uncertainty and Correlation in Seismic Vulnerability Functions of Building Classes," *Earthq. Spectra*, vol. 35, no. 4, pp. 1515–1539, 2019, doi: 10.1193/013018EQS031M.

[117] Y Xie, M Ebad Sichani, J E Padgett, and R DesRoches."The promise of implementing machine learning in earthquake engineering: A state-of-the-art review," *Earthq. Spectra*, vol. 36, no. 4, pp. 1769–1801, 2020, doi: 10.1177/8755293020919419.

[118] S Abeling and J M Ingham."Volume loss fatality model for as-built and retrofitted clay brick unreinforced masonry buildings damaged in the 2010/11 Canterbury earthquakes," *Structures*, vol. 24, pp. 940–954, 2020, doi: 10.1016/j.istruc.2020.02.014.

[119] M Indirli, L A S Kouris, A Formisano, R P Borg, and F M Mazzolani."Seismic damage assessment of unreinforced masonry structures after the Abruzzo 2009 earthquake: The case study of the historical centers of L'Aquila and Castelvecchio Subequo," *International Journal of Architectural Heritage*, vol. 7, no. 5. Taylor and Francis Inc., pp. 536–578, 2013. doi: 10.1080/15583058.2011.654050.

[120] E Samardjieva and J Badal."Estimation of the expected number of casualties caused by strong earthquakes," *Bull. Seismol. Soc. Am.*, vol. 92, no. 6, pp. 2310–2322, 2002, doi: 10.1785/0120010112.

[121] K Jaiswal, D J Wald, and M Hearne."Estimating Casualties for Large Earthquakes Worldwide Using an Empirical Approach," 2009.

[122] L Ceferino, A Kiremidjian, and G Deierlein."Regional Multiseverity Casualty Estimation Due to Building Damage following a Mw 8.8 Earthquake Scenario in Lima, Peru," *Earthq. Spectra*, vol. 34, no. 4, pp. 1739–1761, 2018, doi: 10.1193/080617EQS154M.

[123] S Okada."Description for indoor space damage degree of building in earthquake," 1996.

[124] R Bento."Seismic assessment and strengthening of URM and mixed masonry-RC buildings in Lisbon, Portugal," 2019.

[125] M Piazza, C Baldessari, and R Tomasi."The role of in-plane floor stiffness in the seismic behaviour of traditional buildings," 2008.

[126] V Coias.*Manual de recuparação e conservação do património construído - Técnicas pouco intrusivas*, 1st editio. Lisbon, 2007.

[127] A A AL-Manaseer and W V. Neis."Load Tests on Post-Tensioned Masonry Wall Panels," *Struct. J.*, vol. 84, no. 6, pp. 467–472, 1987, doi: 10.14359/2768.

[128] A Darbhanzi, M S Marefat, and M Khanmohammadi."Investigation of in-plane seismic retrofit of unreinforced masonry walls by means of vertical steel ties," *Constr. Build. Mater.*, vol. 52, pp. 122–129, 2014, doi: 10.1016/J.CONBUILDMAT.2013.11.020.

[129] E Ferretti."Effectiveness of Active Confinement Techniques with Steel Ribbons: Masonry Buildings," *Eur. J. Eng. Form. Sci. Artic.*, vol. 2, 2018, Accessed: Jul. 07, 2021. [Online]. Available: https://ideas.repec.org/a/eur/ejefjr/30.html

[130] E Ferretti and G Pascale."Some of the Latest Active Strengthening Techniques for Masonry Buildings: A Critical Analysis," *Materials (Basel).*, vol. 12, no. 7, 2019, doi: 10.3390/MA12071151.

[131] A B Liel and G G Deierlein."Cost-Benefit Evaluation of Seismic Risk Mitigation Alternatives for Older Concrete Frame Buildings," *Earthq. Spectra*, vol. 29, no. 4, pp. 1391–1411, 2013, doi: 10.1193/030911EQS040M.

[132] A Arya."Non-engineered construction in developing countries - an approach toward the earthquake risk reduction," 2000.

[133] S Diz, A Costa, and A A Costa."Efficiency of strengthening techniques assessed for existing masonry buildings," *Eng. Struct.*, vol. 101, pp. 205–215, 2015, doi: 10.1016/J.ENGSTRUCT.2015.07.017.

[134] M-L Segovia-Verjel, M-V Requena-García-Cruz, E de-Justo-Moscardó, and A Morales-

Esteban."Optimal seismic retrofitting techniques for URM school buildings located in the southwestern Iberian peninsula," *PLoS One*, vol. 14, no. 10, p. e0223491, 2019, doi: 10.1371/JOURNAL.PONE.0223491.

[135] S P Vilanova and J F B D Fonseca."Probabilistic seismic-hazard assessment for Portugal," *Bulletin of the Seismological Society of America*, vol. 97, no. 5. Seismological Society of America, pp. 1702–1717, 2007. doi: 10.1785/0120050198.

[136] C Yepes-Estrada *et al.*"Modeling the Residential Building Inventory in South America for Seismic Risk Assessment," *Earthq. Spectra*, vol. 33, no. 1, pp. 299–322, 2017, doi: 10.1193/101915eqs155dp.

[137] K Jaiswal, D Wald, and K Porter."A Global Building Inventory for Earthquake Loss Estimation and Risk Management," *Earthq. Spectra*, vol. 26, no. 3, pp. 731–748, 2010, doi: 10.1193/1.3450316.

[138] D Montgomery and G Runger.*Applied statistics and probability for engineers*, 3rd editio. New York: John Wiley & Sons, Ltd, 2003.

[139] N Mendes *et al.*"Methods and Approaches for Blind Test Predictions of Out-of-Plane Behavior of Masonry Walls: A Numerical Comparative Study," *Int. J. Archit. Herit.*, vol. 11, no. 1, pp. 59–71, 2017, doi: 10.1080/15583058.2016.1238974.

[140] J-S Jeon, J-H Park, and R DesRoches."Seismic fragility of lightly reinforced concrete frames with masonry infills," *Earthq. Eng. Struct. Dyn.*, vol. 44, no. 11, pp. 1783–1803, 2015, doi: 10.1002/eqe.2555.

[141] M Domaneschi, G P Cimellaro, and G Scutiero."A simplified method to assess generation of seismic debris for masonry structures," *Eng. Struct.*, vol. 186, pp. 306–320, 2019, doi: 10.1016/j.engstruct.2019.01.092.

[142] T M Inc."MATLAB." Natick, Massachusetts, 2018.

[143] R Drysdale, A Hamid, and L Baker.*Masonry structures behaviour and design*, 1st editio. California, 1994.

[144] R Pagaimo."Caracterização morfológica e mecânica de alvenarias antigas. Caso de estudo da vila histórica de Tentúgal," University of Coimbra, 2014.PhD thesis

[145] R Vicente."Estratégias e metodologias para intervenções de reabilitação urbana: Avaliação da vulnerabilidade e do risco sísmico do edificado da Baixa de Coimbra," University of Aveiro, 2008.PhD thesis

[146] S Moreira, L F Ramos, D V. Oliveira, and P B Lourenço."Experimental behavior of masonry wall-to-timber elements connections strengthened with injection anchors," *Eng. Struct.*, vol. 81, pp. 98–109, 2014, doi: 10.1016/j.engstruct.2014.09.034.

[147] A Simões, R Bento, A Gago, and M Lopes."Mechanical Characterization of Masonry Walls With Flat-Jack Tests," *Exp. Tech.*, p. n/a-n/a, 2015, doi: 10.1111/ext.12133.

[148] L Miranda."Ensaios acústicos e de macacos planos em alvenarias resistentes," University of Porto, 2011.PhD thesis

[149] J C Domingues, T M Ferreira, R Vicente, and J Negrão."Mechanical and Typological Characterization of Traditional Stone Masonry Walls in Old Urban Centres: A Case Study in Viseu, Portugal," *Buildings*, vol. 9, no. 1, p. 18, 2019, doi: 10.3390/buildings9010018.

[150] S Medić and M Hrasnica."Modeling Strategies for Masonry Structures," in *Lecture Notes in Networks and Systems*, vol. 28, Springer, 2018, pp. 633–644. doi: 10.1007/978-3-319-71321-

2_55.

[151] H Lovon, V Silva, R Vicente, T M Ferreira, and A A Costa."Characterisation of the masonry building stock in Portugal for earthquake risk assessment," *Eng. Struct.*, vol. 233, p. 111857, 2021, doi: 10.1016/j.engstruct.2021.111857.

[152] T Bakeer.*Collapse Analysis of Masonry Structures Under Earthquake Actions*, vol. 8. 2008.

[153] M A Erberik."Generation of fragility curves for Turkish masonry buildings considering in-plane failure modes," *Earthq. Eng. Struct. Dyn.*, vol. 37, no. 3, pp. 387–405, 2008, doi: 10.1002/eqe.760.

[154] M Bianchini, P Diotallevi, and J Baker."Prediction of inelastic structural response using an average of spectral accelerations," 2008.

[155] M Kohrangi, P Bazzurro, and D Vamvatsikos."Vector and scalar IMs in structural response estimation, Part II: Building demand assessment," *Earthq. Spectra*, vol. 32, no. 3, pp. 1525–1543, 2016, doi: 10.1193/053115EQS081M.

[156] C Casotto, V Silva, H Crowley, R Nascimbene, and R Pinho."Seismic fragility of Italian RC precast industrial structures," *Eng. Struct.*, vol. 94, pp. 122–136, 2015, doi: 10.1016/j.engstruct.2015.02.034.

[157] N Luco, B Ellingwood, R Hamburger, J Hooper, J Kimball, and C Kircher."Risk-Targeted versus Current Seismic Design Maps for the Conterminous United States," *undefined*, 2007.

[158] J Douglas, T Ulrich, and C Negulescu."Risk-targeted seismic design maps for mainland France," *Nat. Hazards 2012 653*, vol. 65, no. 3, pp. 1999–2013, 2012, doi: 10.1007/S11069-012-0460-6.

[159] V Silva, H Crowley, and P Bazzurro."Exploring Risk-Targeted Hazard Maps for Europe:," *https://doi.org/10.1193/112514eqs198m*, vol. 32, no. 2, pp. 1165–1186, 2019, doi: 10.1193/112514EQS198M.

[160] S N Jonkman, P H A J M Van Gelder, and J K Vrijling."An overview of quantitative risk measures for loss of life and economic damage," *J. Hazard. Mater.*, vol. 99, no. 1, pp. 1–30, 2003, doi: 10.1016/S0304-3894(02)00283-2.

[161] H H Tsang and F Wenzel."Setting structural safety requirement for controlling earthquake mortality risk," *Saf. Sci.*, vol. 86, pp. 174–183, 2016, doi: 10.1016/J.SSCI.2016.02.028.

[162] N Lazar Sinković and M Dolšek."Fatality risk and its application to the seismic performance assessment of a building," *Eng. Struct.*, vol. 205, p. 110108, 2020, doi: 10.1016/J.ENGSTRUCT.2019.110108.

[163] C Yepes-Estrada *et al.*"The Global Earthquake Model Physical Vulnerability Database:," *https://doi.org/10.1193/011816EQS015DP*, vol. 32, no. 4, pp. 2567–2585, 2016, doi: 10.1193/011816EQS015DP.

[164] A B Liel and G G Deierlein."Assessing the collapse risk of California's existing reinforced concrete frame structures: Metrics for seismic safety decisions.," California, 2008.

[165] M D'Amato, R Laguardia, G Di Trocchio, M Coltellacci, and R Gigliotti."Seismic Risk Assessment for Masonry Buildings Typologies from L'Aquila 2009 Earthquake Damage Data," *https://doi.org/10.1080/13632469.2020.1835750*, 2020, doi: 10.1080/13632469.2020.1835750.

[166] D N Grant *et al.*"Explicit modelling of collapse for Dutch unreinforced masonry building typology fragility functions," *Bull. Earthq. Eng.*, vol. 19, no. 15, pp. 6497–6519, 2021, doi:

10.1007/S10518-020-00923-Y/FIGURES/6.

[167] LSTC."LS-PRE/POST," Livermore, California, 2002.

[168] H Crowley, R Pinho, B Polidoro, and P Stafford."Development of v2 partial collapse fragility and consequence functions for the Groningen field," London, 2015.

[169] S Lagomarsino."Damage assessment of churches after L'Aquila earthquake (2009)," *Bull. Earthq. Eng.*, vol. 10, no. 1, pp. 73–92, 2012, doi: 10.1007/s10518-011-9307-x.

[170] A Penna *et al.*"Damage to churches in the 2016 central Italy earthquakes," *Bull. Earthq. Eng.*, vol. 17, no. 10, pp. 5763–5790, 2019, doi: 10.1007/s10518-019-00594-4.

[171] M De Risi, C Del Gaudio, and G Verderame."Evaluation of Repair Costs for Masonry Infills in RC Buildings from Observed Damage Data: the Case-Study of the 2009 L'Aquila Earthquake," *Buildings*, vol. 9, no. 5, p. 122, 2019, doi: 10.3390/buildings9050122.

[172] "The L'Aquila earthquake - Photos - The Big Picture." http://archive.boston.com/bigpicture/2009/04/the_laquila_earthquake.html (accessed Mar. 16, 2021).

[173] H Lovon, V Silva, R Vicente, and T-M Ferreira."Seismic vulnerability Assessment of Portuguese masonry buildings (under revision)," *Eng. Struct.*, 2021.

[174] J K Vrijling, P H A J M van Gelder, and S J Ouwerkerk."Criteria for Acceptable Risk in the Netherlands," *Infrastruct. Risk Manag. Process. Nat. Accid. Deliberate Hazards*, pp. 143–157, 2006, doi: 10.1061/9780784408155.CH05.

[175] R E (Robert E . Melchers and A T Beck.*Structural reliability analysis and prediction*, 2nd ed. 2018.

[176] I O for S (ISO)."2394:1998(E) - General principles on reliability for structures," 1998.

[177] B J M Ale."Tolerable or Acceptable: A Comparison of Risk Regulation in the United Kingdom and in the Netherlands," *Risk Anal.*, vol. 25, no. 2, pp. 231–241, 2005, doi: 10.1111/J.1539-6924.2005.00585.X.

[178] B Bhattacharya, R Basu, and K T Ma."Developing target reliability for novel structures: the case of the Mobile Offshore Base," *Mar. Struct.*, vol. 14, no. 1–2, pp. 37–58, 2001, doi: 10.1016/S0951-8339(00)00024-1.

[179] K Fischer, C Viljoen, J Köhler, and M H Faber."Optimal and acceptable reliabilities for structural design," *Struct. Saf.*, vol. 76, pp. 149–161, 2019, doi: 10.1016/J.STRUSAFE.2018.09.002.

[180] D Diamantidis, S Duzgun, F Nadim, and M Whorle."On the acceptable risk for structures subjected to geohazards," 2006.

[181] L Mendes-Victor, C S Oliveira, I Pais, and P Teves-Costa."Earthquake Damage Scenarios in Lisbon for Disaster Preparedness," *Issues Urban Earthq. Risk*, pp. 265–289, 1994, doi: 10.1007/978-94-015-8338-1_18.

[182] C S Oliveira."The Influence of Scale on Microzonation and Impact Studies," in *Recent Advances in Earthquake Geotechnical Engineering and Microzonation*, Springer, Dordrecht, 2004, pp. 27–65. doi: 10.1007/1-4020-2528-9_3.

[183] B Sengezer and E Koç."A critical analysis of earthquakes and urban planning in Turkey," *Disasters*, vol. 29, no. 2, pp. 171–194, 2005, doi: 10.1111/J.0361-3666.2005.00279.X.

[184] A Carvalho, G Zonno, G Franceschina, J Bilé Serra, and A Campos Costa."Earthquake

shaking scenarios for the metropolitan area of Lisbon," *Soil Dyn. Earthq. Eng.*, vol. 28, no. 5, pp. 347–364, 2008, doi: 10.1016/J.SOILDYN.2007.07.009.

[185] C S Oliveira."Lisbon earthquake scenarios: A review on uncertainties, from earthquake source to vulnerability modelling," *Soil Dyn. Earthq. Eng.*, vol. 28, no. 10–11, pp. 890–913, 2008, doi: 10.1016/J.SOILDYN.2007.11.002.

[186] M Pagani *et al.*"OpenQuake Engine: An Open Hazard (and Risk) Software for the Global Earthquake Model," *Seismol. Res. Lett.*, vol. 85, no. 3, pp. 692–702, 2014, doi: 10.1785/0220130087.

[187] V Silva, H Crowley, H Varum, and R Pinho."Seismic risk assessment for mainland Portugal," *Bull. Earthq. Eng.*, vol. 13, no. 2, pp. 429–457, 2014, doi: 10.1007/s10518-014-9630-0.

[188] G M Atkinson and D M Boore."Earthquake ground-motion prediction equations for eastern North America," *Bull. Seismol. Soc. Am.*, vol. 96, no. 6, pp. 2181–2205, 2006, doi: 10.1785/0120050245.

[189] S Akkar and J J Bommer."Empirical Equations for the Prediction of PGA, PGV, and Spectral Accelerations in Europe, the Mediterranean Region, and the Middle East," *Seismol. Res. Lett.*, vol. 81, no. 2, pp. 195–206, 2010, doi: 10.1785/GSSRL.81.2.195.

[190] M Uranjek, V Bosiljkov, R Žarnić, and V Bokan-Bosiljkov."In situ tests and seismic assessment of a stone-masonry building," *Mater. Struct. Constr.*, vol. 45, no. 6, pp. 861–879, 2012, doi: 10.1617/S11527-011-9804-Z/FIGURES/17.

[191] C Del Gaudio *et al.*"Empirical fragility curves for masonry buildings after the 2009 L'Aquila, Italy, earthquake," *Bull. Earthq. Eng.*, vol. 17, no. 11, pp. 6301–6330, 2019, doi: 10.1007/S10518-019-00683-4/TABLES/8.

[192] G Guerrini *et al.*"Experimental and Numerical Assessment of Seismic Retrofit Solutions for Stone Masonry Buildings," *Geosci. 2021, Vol. 11, Page 230*, vol. 11, no. 6, p. 230, 2021, doi: 10.3390/GEOSCIENCES11060230.

[193] S S Lucchini, L Facconi, F Minelli, and G Plizzari."Retrofitting unreinforced masonry by steel fiber reinforced mortar coating: uniaxial and diagonal compression tests," *Mater. Struct. Constr.*, vol. 53, no. 6, pp. 1–22, 2020, doi: 10.1617/S11527-020-01574-W/FIGURES/12.

[194] NF P 18-891.*Produits spe´ciaux destines aux constructions en be´ton hydraulique—Produits pour injections dans des structures en be´ton—Essai d´ injectabilite´ a` la colonne de sable en milieux sec et humide, French Standard (In French)*. 1986.

[195] A American Society for Testing Materials.*ASTM C476-20, Standard Specification for grout for masonry*. United states: ASTM, 2020. doi: 10.1520/C0476-20.

[196] L Binda, C Modena, G Baronio, and S Abbaneo."Repair and investigation techniques for stone masonry walls," *Constr. Build. Mater.*, vol. 11, no. 3, pp. 133–142, 1997, doi: 10.1016/S0950-0618(97)00031-7.

[197] L Miranda, J Milosevic, and R Bento."Cyclic behaviour of stone masonry walls strengthened by grout injection," *Mater. Struct. Constr.*, vol. 50, no. 1, pp. 1–17, 2017, doi: 10.1617/S11527-016-0911-8/FIGURES/12.

[198] B Silva, M Dalla Benetta, F Da Porto, and C Modena."Experimental assessment of in-plane behaviour of three-leaf stone masonry walls," *Constr. Build. Mater.*, vol. 53, pp. 149–161, 2014, doi: 10.1016/J.CONBUILDMAT.2013.11.084.

[199] P D, V MR, S A, Binda L, and M C."Repair and strengthening of historic masonry buildings in seismic areas," 2001.

[200] D M, N D, P F, and M R."The CAM system for the retrofit of masonry structures," 2001.

[201] F Ersubasi and H H Korkmaz."Shaking table tests on strengthening of masonry structures against earthquake hazard," *Nat. Hazards Earth Syst. Sci.*, vol. 10, no. 6, pp. 1209–1220, 2010, doi: 10.5194/NHESS-10-1209-2010.

[202] N Mazzon, C M M Chavez, M R Valluzzi, F Casarin, and C Modena."Shaking Table Tests on Multi-Leaf Stone Masonry Structures: Analysis of Stiffness Decay," *Adv. Mater. Res.*, vol. 133–134, pp. 647–652, 2010, doi: 10.4028/WWW.SCIENTIFIC.NET/AMR.133-134.647.

[203] E Toumbakari."Lime-pozzolan-cement grouts and their structural effects on composite masonry walls," Catholic University of Leuven, 2002.PhD thesis

[204] M Corradi, A Borri, and A Vignoli."Strengthening techniques tested on masonry structures struck by the Umbria–Marche earthquake of 1997–1998," *Constr. Build. Mater.*, vol. 16, no. 4, pp. 229–239, 2002, doi: 10.1016/S0950-0618(02)00014-4.

[205] M R Valluzzi, F da Porto, and C Modena."Behavior and modeling of strengthened three-leaf stone masonry walls," *Mater. Struct. 2004 373*, vol. 37, no. 3, pp. 184–192, 2004, doi: 10.1007/BF02481618.

[206] E Vintzileou and A Miltiadou-Fezans."Mechanical properties of three-leaf stone masonry grouted with ternary or hydraulic lime-based grouts," *Eng. Struct.*, vol. 30, no. 8, pp. 2265–2276, 2008, doi: 10.1016/J.ENGSTRUCT.2007.11.003.

[207] C Almeida, J P Guedes, A Arêde, C Q Costa, and A Costa."Physical characterization and compression tests of one leaf stone masonry walls," *Constr. Build. Mater.*, vol. 30, pp. 188–197, 2012, doi: 10.1016/J.CONBUILDMAT.2011.11.043.

[208] D V. Oliveira, R A Silva, E Garbin, and P B Lourenço."Strengthening of three-leaf stone masonry walls: An experimental research," *Mater. Struct. Constr.*, vol. 45, no. 8, pp. 1259–1276, 2012, doi: 10.1617/S11527-012-9832-3/FIGURES/18.

[209] B Silva, M Dalla Benetta, F Da Porto, and M R Valluzzi."Compression and Sonic Tests to Assess Effectiveness of Grout Injection on Three-Leaf Stone Masonry Walls," *https://doi.org/10.1080/15583058.2013.826300*, vol. 8, no. 3, pp. 408–435, 2013, doi: 10.1080/15583058.2013.826300.

[210] E Luso and P B Lourenço."Mechanical Behavior of Two-Leaf Masonry Wall–Strengthening Using Different Grouts," *J. Mater. Civ. Eng.*, vol. 31, no. 7, p. 04019096, 2019, doi: 10.1061/(ASCE)MT.1943-5533.0002712.

[211] T Sevil, M Baran, T Bilir, and E Canbay."Use of steel fiber reinforced mortar for seismic strengthening," *Constr. Build. Mater.*, vol. 25, no. 2, pp. 892–899, 2011, doi: 10.1016/J.CONBUILDMAT.2010.06.096.

[212] L Facconi, F Minelli, S Lucchini, and G Plizzari."Experimental Study of Solid and Hollow Clay Brick Masonry Walls Retrofitted by Steel Fiber-Reinforced Mortar Coating," *https://doi.org/10.1080/13632469.2018.1442264*, vol. 24, no. 3, pp. 381–402, 2018, doi: 10.1080/13632469.2018.1442264.

[213] L Kheddache, C Aribi, K Chahour, and B Safi."Highlighting of the distribution effect of steel hook fibers at low and high dosage on the flexural strength of self-compacting mortars," *Mater. Today Proc.*, vol. 52, pp. 1384–1390, 2022, doi: 10.1016/J.MATPR.2021.11.125.

[214] P Pierre, R Pleau, and M Pigeon."Mechanical Properties of Steel Microfiber Reinforced Cement Pastes and Mortars," *J. Mater. Civ. Eng.*, vol. 11, no. 4, pp. 317–324, 1999, doi: 10.1061/(ASCE)0899-1561(1999)11:4(317).

[215] ISO."Risk management - Risk assessment techniques," Geneva, Switzerland, 2019.

[216] E L Krinitzsky."Deterministic versus probabilistic seismic hazard analysis for critical structures," *Eng. Geol.*, vol. 40, no. 1–2, pp. 1–7, 1995, doi: 10.1016/0013-7952(95)00031-3.

[217] J J Bommer."Deterministic vs. probabilistic seismic hazard assessment: An exaggerated and obstructive dichotomy," *J. Earthq. Eng.*, vol. 6, no. SPEC. ISS. 1, pp. 43–73, 2002, doi: 10.1142/S1363246902000644.

[218] J Baker, B Bradley, and P Stafford.*Seismic Hazard and Risk Analysis*. Cambridge University Press, 2021. doi: 10.1017/9781108425056.

[219] E 1998-1.*Eurocode 8 : design of structures for earthquake resistance*. European Union, 1996.

[220] ASCE/SEI 7-10."Minimum Design Loads and Associated Criteria for Buildings and Other Structures. Structural Engineering Institute of the American Society of Civil Engineering, Reston," 2013.

[221] G Baltzopoulos, A Grella, and I Iervolino."Seismic reliability implied by behavior-factor-based design," *Earthq. Eng. Struct. Dyn.*, vol. 50, no. 15, pp. 4076–4096, 2021, doi: 10.1002/EQE.3546.

[222] V Silva, H Crowley, and P Bazzurro."Exploring Risk-Targeted Hazard Maps for Europe:," *https://doi.org/10.1193/112514eqs198m*, vol. 32, no. 2, pp. 1165–1186, 2019, doi: 10.1193/112514EQS198M.

[223] O C, A Campos-Costa, and M Sousa."Estimativa dos Danos Causados por Sismos no Parque Habitacional do Continente Português Contribuição para a Definição de Uma Política de Seguros," Lisbon, Portugal, 1997.

[224] J Antonio, P P Montilla, C Lo´pez, and L L Casado."Seismic Hazard Estimate at the Iberian Peninsula," *pure Appl. Geophys. 2002 15911*, vol. 159, no. 11, pp. 2699–2713, 2002, doi: 10.1007/S00024-002-8754-3.

[225] IGN."The Seismicity Catalog," 1992.

[226] M Sousa, A Martins, and C Oliveira."Compilação de catálogos sísmicos da região Ibérica," Lisbon, Portugal, 1992.

[227] J Stepp."Analysis of completeness of the earthquake sample in the Puget Sound area and its effect on statistical estimates of earthquake hazard," 1972.

[228] D Albarello, R Camassi, and A Rebez."Detection of Space and Time Heterogeneity in the Completeness of a Seismic Catalog by a Statistical Approach: An Application to the Italian Area," *Bull. Seismol. Soc. Am.*, vol. 91, no. 6, pp. 1694–1703, 2001, doi: 10.1785/0120000058.

[229] H Crowley, J J Bommer, R Pinho, and J Bird."The impact of epistemic uncertainty on an earthquake loss model," *Earthq. Eng. Struct. Dyn.*, vol. 34, no. 14, pp. 1653–1685, 2005, doi: 10.1002/EQE.498.

[230] E Delavaud *et al.*"Toward a ground-motion logic tree for probabilistic seismic hazard assessment in Europe," *J. Seismol.*, vol. 16, no. 3, pp. 451–473, 2012, doi: 10.1007/S10950-012-9281-Z/TABLES/15.

[231] K W Campbell."Prediction of Strong Ground Motion Using the Hybrid Empirical Method and Its Use in the Development of Ground-Motion (Attenuation) Relations in Eastern North America," *Bull. Seismol. Soc. Am.*, vol. 93, no. 3, pp. 1012–1033, 2003, doi: 10.1785/0120020002.

[232] G Toro."Prediction of strong ground motion using the hybrid empirical method and its use in the development of ground-motion (attenuation) relations in eastern North America," 2002.

[233] C Cauzzi and E Faccioli."Broadband (0.05 to 20 s) prediction of displacement response spectra based on worldwide digital records," *J. Seismol. 2008 124*, vol. 12, no. 4, pp. 453–475, 2008, doi: 10.1007/S10950-008-9098-Y.

[234] J X Zhao *et al.*"Attenuation Relations of Strong Ground Motion in Japan Using Site Classification Based on Predominant Period," *Bull. Seismol. Soc. Am.*, vol. 96, no. 3, pp. 898–913, 2006, doi: 10.1785/0120050122.

[235] B S J Chiou and R R Youngs."An NGA Model for the Average Horizontal Component of Peak Ground Motion and Response Spectra:," *https://doi.org/10.1193/1.2894832*, vol. 24, no. 1, pp. 173–215, 2019, doi: 10.1193/1.2894832.

[236] S Kramer.*Geotechnical earthquake engineering*. New Jersey: Prentice Hall, 1996.

[237] E H Field, T H Jordan, and C A Cornell."OpenSHA: A Developing Community-modeling Environment for Seismic Hazard Analysis," *Seismol. Res. Lett.*, vol. 74, no. 4, pp. 406–419, 2003, doi: 10.1785/GSSRL.74.4.406.

[238] J A Valcárcel, M G Mora, O D Cardona, L G Pujades, A H Barbat, and G A Bernal."Methodology and applications for the benefit cost analysis of the seismic risk reduction in building portfolios at broadscale," *Nat. Hazards*, vol. 69, no. 1, pp. 845–868, 2013, doi: 10.1007/S11069-013-0739-2/FIGURES/14.

[239] R Marques, P Lamego, P B Lourenço, and M L Sousa."Efficiency and Cost-Benefit Analysis of Seismic Strengthening Techniques for Old Residential Buildings in Lisbon," *https://doi.org/10.1080/13632469.2017.1286616*, vol. 22, no. 9, pp. 1590–1625, 2017, doi: 10.1080/13632469.2017.1286616.

[240] D Cardone, G Gesualdi, and G Perrone."Cost-Benefit Analysis of Alternative Retrofit Strategies for RC Frame Buildings," *https://doi.org/10.1080/13632469.2017.1323041*, vol. 23, no. 2, pp. 208–241, 2017, doi: 10.1080/13632469.2017.1323041.

[241] W K Viscusi and C J Masterman."Income Elasticities and Global Values of a Statistical Life," *J. Benefit-Cost Anal.*, vol. 8, no. 2, pp. 226–250, 2017, doi: 10.1017/BCA.2017.12.

[242] O AlShawa, D Liberatore, and L Sorrentino."Dynamic One-Sided Out-Of-Plane Behavior of Unreinforced-Masonry Wall Restrained by Elasto-Plastic Tie-Rods," *https://doi.org/10.1080/15583058.2018.1563226*, vol. 13, no. 3, pp. 340–357, 2019, doi: 10.1080/15583058.2018.1563226.